# Trends, composition, and sources of carbonaceous aerosol at the Birkenes Observatory, Northern Europe, 2001-2018

Karl Espen Yttri[1], Francesco Canonaco[2,7], Sabine Eckhardt[1], Nikolaos Evangeliou[1], Markus Fiebig[1], Hans Gundersen[1], Anne-Gunn Hjellbrekke[1], Cathrine Lund Myhre[1], Stephen Matthew Platt[1], André S. H. Prévôt[2], David Simpson[3,4], Sverre Solberg[1], Jason Surratt[5], Kjetil Tørseth[1], Hilde Uggerud[1], Marit Vadset[1], Xin Wan[6], and Wenche Aas[1]

[1] NILU - Norwegian Institute for Air Research, P.O. Box 100, N-2027 Kjeller, Norway

[2]Paul Scherrer Institute (PSI), 5232 Villigen-PSI, Switzerland

[3]EMEP MSC-W, Norwegian Meteorological Institute, Oslo, Norway

[4]Department of Earth & Space Sciences, Chalmers Univ. Technology, Gothenburg, Sweden

[5] Department of Environmental Sciences & Engineering, University of North Carolina

[6] Key Laboratory of Tibetan Environment Changes and Land Surface Processes, Institute of Tibetan Plateau Research, Chinese Academy of Sciences Courtyard 16, Lin Cui Road, Chaoyang District, Beijing 100101, P.R. China

[7] Datalystica Ltd., 5234 Villigen, Switzerland

*_To whom correspondence should be addressed:_ Karl Espen Yttri, e-mail address: key@nilu.no

**Abstract**

We present 18 years (2001–2018) of aerosol measurements: organic and elemental carbon (OC and EC), organic tracers (levoglucosan, arabitol, mannitol, trehalose, glucose, 2-methyltetrols), trace elements and ions at the Birkenes Observatory (Southern Norway), a site representative of the Northern European region. The OC/EC (2001–2018) and the levoglucosan (2008–2018) time series are the longest in Europe, with OC/EC available for the $PM_{10}$, $PM_{2.5}$ (fine) and $PM_{10-2.5}$ (coarse) size fractions, providing the opportunity for a nearly two-decade long assessment. Using positive matrix factorization (PMF) we identify seven carbonaceous aerosol sources at Birkenes: Mineral dust dominated (MIN), traffic/industry-like (TRA/IND), short range transported biogenic secondary organic aerosol ($BSOA_{SRT}$), primary biological aerosol particles (PBAP), biomass burning (BB), ammonium nitrate dominated ($NH_4NO_3$), and (one low carbon fraction) sea salt (SS).

We observed significant ($p<0.05$), large decreases of EC in $PM_{10}$ (-3.9% $yr^{-1}$) and $PM_{2.5}$ (-4.2% $yr^{-1}$), and a smaller decline in levoglucosan (-2.8% $yr^{-1}$), suggesting that OC/EC from traffic and industry is decreasing, while abatement of OC/EC from biomass burning has been slightly less successful. EC abatement of anthropogenic sources is further supported by decreasing EC fractions in $PM_{2.5}$ (-3.9% $yr^{-1}$) and $PM_{10}$ (-4.5% $yr^{-1}$). PMF apportioned 72% of EC to fossil fuel sources, further supported by PMF applied to absorption photometer data, which yielded a two-factor solution with a low aerosol Ångstrøm exponent (AAE=0.93) fraction assumed to be equivalent black carbon from fossil fuel combustion ($eBC_{ff}$), contributing 78% to eBC mass. The higher AAE fraction (AAE=2.04) is likely eBC from BB

($eBC_{bb}$). Source receptor model calculations (FLEXPART) showed that Continental Europe and western Russia were the main source regions both of elevated $eBC_{bb}$ and $eBC_{ff}$.

Dominating biogenic sources explain why there was no downward trend for OC. A relative increase in the OC fraction in $PM_{2.5}$ (+3.2% $yr^{-1}$) and $PM_{10}$ (+2.3% $yr^{-1}$) underscores the importance of biogenic sources at Birkenes (BSOA and PBAP), which were higher in the vegetative season and dominated both fine (53%) and coarse (78%) OC. Furthermore, 77–91% of OC in $PM_{2.5}$, $PM_{10-2.5}$ and $PM_{10}$ was attributed to biogenic sources in summer vs. 22-37% in winter. The coarse fraction had the highest share of biogenic sources regardless of season and was dominated by PBAP, except in winter.

Our results show a shift in aerosol composition at Birkenes and thus also in the relative source contributions. The need for diverse off-line and on-line carbonaceous aerosol speciation to understand carbonaceous aerosol sources, including their seasonal, annual, and long-term variability has been demonstrated.

## 1. Introduction

Carbonaceous aerosol has been studied intensively over the last 20 years due to its influence on radiative forcing (Bond et al., 2013; Myhre and Samset, 2015; Lund et al., 2018), both directly by scattering and absorption of sunlight, and semi directly and indirectly by influencing cloud properties (Boucher et al., 2013; Hodnebrog et al., 2014; Myhre et al., 2013). It also contributes to the burden of respiratory and cardiovascular disease (Janssen et al., 2012; WHO, 2013). Consequently, carbonaceous aerosol [here: elemental carbon (EC) and organic carbon (OC)] is measured regularly in major air monitoring networks such as e.g., EMEP and IMPROVE (e.g., Malm et al. 1994; Tørseth and Hov, 2003; Tørseth et al., 2012; UNECE, 2019; Hjellbrekke, 2020). Carbonaceous aerosol has an atmospheric lifetime of days to a few weeks and is thus relevant for atmospheric long-range transport. Accordingly, the European Monitoring and Evaluation Programme (EMEP) included OC/EC measurements in 2004 after a pioneering measurement campaign at 12 European sites from 2002–2003 (Yttri et al., 2007a; Tørseth et al., 2012), showing that carbonaceous aerosol was a major constituent of the ambient aerosol in the European rural background environment, accounting for 9–37% (OM = organic matter) and 1–5% (EC) of $PM_{10}$, and that OM was more abundant than sulfate ($SO_4^{2-}$) at sites reporting both variables (Yttri et al., 2007a). Similar conclusions were found from another long-term campaign, CARBOSOL (Gelencsér et al., 2007; Pio et al., 2007), which monitored atmospheric aerosol and its components for two years at six sites along a west-east transect extending from the Azores, in the mid-Atlantic Ocean, to K-Kuszta (Hungary), in centra Europe.

There are numerous carbonaceous aerosol sources, both anthropogenic, e.g. emissions from combustion of fossil fuel and biomass, and biogenic, e.g. vegetation emitted terpene/isoprene oxidation, and primary biological aerosol particles (PBAP) from e.g. plants and fungi (Bauer et al., 2002; Donahue et al., 2009; Hallquist et al., 2009; Fröhlich-Nowoisky et al., 2016).

Detailed source apportionment and quantification of carbonaceous aerosol is challenging due to it numerous sources, the complexity of atmospheric formation and the vast number of organic compounds associated with carbonaceous aerosols. A few studies have addressed carbonaceous aerosol sources in the European rural background environment using source-specific organic tracers (Gelencsér et al., 2007; Szidat et al., 2009; Genberg et al., 2011; Gilardoni et al., 2011; Yttri et al., 2011a,b). These consistently show that residential wood burning dominates OC in winter, whereas biogenic secondary organic aerosol (BSOA) is the major source in summer. PBAP makes a significant contribution to $PM_{10}$ in the vegetative season in the Nordic countries, second only to BSOA (Yttri et al., 2011a,b). Fossil fuel sources typically dominate EC regardless of season but residential wood burning emissions can be equally important and occasionally dominate in the heating season (Zotter et al., 2014; Yttri et al., 2019). On-line high time-resolution measurements by aerosol mass spectrometer (AMS) and aerosol chemical speciation monitors (ACMS) have become available in recent years, complementing off-line analysis of organic tracers. In the comprehensive study by Crippa et al. (2014), including 15 European rural background sites and 2 urban sites, covering winter, spring and fall, hydrocarbon-like organic aerosol (OA) (11±5%) and biomass burning OA (12±5%) contributed almost equally to the total OA concentration. The vast majority was however attributed to secondary sources; i.e., semi volatile oxygenated OA (34±11%) and low-volatility oxygenated OA (50±16%). Secondary oxygenated OA (OOA) can be both anthropogenic and biogenic; however Crippa et al. (2014) did not draw any conclusions on this. Results presented by Bougiatioti et al. (2014) show how freshly emitted biomass burning OA can be transformed to more oxidized OOA after just a short time in the atmosphere when subject to high temperatures and high solar radiation.

Over the last decades, European anthropogenic emissions of secondary inorganic aerosol precursors, e.g. ammonia ($NH_3$) and nitrogen oxides ($NO_x$), and non-methane volatile organic compounds (NMVOC) have stabilized, and those of sulfur dioxide ($SO_2$) significantly reduced, following implementation of the Gothenburg Protocol (Reis et al., 2012; UNECE, 2013; Matthews et al., 2020). The anthropogenic carbonaceous aerosol is not regulated by any binding international protocol, although co-benefit is expected from the regulation of $NO_X$ and NMVOC, which act as precursors of secondary organic aerosol (Hallquist et al., 2009). $PM_{2.5}$ was included in the revised version of the Gothenburg protocol (UNECE, 2013) in 2012, which states that effort should be directed towards sources that also emit black carbon (BC), which inevitably also will influence OC.

Residential wood burning is a major source of carbonaceous aerosol in circumpolar countries (e.g. Yttri et al., 2014) and even considered the most important source in Norway, accounting for 48% (2017) of $PM_{2.5}$ (Grythe et al., 2019). This region also regularly experiences major wild and agricultural fires (e.g. Stohl et al., 2006 and 2007). A growing number of studies show that residential wood burning is more widespread in continental Europe than previously assumed and that its contribution to the ambient carbonaceous aerosol can be substantial (Sillanpää et al., 2005; Gelencsér et al., 2007; Puxbaum et al., 2007; Lanz et al., 2010; Maenhaut et al., 2012; Genberg et al., 2011; Fuller et al., 2014; Yttri et al.,

2019) and even dominating (Szidat et al., 2007; Herich et al., 2014). Residential wood burning is a decentralized source in Europe and combustion typically takes place in small units where the emissions are emitted without after-treatment. An economic downturn in Greece compelled households to burn firewood and waste material as fuel costs rose, increasing residential wood burning emissions in urban areas by 30% (Saffari et al., 2013). Future increases in European wood burning emissions might occur due to climate change mitigation policies supporting the use of renewable and biofuels (van der Gon et al., 2015). Denier van der Gon et al. (2015) conclude that European emissions from residential wood burning are significantly underestimated, thus it appears timely to address how ambient carbonaceous aerosol -particularly from biomass burning -has developed over the last two decades.

Kahnert et al. (2004) and Tørseth et al. (2012) highlight the importance of long-term measurements (> 10 years) of carbonaceous aerosol. The Birkenes Observatory in southern Norway holds the longest time series of OC and EC in Europe, dating back to 2001, including measurements in both the $PM_{10}$ and the $PM_{2.5}$ fractions. Infleunced by major anthropogenic emission regions in Europe, the Birkenes Observatory is well suited to monitor air pollution from Continental Europe.

Here we apply positive matrix factorization (PMF) to identify sources of carbonaceous aerosol at the Birkenes Observatory. Measurements of complementary species accompany OC/EC monitoring, allowing us to understand these sources, their contribution and variability at time scales from minutes to decades: organic tracers for biomass burning (levoglucosan), PBAP (arabitol, mannitol, trehalose and glucose) and BSOA (2-methyltetrols), as well as high time resolution equivalent black carbon resulting from biomass ($eBC_{bb}$) and fossil ($eBC_{ff}$) fuel combustion, derived from multiwavelength aethalometer measurements.

## 2. Methodology

### 2.1 Sampling site

The Birkenes Observatory (58°23'N, 8°15'E, 219 m above sea level, asl) is an EMEP/GAW (Global Atmospheric Watch) supersite in southern Norway (Figure 1) situated 100 m south-east of the old Birkenes site, initiating measurements in 2009. The observatory is in the Boreo-nemorale zone with mixed coniferous and deciduous trees (65% of the land use near the site); the remainder being meadows (10%), low intensity agricultural areas (10%), and freshwater lakes (15%). Close to the Skagerrak coast (~20 km) and at low altitude, the observatory experiences a maritime climate with relatively mild winters and moderately warm summers. The prevailing wind is westerly/south westerly. Figure S 1 shows ambient temperature and precipitation (2001–2018) at Birkenes. The nearest city is Kristiansand (population ~61 000) 25 km to the south/south-west.

### 2.2 Measurements and procedures

#### 2.2.1 Off-line filter measurements

We collected OC/EC, organic tracers and PM mass filter samples using two low-volume samplers with

a $PM_{10}$ and a $PM_{2.5}$ inlet. Quartz fiber filters (Whatman QM-A; 47 mm in diameter) were pre-fired (850 °C; 3 h). We conditioned the filters [20 ± 1°C; 50 ± 5% RH (relative humidity)] for 48 h before and after exposure and weighed them to obtain PM mass. We kept filters in petri slides and stored them at 4 °C after weighing and before OC/EC analysis. After OC/EC analysis and prior to organic tracer analysis the samples were stored at -18 °C. Two field blanks were assigned to each month of sampling and were treated in exactly the same manner regarding preparation, handling, transport and storage as the exposed filters, except that they were not inserted in the samplers. We collected one sample per sampler per week (168 hours), except for 14 August 2002–17 September 2008, when two samples were collected per sampler per week; at 24 h and 144 h intervals. The sampling inlets are 2 m above the Observatory roof, 5 m above the ground level (~226 m asl). The OC/EC and PM mass time series date back to February 2001 and organic tracers back to January 2008 (monosaccharide anhydrides) and January 2016 (sugars, sugar-alcohols and 2-methyltetrols).

We performed thermal-optical analysis (TOA, Sunset Laboratory OC/EC instrument), using transmission for charring correction. We used the Quartz temperature programme in 2001–2008 and EUSAAR-2 (Cavalli et al., 2010) from 2008. We compare the two temperature programmes for $PM_{2.5}$ samples collected in 2014 in Supplementary Sect. S1. OC/EC instrument performance is regularly inter-compared under the joint EMEP/ACTRIS quality assurance and quality control effort (e.g. Cavalli et al., 2013).

Until 2014, we determined monosaccharide anhydrides (levoglucosan, mannosan, galactosan) in $PM_{10}$ using high-performance liquid chromatography high-resolution time-of-flight mass spectrometry (HPLC-HR-TOFMS) in negative electrospray ionization mode according to the method of Dye and Yttri (2005). After 2014, we use ultra-performance liquid chromatography (UPLC), with two Waters columns (2 x 2.1 x 150 mm HSS T3, 1.8 µm, Waters Inc.). Changing the column improved the chromatographic resolution, allowing the analysis of sugars, sugar-alcohols and 2-methyltetrols. We identified the monosaccharide anhydrides based on retention time and mass spectra (accurate mass and isotope pattern) of authentic standards (Table S 1). Isotope-labelled standards of levoglucosan, galactosan, arabitol, mannitol, trehalose and glucose were used as internal recovery standard (Table S 1).

Weekly OC/EC, $PM_{10}$, $PM_{2.5}$ are publicly available on EBAS (http://ebas.nilu.no). Mean values (daily/weekly/seaonal/annual) used below, merging of data from the old and new Birkenes sites, and quality assurance of the filter data are detailed in Sect. S1. We used the Mann-Kendall test (Mann, 1945; Kendall, 1975; Gilbert, 1987) to identify significant trends in the filter based measurements, and the Theil-Sen slope (Theil, 1950; Sen, 1968; Gilbert, 1987) to quantify the trends (Sect. S2).

### 2.2.2 Online measurement and source apportionment of absorption coefficients

We determined Absorption coefficients ($B_{Abs}$) using a multi-wavelength absorption photometer (AE33 Aethalometer, Magee Scientific). Here we performed source apportionment using the aethalometer

model (Sandradewi et al., 2008) to determine $eBC_{bb}$/$eBC_{ff}$. However, the aethalometer model requires *a-priori* knowledge of the aerosol Ångstrøm exponents (AAE), uncertainties which can lead to large variation in the magnitude of the resulting time series and negative concentrations during some periods. Often, the aethalometer model yields negative concentrations for any single input AAE pair. Therefore, we also used a novel PMF application (Platt et al., in prep.) finding two factors, a low AAE factor (0.9) and a higher AAE factor (2.04) identified as $eBC_{ff}$ and $eBC_{bb}$, respectively. Uncertainties were assessed using bootstrapping ($n$=2000). The advantages of the PMF are that no *a-priori* knowledge of the factor AAEs is required, no periods of negative concentration result, deviations from a strict power-law dependence of $B_{Abs}$ on wavelength (e.g. due to degradation of light absorbing components in the atmosphere or instrument errors/bias) are permitted, and poorly fitting data are assigned to a residual. Meanwhile bootstrapping allows estimation of uncertainties, the methodology of the PMF analysis and aethalometer data post-processing are detailed in Sect. S3 (Table S 2).

### 2.3 FLEXPART model simulations

We investigated the origin of the observed eBC with a Lagrangian transport model (FLEXPART v10.4, Pisso et al., 2019). The model, powered by European Centre for Medium-Range Weather Forecasts with 137 vertical layers and a horizontal resolution of 0.1°×0.1° tracks simulated particles arriving at the receptor 30 days backwards in time (retro-plume mode) and accounts for gravitational settling, dry and wet deposition (Grythe et al., 2017), turbulence (Cassiani et al., 2014), unresolved mesoscale motions (Stohl et al., 2005) and includes a deep convection scheme (Forster et al., 2007). Output consists of an emission sensitivity (0.5°×0.5° resolution), a quantitative measure for the particle mass concentration at the receptor resulting from a unit emission flux at the Earth's surface. The emission sensitivity can also be interpreted as a probability distribution field of the particle's origin, used in the present study to identify possible source regions of eBC.

### 2.4 Positive Matrix Factorization analysis on filter data

We performed PMF ME2 (Canonaco et al., 2013) (See Sect. S3 for a description of the analysis principle and S4 for its application to filter data) for samples collected in 2016-2018 (151 samples), using the following as input data: OC (in $PM_{2.5}$ and $PM_{10-2.5}$), EC (in $PM_{10}$), levoglucosan, mannosan, galactosan, arabitol, mannitol, trehalose, glucose, 2-methylerythritol, 2-methylthreitol, V, Mn, Ti, Fe, Co, Ni, Cu, Zn, As, Cd, and Pb (all in $PM_{10}$), $SO_4^{2}$, $NO_3^{-}$, $NH_4^{+}$, $Ca^{2+}$, $Mg^{2+}$, $K^{+}$, $Na^{+}$, $Cl^{-}$ (from open filter face). Table S 3 shows miscellaneous settings of the PMF analysis of these data including missing data treatment and an assessment of the PMF performance. The input data and error estimates were prepared using the procedure suggested by Polissar et al. (1998) and Norris et al. (2014), see Sect. S3.

Source apportionment by PMF is based on the temporal variability of the components. It is expected that significant contributions to carbonaceous aerosol at Birkenes is via long-range atmospheric transport (LRT), alongside more local sources. Local and LRT sources will have different

temporal variability, and significant mixing of air masses and chemical transformation is expected for the latter, i.e., factor profiles at Birkenes are expected to differ somewhat from emission profiles at the source, even though the profile is distinctive enough for source attribution. Because of this we did not attempt to constrain factor profiles via e.g. ME-2 (Canonaco et al., 2013) since Birkenes, as a relatively clean rural background site, is unlikely to receive unprocessed emissions. Furthermore, mixed contributions to a factor can in some cases be resolved *a posteriori* for source quantification (i.e. if it is clear where mass should be reassigned), without potentially perturbing the output factor time series.

*Two previous studies have used factor analysis to study PM sources at Birkenes (Aamundsen et al. (1992; Maenhaut, 2018). The present study focuses on carbonaceous aerosol, using OC, EC and highly source specific organic tracers as input in addition to inorganic species and elements used by Aamundsen et al. (1992) and Maenhaut (2018). This provides a different set of factors, based on different input, hampering any reliable comparison of these studies.*

### 2.4.1 Identification of PMF factors

The biomass burning (BB) factor appears well confined in the PMF solution (Figure 2, Table S 4), explaining all the monosaccharide anhydrides (95–98%). $OC_{BB}$ was almost exclusively (87%) in the fine fraction of $PM_{10}$. Other key qualifiers derived from the BB factor are the ratios listed in Table 1, which are highly comparable to the results obtained by $^{14}C$-analysis reported in the comprehensive study by Zotter et al. (2014). The BB factor is elevated in the heating season and peaks in winter, pointing to residential heating as the major source.

The TRA/IND factor explained most EC (50%), the majority of the trace elements Pb (84%), Zn (82%), Cd (81%), As (78%), V (70%), Ni (69%), Cu (62%) and Co (42%) and a noticeable fraction of $SO_4^{2-}$ (20%), which suggests influence of various anthropogenic emissions. TRA/IND explained a small fraction of fine OC (10%) and a negligible fraction of coarse OC (4%). The majority of OC (88%) resides in the fine fraction, which is in line with its combustion-derived origin. The high EC fraction unambiguously points to combustion processes, and the low OC/EC ratio (1.4 for $PM_{2.5}$) towards a substantial, but not exclusive, influence from vehicular traffic. Cu and Zn result from brake wear (Fomba et al., 2018), whereas tire wear is an additional source of Zn (Pacyna et al., 1986), corroborating the influence of vehicular traffic to the TRA/IND factor. Ni and V are commonly associated with combustion of heavy oil (Viana et al., 2008), As, Cd and Pb with combustion of coal, and to a lesser extent oil, but also from metallurgic activity (Pacyna et al., 1986). The TRA/IND factor has a minimum in summer and shows minor variability for the rest of the year. A similar drop in the vehicular traffic factor in summer for Helsinki was shown by Saarikoski et al. (2008).

The PMF analysis confined the majority of coarse OC (53%) and essentially all (82–93%) of the PBAP tracers (arabitol, mannitol, trehalose, and glucose) within one factor (PBAP). The PBAP factor has a pronounced seasonal variability with increased levels in the vegetative season and nearly absent outside of it, as previously described for coarse OC (Yttri et al., 2007a) and PBAP tracers (Yttri

et al., 2007b) at Birkenes.

2-methyltetrols (92–96%) are oxidation products of isoprene (Claeys et al., 2004) and are almost exclusively attributed to the $BSOA_{SRT}$ (SRT=Short Range Transport) factor, which explains 9% of fine OC and 13% of coarse OC. The complete absence of EC and the presence of $SO_4^{2-}$ (17%) underpins the secondary nature of this factor, which is present in summer with tail ends in late spring an early fall. The $BSOA_{SRT}$ time series increases abruptly in the transition May/June, as leaves unfold, and subsides equally rapid in the beginning of October when trees shed their leaves. The near absence of 2-methyltetrols prior to May/June suggests that the 0.5–1.5 months earlier onset of the vegetative season in Continental Europe (Rötzer and Chmielewski, 2001) is not reflected by the 2-methyltetrols observations at Birkenes, indicating a short atmospheric lifetime for 2-methyltetrols. Consequently, local isoprene emissions likely explain the observed concentrations of 2-methyltetrols at Birkenes, questioning to what extent the $BSOA_{SRT}$ factor includes a continental BSOA contribution. Similar sources (deciduous and coniferous trees), temperature dependent emissions, and formation rates, suggest that particulate phase oxidation products of mono- and sesquiterpenes are accounted for by the isoprene-derived $BSOA_{SRT}$-factor as well, but with a similar issue concerning local versus LRT contribution, as proposed for the 2-methyltetrols.

The MIN factor is defined by its content of Ti (93% of total), Fe (75%), Mn (52%) and $Ca^{2+}$ (39%) (Figure 2, Table S 4), well-known constituents of mineral dust (e.g. Alastuey et al., 2016). It also contains some of the elements that dominate the TRA/IND factor, including Co (43%), Cu (20%), Ni (17%) and V (14%), indicating anthropogenic influence. Notably, 31% of fine OC is attributed to the MIN factor, whereas it explains 13% of coarse OC. This corresponds to that reported by Kyllönen et al. (2020) for the Subarctic site Pallas (Finland) where 29% of the fine OC was apportioned to the mineral dust factor. Waked et al. (2014) found a similar result for Lens (France) where the mineral dust factor explained 15% of OC. No information on the size distribution was available in Kyllönen et al. (2020) and Waked et al. (2014), whereas in the present study 86% of OC in the MIN factor resides in the fine fraction of $PM_{10}$. Since mineral dust typically resides in the coarse fraction of $PM_{10}$ (Ripoll et al., 2015), one would expect the same for its carbon content, e.g. as $CaCO_3$. More efficient deposition of coarse mode mineral dust during LRT is one possible explanation but mixing of air masses is more likely, as 13% of the EC also resides in this factor. The high OC/EC ratio in the unweighted MIN factor profile (18 for $PM_{2.5}$) indicates a minor primary combustion particle influence, and the absence of levoglucosan shows that the EC content originates from fossil fuel combustion (consistent with some TRA/IND influence). Using Eq. (1), 8% of the MIN factor's fine OC content is attributed to combustion of fossil fuel OC ($OC_{PrimFF}$), whereas the corresponding percentage for $PM_{10}$ OC is 7%. If all $Ca^{2+}$ and $Mg^{2+}$ in the MIN factor was present as either Calcite ($CaCO_3$) or Dolomite $CaMg(CO_3)_2$, the $CO_3^{2-}$-carbon would account for no more than 3% of the factor's $PM_{10}$ OC content, and 22% if all reside in its coarse fraction. This shows that the OC content of the MIN factor mostly originates from other sources than mineral dust and combustion of fossil fuel. The MIN factor is most abundant in spring and early summer, as

seen by Waked et al. (2014), and is associated with southern air masses, as seen for the dry and warm period in the transition of May/June 2018 (Figure 3) when there was a pronounced peak in the MIN factor time series (Figure 2). Indeed, the mean ambient temperature was 4˚C higher in May 2018 than for May 2001–2018, whereas it was 2.4˚C higher for June 2018 than for June 2001–2018. We thus suggest that the climatological conditions that activate mineral dust sources also favour BSOA formation and that the majority of both fine (92%) and coarse fraction (78%) OC in the MIN factor is LRT BSOA ($OC_{BSOA,LRT}$).

$$OC_{Fossil,primary,MIN} = [EC_{MIN}]\ x\ \left(\frac{OC}{EC}\right)_{TRA/IND}, \left(\frac{OC}{EC}\right)_{TRA/IND} = 1.4 \qquad Eq.1$$

The majority of $NH_4^+$ (77%) and $NO_3^-$ (68%) reside in the $NH_4NO_3$ factor, which points to secondary inorganic aerosol (SIA) formation during LRT. This is supported by a noticeable contribution of $SO_4^{2-}$ (35%) to the $NH_4NO_3$ factor, as well. The factors content of $NO_2$ (30%) points towards a combustion-derived origin of $NO_3$, as does EC (13%). The factor's OC content is comparable to that seen for the BB factor. The factor is most pronounced in winter and spring.

The sea salt (SS) aerosol factor was recognized by its high $Cl^-$ (96%), $Na^+$ (87%) and $Mg^{2+}$ (79%) fractions. The $K^+/Na^+$ (0.036), $Ca^{2+}/Na^+$ (0.034) and $SO_4^{2-}/Na^+$ (0.282) ratios derived from the SS factor closely resemble these ratios in sea water (0.037, 0.038 and 0.252) (Stumm and Morgan, 1996), further demonstrating the successful separation of this factor.

## 3. Results and discussion

### 3.1 Levels and trends of carbonaceous aerosol and organic tracers

Annual mean carbonaceous aerosol concentrations at Birkenes (2001–2018) are among the lowest in Europe (Yttri et al., 2007a; Yttri et al., 2019), with OC from 0.56–1.07 µg C $m^{-3}$ for $PM_{10}$ and 0.50–0.93 µg C $m^{-3}$ for $PM_{2.5}$, and EC from 0.05–0.15 µg C $m^{-3}$ (Figure 4; Table S 4). EC, being from combustion that generates fine PM, was almost exclusively associated with $PM_{2.5}$, whereas OC was abundant also in the coarse fraction ($PM_{10-2.5}$), particularly in summer and fall (Figure 4). The correlation between OC and EC varied by season (Table S 6) and was highest in the heating season, reflecting the contribution of biogenic, non-EC sources, such as BSOA and PBAP in the vegetative season. The higher $R^2$-values for $PM_{2.5}$ compared to $PM_{10}$ can partly be attributed to PBAP, which mainly resides in $PM_{10-2.5}$.

The variability of the annual mean OC (15–22%) and EC (27%) concentrations was comparable to the major secondary inorganic aerosol (SIA) ($SO_4^{2-}$, $NO_3^-$, $NH_4^+$) and sea salt (SS) aerosol species ($Na^+$, $Mg^{2+}$, $Cl^-$) (25–31%). A difference of > 60% between consecutive years was observed for OC and EC in $PM_{10}$ and $PM_{2.5}$, whereas 160% was seen for OC in $PM_{10-2.5}$. It is important to note that despite decades of $SO_2$, $NH_3$ and $NO_x$ mitigation efforts, SIA dominates $PM_{10}$ mass (29–52%) most years, followed by carbonaceous aerosol (24–40%) and SS aerosol (10–28%) (Figure 5; Table S 7). SIA

constituents were also the largest $PM_{10}$ fraction during air pollution episodes (Table S 8), reflecting that Birkenes is affected by major SIA precursor emission regions in Continental Europe.

Levels of total carbon (TC) and PM fractions are shown in Table S 9 and Table S 10, respectively for completeness. In the following sections we discuss the OC and EC fractions separately in detail.

### 3.1.1 Organic carbon

We found no significant trend for OC in $PM_{10}$ ($OC_{PM10}$). For fine OC in $PM_{2.5}$ ($OC_{PM2.5}$) there was a minor decrease (-0.8% $yr^{-1}$), whereas there was a minor increase for coarse OC ($OC_{PM10-2.5}$) (0.8% $yr^{-1}$) (Table S 11). The anthropogenic fraction of OC observed at Birkenes likely has a downward trend as found for EC (Sect. 3.1.2), but the substantial influence of natural sources demonstrated in the present, as well as in previous, studies (Yttri et al., 2011b), explains the general lack of trends for OC.

The OC time series are characterized by two years where the annual mean was substantially higher (2006) and lower (2012) than the proceeding and the following year (Figure 4). The increased level in 2006 was most pronounced in the fine fraction and in all seasons except spring, whereas the drop in 2012 mainly was attributed to the coarse fraction and was observed in all seasons. The $OC_{PM10-2.5}$ annual mean time series is characterised by a stepwise increase from 2001 up to, and including, 2006, after which the concentration dropped and showed minor annual variability, except for the very low annual mean of 2012. After 2015, there are indications of a similar stepwise increase as seen for 2001–2006.

The $OCPM_{10-2.5}$ contribution to $OC_{PM10}$ ranged from 18–35% on an annual basis (2001 excluded due to data capture <50%), and levels were highest in summer and fall. Previous studies (Simpson et al., 2007; Yttri et al., 2011a,b) showed that BSOA largely dominates the fine carbonaceous aerosol in summer at Birkenes, whereas the present study shows that Birkenes regularly experiences major air pollution events in spring, as a result of LRT (Table S 4, Table S 7 and Table S 8). Hence, both biogenic sources and LRT explain the observed seasonality of fine OC.

We attribute elevated $OC_{PM2.5}$ in winter 2010 to residential wood burning emissions as discussed in Sect. 3.2.1. Only on five occasions did the seasonal mean of $OC_{PM2.5}$ exceed 1 µg C $m^{-3}$, four of those in the first three years of the time series. The highest mean was observed in summer 2002 (1.4 µg C $m^{-3}$) when wildfires in Eastern Europe influenced Birkenes (Yttri et al., 2007a). The four other occasions, spring (2001, 2002, 2003 and 2018), also saw prolonged episodes of PM air pollution with the hallmark of LRT; i.e., elevated $SO_4^{2-}$, $NO_3^-$ and $NH_4^+$. According to our PMF analysis (See Sect. 3.2) there are several anthropogenic and biogenic sources likely to contribute to fine OC at Birkenes, whereas coarse fraction OC is dominated by a single source, PBAP (Yttri et al., 2007 a,b; Yttri et al., 2011 a,b; Glasius et al., 2018). Hence, it is not surprising that $OC_{PM2.5}$ was the dominant OC fraction, accounting for 70–89% $OC_{PM10}$ on an annual basis.

### 3.1.2 Elemental carbon

Notably, EC levels dropped from 2007–2008, contrasting with the annual mean OC time series, (Figure 4 and Table S 5). This major downward trend of EC clearly points to changing source contributions to EC at Birkenes. We rarely observed seasonal means exceeding 0.15 µg C $m^{-3}$; only in winter 2006, 2007 and 2010, spring 2001, 2003 and 2007, and fall 2005 and 2011. Weekly samples exceeded 0.5 µg C $m^{-3}$ for three samples only, all associated with LRT.

A statistically significant reduction was calculated for EC in $PM_{10}$ (-3.9% $yr^{-1}$) and $PM_{2.5}$ (-4.2% $yr^{-1}$) (Table S 11), corresponding well with $SO_4^{2-}$ (-3.8% $yr^{-1}$) and $PM_{2.5}$ (-4.0% $yr^{-1}$). The trend for EC was most pronounced in spring and summer (-4.0 – -5.9% $yr^{-1}$) (Table S 12), as seen for $SO_4^{2-}$ (-4.2 – -6.4% $yr^{-1}$) and $PM_{2.5}$ (-3.0 – -4.4% $yr^{-1}$) (Table S 12). The EMEP model finds a somewhat lower reduction for EC (-3.0 % $yr^{-1}$) for 2001–2017 (EEA, 2020) with the largest emission reductions for the road transport (83 kt; -3.6% $yr^{-1}$) and off-road categories (44 kt; -3.7 % $yr^{-1}$) (https://www.ceip.at), which are sectors with a minor seasonal variability. We suggest that these sectors explain the downward trend observed for EC at Birkenes, and that the seasonality of the EC trend is due to the substantial contribution from less abated sources, such as domestic heating in winter and fall. Notably, modelled EC emissions are unchanged for the category other stationary combustion for 2001–2016 (-1 kt; -0.08% $yr^{-1}$) (https://www.ceip.at), which includes residential heating, and wood burning in particular.

Effective abatement of SIA precursors and fossil EC, along with a high natural source contribution to OC, largely explains why the OC fraction increased significantly for $PM_{2.5}$ (+3.2% $yr^{-1}$) and $PM_{10}$ (+2.4% $yr^{-1}$), whereas it decreased for the EC fraction (-3.9 – -4.5% $yr^{-1}$) (Table S 13). The largest increase (OC) and decrease (EC) was seen in the vegetative season (Table S 14) when BSOA and PBAP increase and the influence of poorly abated sources such as domestic heating is low. Consequently, these results demonstrate a long-term change in the aerosol chemical composition at Birkenes and thus also in the relative source composition of PM.

### 3.1.3 Levoglucosan

Levels of levoglucosan and other organic tracers are given in Table S 15, whereas other organic tracers (arabitol, mannitol, trehalose, glucose, and 2-methyltetrols) are discussed in Sect. S6.

The statistically significant decrease of levoglucosan (-2.8% $yr^{-1}$) at Birkenes for 2008–2018 (Figure 6; Table S 11), and the fact that biomass burning levels observed at Birkenes are largely explained by continental emissions (Figure 7) might indicate that wood burning emissions in continental Europe are declining. However, surprisingly, we find no significant trend for levoglucosan on a seasonal basis (Table S 12). Furthermore, and although one should be careful drawing conclusions from non-significant outcomes, it is worth noting that the levoglucosan to EC ratio most likely increased (+2.8% $yr^{-1}$ ($PM_{10}$), CI (Confidence Interval) = -3.5 – +6.5% $yr^{-1}$ and +2.3% $yr^{-1}$ ($PM_{2.5}$), CI = -2.2 – 5.0 % $yr^{-1}$) for the period 2008–2018, whereas it most likely decreased (-1.8% $yr^{-1}$ ($PM_{10}$), CI = -10.6 – +1.8 and -3.6% $yr^{-1}$ ($PM_{2.5}$), CI = -9.8 – +1.3% $yr^{-1}$) for the levoglucosan to OC ratio (Table S 13). A more efficient abatement of fossil sources than biomass burning would explain the levoglucosan to EC

increase, whereas we fail to see a similar trend for the levoglucosan to OC ratio, as prevailing natural sources mask the assumed reduction in fossil OC of anthropogenic origin.

The levoglucosan time-series provides a hitherto unprecedented opportunity to validate European residential wood burning emission inventories at a decadal time basis. Unfortunately, the inventories suffer from non-harmonized emission reporting and lack of condensable organics (van der Gon et al., 2015, Simpson et al., 2019), which hampers any reliable attempt for such validation. Given the uncertainties in the trend calculations (i.e. annual vs. seasonal trends), more work is needed to investigate trends in levoglucosan and biomass burning, foremost by continuation of the actual time series. Such efforts should be initiated immediately given the numerous studies that point to residential wood burning as a major source of air pollution in Europe (e.g. Denier van der Gon et al., 2015; Yttri et al., 2019).

### 3.2 Sources of carbonaceous aerosol at Birkenes

We used PMF to apportion carbonaceous aerosol at Birkenes for 2016–2018. The time period was restricted by organic tracer data availability. Carbonaceous aerosol annual means for 2016–2018 were within the long-term annual mean (±SD) for OC, and only slightly lower for EC in 2016 and 2017 and are thus representative of the longer time series. Six out of seven factors identified in contribution-weighted relative profiles from PMF (Figure 2; Table S 4) were associated with significant amounts of carbonaceous aerosol. This includes factors for mineral dust-dominated (MIN), which OC content is associated mainly with LRT BSOA ($BSOA_{LRT}$), traffic/industrial-like (TRA/IND), biogenic secondary organic aerosol ($BSOA_{SRT}$), which is short-range transported, primary biological aerosol particles (PBAP), biomass burning (BB), and ammonium nitrate dominated ($NH_4NO_3$). The sea salt aerosol factor (SS) had a negligible (<1%) carbonaceous aerosol content.

The MIN factor (31%) explained the largest fraction of fine OC, whereas BB (17%), $NH_4NO_3$ (17%) and PBAP (16%) had almost equally large shares, as did TRA/IND (10%) and $BSOA_{SRT}$ (9%) (Figure 8). Coarse OC was by far most abundant in the PBAP factor (53%), whereas $BSOA_{SRT}$ (13%), MIN (13%) and $NH_4NO_3$ (12%) explained almost equally large shares. For the other factors, coarse OC was minor. EC was apportioned to only five factors of which TRA/IND (50%) dominated by far. BB made a 21% contribution and MIN and $NH_4NO_3$ equally large shares (13%). The 3% apportioned to PBAP is an assumed analytical artefact (See Sect. 3.2.2 for details).

The BB, $NH_4NO_3$ and TRA/IND factors are considered entirely anthropogenic, $BSOA_{SRT}$ and PBAP exclusively natural, whereas MIN is mixed (Figure 8). Natural (54%) and anthropogenic (46%) sources contributed almost equally to fine OC (Figure 8) annually, so also in spring and fall (51% natural), whereas natural sources prevailed in summer (77%) and anthropogenic in winter (78%). Natural sources dominated coarse OC annually (78%) and in all seasons (70–91%), except winter (37%). We consider the minor fraction of coarse OC attributed to carbonate-carbon (3%) to be of natural origin. The findings for OC in $PM_{10}$ are rather like that of $PM_{2.5}$, only that the natural contribution is somewhat

more pronounced due to the influence from a mostly naturally influenced coarse OC fraction.

### 3.2.1 Anthropogenic carbonaceous aerosol sources

According to PMF, BB accounted for 14–17% of OC annually, considering both $PM_{2.5}$ and $PM_{10}$ vs. only 6% of coarse OC. BB was by far the major contributor to OC in winter (35–37%) and by far the most minor contributor in summer (2–3%) (not considering SS). Spring and fall are transition seasons where BB still made a substantial 14–19% contribution to OC. BB explained 22% of EC annually (excluding $EC_{PBAP}$, which we assume is an analytical artefact, see Sect. 3.2.2), hence fossil fuel combustion (78%) was the major source. Emissions from residential wood burning increased in the heating season but fossil fuel sources dominated EC even in winter (66%). It cannot be excluded that part of levoglucosan originates from wildfires in summer, spring, and fall, though this itself may be due to anthropogenic activity. However, the levoglucosan/mannosan (L/M) ratio indicates minor variability in the source composition throughout the year (See Sect. S5), suggesting one dominating source.
The 78%:22% split of EC into fossil fuel combustion and biomass burning derived from PMF is supported by high time resolved concentrations of $eBC_{BB}$ and $eBC_{FF}$ derived from multiwavelength aethalometer measurements of the absorption coefficient, following the PMF-approach of Platt et al. (in prep.). With this approach we find $eBC_{BB}/eBC_{TOT}$=28% (Table 2). Meanwhile, using the aethalometer model and $AAE_{FF}$=0.9 and $AAE_{BB}$=1.68 (Zotter et al. 2017) as input we find $eBC_{BB}/eBC_{TOT}$=48%, however the aethalometer model is extremely sensitive to the input AAE and the AAE values suggested by Zotter et al. (2017) are only recommended where no *a priori* information on the AAEs is available and a significant advantage of the PMF approach by Platt et al. (in prep.) is that the AAE is an output.

Source regions of elevated (70$^{th}$ percentile) and low (30$^{th}$) winter and summertime $eBC_{BB}$ (and $eBC_{FF}$) observed at Birkenes for 2018 were studied using the approach of Hirdman et al. (2010). The results show that Birkenes is a receptor of LRT exclusively from Continental Europe for elevated $eBC_{BB}$ and $eBC_{FF}$ levels (Figure 7), both in summer and winter. This is consistent with a lack of diurnal variation in either $eBC_{BB}$ or $eBC_{FF}$, likely because there are few local sources at Birkenes. The main source regions extend from the Atlantic coast in the west to the Ural Mountains in winter, whereas the regions in summer are confined to Eastern Europe and western Russia (but not as far east as the Urals). Notably, the Nordic countries do not contribute to elevated levels except for southern parts of Finland in summer. The footprints are almost identical for $eBC_{BB}$ and $eBC_{FF}$ both for summer and winter. High similarity in winter is not a surprise, as the footprint covers such a wide area and because wood burning for residential heating is common in several European countries. The summertime footprint is a subsection of the wintertime footprint that covers an area well-known for severe wildfires and agricultural fires (Stohl et al., 2007 and Yttri et al., 2007a), and thus agrees with previous studies. Further, Sciare et al. (2008) point to the European countries bordering the Black Sea as having high

carbonaceous aerosol of fossil origin. Low $eBC_{BB}$ and $eBC_{FF}$ levels at Birkenes are consistent with air masses that have an oceanic or terrestrial origin at high latitudes, mainly from the Arctic. Notably, the 30% highest values explain 74% of $eBC_{BB}$ at Birkenes for the actual period, hence LRT is decisive not only for episodes of high concentrations but also largely explains the mean concentration. All $eBC_{BB}$ and $eBC_{FF}$ observations included in the 70$^{th}$ percentile was made in winter despite the less pronounced seasonality of $eBC_{FF}$ compared to $eBC_{BB}$.

To generate a longer BB time series of $OC_{BB}$ and $EC_{BB}$ we combine the levoglucosan time series (2008–2018) with levoglucosan/OC and levoglucosan/EC ratios derived from the BB factor of the PMF analysis (Table 1; See Sect. S 5 for details). Depletion of levoglucosan by OH oxidation is more likely in summer (Hoffmann et al., 2010; Yttri et al., 2014), still we assume that levels mostly reflect biomass burning emissions in all seasons.

$EC_{BB}$ levels were elevated in the heating season (Figure 9; Table S 16). A strong temperature influence is illustrated by a 9°C difference in the 25$^{th}$ percentile of wintertime temperatures in 2015 (-0.3°C) and 2010 (-9.3°C) (Figure S 1), which experienced the lowest (19 ng m$^{-3}$) and the highest (84 ng m$^{-3}$) winter-time mean concentration of $EC_{BB}$, respectively. Winter 2010 was exceptionally cold due to a negative North Atlantic Oscillation, and the only occasion when $EC_{BB}$ exceeded $EC_{FF}$, with annual mean $EC_{BB}$>60% higher than the long-term mean. Pronounced interannual variability was seen for the wood burning contribution in winter, from 21–60% to EC, with the lowest fractions occasionally matched by those in spring and fall, typically ranging between 20–30%. $EC_{BB}$/EC was small in summer (4–15%), considerably less than other seasons, except in 2008, where we calculate a substantial 30–40% contribution. Levoglucosan cannot be used to differentiate emissions from residential wood burning, wildfires and agricultural fires; exceptions are major wildfire and agricultural fire episodes identifiable by unusual high concentrations and traced by source receptor models/satellite data for plumes/burnt areas (Yttri et al., 2007a, Stohl et al., 2007). Influence from major wildfires in Eastern Europe caused a summertime peak in fine OC and EC in 2002 at Birkenes (Yttri et al., 2007a). In June 2008, the largest wildfire in Norway since the Second World War raged 25 km northeast of the Birkenes Observatory, with an area of 30 km$^2$ burnt. The observatory was downwind of the fire on only one day, according to FLEXPART (Figure S 2). Despite this, the levoglucosan concentration for the weekly filter sample was 153 ng m$^{-3}$, by far the highest in one decade of sampling. Notably, the annual mean concentration of levoglucosan for 2008 increased by nearly 35% and $EC_{bb}$ contributed significantly to EC for summer 2008.

The seasonality of $OC_{BB}$ (Figure 9) was like $EC_{bb}$. Mean wintertime $OC_{BB}$/OC was 39–40% and >50% in 2010 and 2012, considering both $PM_{10}$ and $PM_{2.5}$. The summertime contribution was typically <5%, reflecting both low levoglucosan levels and major influences from BSOA and PBAP, which peak in summer. Notably, five of the seven highest weekly OC concentrations for the $PM_{10}$ time-series were attributed to emissions from major wildfires in Eastern Europe, i.e., August 2002, and May/September 2006, and thus prior to the initiation of the levoglucosan time series. The local wildfire episode in

summer 2008 caused a substantial increase in $OC_{bb}$/OC (13–18%), which is within the lower range of that observed for spring (12–27%) and fall (13–39%).

### 3.2.2 Biogenic carbonaceous aerosol sources

The general lack of PBAP tracers in the MIN (<1%) and SS (<2%) factors and no sea salt and Ti in the PBAP factor, implies that soil and sea spray aerosol do not contribute to PBAP at Birkenes, although this has been shown elsewhere (O'Dowd et al., 2004; Jia and Fraser, 2011). PBAP represented by glucose, arabitol and mannitol appears to be associated with leaves rather than soil material and to be a source of local origin (Samaké et al., 2019). However, even large PBAP, such as birch pollen (avg. diam. 22 µm), has a potential for long range atmospheric transport of 1000 km due to its low density, hydrophobic nature, release during favourable dispersion conditions, and (often) emission height > 10 m (e.g. Sofiev et al., 2006; Skjøth et al., 2007).

The PBAP factor concentration was nearly one order of magnitude higher in summer and fall than in winter and was the major contributor to coarse OC for all seasons except winter, particularly in summer (54%) and fall (69%) (Figure 8). These are conservative estimates, as 3–9% of the PBAP tracers reside in the $BSOA_{SRT}$ factor, likely due to co-variability, as there is no scientific evidence linking biologically formed sugars and sugar-alcohols to abiotic formation of BSOA. Notably, the PBAP factor explained 20–26% of fine OC in summer and fall, being the major contributor in fall. Consequently, PBAP was the major contributor to OC even in $PM_{10}$ in summer (31%) and fall (40%). The PBAP factor even explained 16% of fine OC (Figure 8) annually, corresponding to 0.084 µg C $m^{-3}$, which is marginally lower than the factor's content of coarse OC (0.113 µg C $m^{-3}$). Combined, this made PBAP the most abundant contributor to OC in $PM_{10}$ along with the MIN factor (both 26%). Some PBAP tracers partly reside in the fine mode (Carvalho et al., 2003; Yttri et al., 2007b) but the 43% $OC_{PBAP}$ found in the fine fraction in the present study is higher than what has previously been reported for the actual PBAP tracers at Birkenes; i.e. 6–7% (arabitol and mannitol), 20% (trehalose), and 33% (glucose) (Yttri et al., 2007b). It cannot be excluded that the PBAP factor contains some fine OC from other sources e.g. due to condensation, but although there is a seasonal co-variability with the $BSOA_{SRT}$ factor, only 2–3% of the 2-methyltetrols were explained by the PBAP factor and there was a low correlation between the PBAP and the $BSOA_{SRT}$, which questions this hypothesis.

Arabitol and mannitol are well-known tracers of fungal spores (Bauer et al., 2008), one of the most abundant sources of PBAP (Elbert et al., 2007). Applying an OC to mannitol ratio of 5.2–10.8 for fungal spores (Bauer et al., 2008; Yttri et al., 2011a), we estimate that 11–22% of $OC_{PBAP}$ (in $PM_{10}$) comes from this source. Glucose is one of the primary molecular energy sources for plants and animals, a building block of natural dimers and polymers (e.g. sucrose and cellulose), and thus ubiquitous in nature and considered a PBAP tracer of general character, and clearly important for allocation of carbon mass to PBAP. Nevertheless, a wider range of organic tracers ought to be tested in future PMF studies to explore the potential of further separation of the highly heterogenic PBAP source, including cellulose,

but also amino acids. A greater diversity of PBAP tracers may also provide a more correct PBAP estimate. The PMF approach used in the present study gives a somewhat higher, but overlapping, estimate of $OC_{PBAP}$ at Birkenes for August 2016–2018 than Latin Hypercube sampling (LHS) for August 2009 (Yttri et al., 2011b) (Table 3). The LHS approach was based on *a priori* emission ratios, with uncertainty ranges estimated in a similar way to a Monte Carlo analysis (though less computationally extensive), and considered only the sum of fungal spores and plant debris as $OC_{PBAP}$, based on mannitol (fungal spores) and cellulose (plant debris), whereas the PMF approach may pick other contributing, i.e. co-varying, sources.

The 3% EC in the PBAP factor is substantially less than the 16% reported by Waked et al. (2014), which stated that atmospheric mixing, PMF limitations and artifacts caused by thermal-optical analysis could be plausible explanations. In the present study, low levels of coarse fraction EC occasionally appear in summer and fall (Table S 5), following the seasonality of PBAP. This finding does not exclude any of the three possibilities proposed by Waked et al., (2014), but supports the suggestion by Dusek et al. (2017) that PBAP, or at least some types of PBAP, chars and evolves as modern carbon EC during thermal-optical analysis. If $EC_{PBAP}$ indeed is an analytical artefact, then constraining the PBAP factor to contain no EC, as suggested by Weber et al. (2019), should be done with caution, as it will wrongfully apportion pyrolytic carbon generated from PBAP as EC to another source. Thus, $EC_{PBAP}$ should rather be interpreted as $OC_{PBAP}$. With no $EC_{SS}$, no $EC_{BSOA,SRT}$ and $EC_{PBAP}$ an assumed analytical artefact, EC can be apportioned into a fossil fuel category ($EC_{FF}$), consisting of the MIN, TRA/IND, and $NH_4NO_3$ factors (explains 0.2% of levoglucosan), and a non-fossil biomass burning category ($EC_{BB}$), the BB factor. Some EC has been reported from meat cooking (Rogge et al., 1991), which is a non-fossil source, but its influence is minor at Birkenes, as it has not been observed based on concurrent ACSM-measurements and is not accounted for by levoglucosan.

Our PMF results support the use of $OC_{PM10-2.5}$ as a proxy of $OC_{PBAP}$, which has a pronounced seasonality (Figure 4) with the highest seasonal mean concentration observed in summer for 15 of the studied years and in fall for the three others (Table S 5). The seasonal mean exceeded 0.5 µg C $m^{-3}$ on two occasions only; fall 2005 and fall 2006. With a few exceptions, $OC_{PM10-2.5}$ contributed more than 30% to $OC_{PM10}$ in summer and fall. The highest relative contribution (45–50%) to $OC_{PM10}$ were exclusively observed in fall (2004, 2005, 2006, 2008, 2014, 2017), likely reflecting a combination of high $OC_{PM10-2.5}$ concentrations and fine fraction $OC_{BSOA}$ declining at this time of the year. $OC_{PM10-2.5}$ made a substantially lower contribution to $OC_{PM10}$ in winter (mean: 13%) and in spring (mean: 19%) compared to summer and fall, although contributions exceeding 25% were observed in spring for certain years. Notably however, the PBAP factor explains 16% of fine OC, which would not be accounted for using coarse OC as a proxy of $OC_{PBAP}$.

These numbers suggest that PBAP is a major, continuous contributor to OC in $PM_{10}$ at Birkenes for a period of nearly two decades, and that it largely explains the seasonality. Estimates of PBAP levels in the continental European rural background environment are largely lacking and should be undertaken

to explore PBAPs potential importance. With a longer vegetative season and a different climate, the PBAP flux might be larger in more southerly countries, although the relative contribution might be lower due higher overall OC levels. Waked et al. (2014) found that $OC_{PBAP}$ accounted for 17% of OC in $PM_{10}$ on an annual basis for an urban background site in Lens (Northern France), and between 5–6% in winter/spring and 27–37% in summer/fall using PMF for source apportionment. These fractions are comparable to those observed in the present study, albeit concentrations calculated by Waked et al. (2014) were higher.

PBAP is a large OC source not included in many models. OC model closure, both for overall levels and seasonality, would thus likely be improved in many cases by its inclusion. This appears to be particularly important for regions with low anthropogenic influence. Birkenes is situated in the Boreo-nemorale zone, a transition zone of the Nemorale and the Boreal zone, hence, findings made for this site likely gives an indication of what can be expected for this scarcely populated, circumpolar region, which by far is the largest terrestrial biome of the Northern Hemisphere. Hence, measurements in unperturbed areas should include PBAP for a better understanding of background conditions. In turn, such measurements may improve e.g. climate models; i.e., the aerosol climate effect under relatively clean conditions.

Modelled estimates suggest a 10–40% contribution of BSOA to fine OC annually at Birkenes (Simpson et al., 2007; Bergström et al., 2012). Hence, the 9% contribution of $OC_{BSOA,SRT}$ to fine OC, and the 13% contribution to coarse OC (10% to OC in $PM_{10}$) found in the present study by PMF, appears to be in the lower range. Further, 3–9% of the PBAP tracers reside in the $BSOA_{SRT}$ factor, hence some of its OC content may rather be attributed to PBAP, further lowering the OC content of the $BSOA_{SRT}$ factor but strengthening coarse OC as a proxy of PBAP. $BSOA_{SRT}$ made a negligible contribution to fine, coarse and $PM_{10}$ OC in all seasons, except in summer (22–25%), apparently contradicting previous studies that unambiguously point to BSOA as the major carbonaceous aerosol source at Birkenes in the vegetative season (Simpson et al., 2007; Yttri et al., 2011b). Note that a prevailing BSOA source in summer is considered a normal situation also for European rural background environment in general (e.g. Gelenscer et al., 2007), not only for Birkenes. Table 3 shows that $OC_{BSOA,SRT}$ obtained by PMF for August 2016–2018 is substantially lower than that obtained by LHS for August 2009 (Yttri et al., 2011b). Although not obtained for the same year, we argue that methodology rather than climatology explains most of the difference. $OC_{BSOA,LHS}$ provides an upper estimate including all modern carbon, local and from LRT (excluding biomass burning and PBAP fungal spores and plant debris), whereas $OC_{BSOA,SRT}$ gives a lower estimate accounting for locally formed BSOA.

It is less likely that anthropogenic secondary organic aerosol (ASOA) resides in the $BSOA_{SRT}$-factor, as ASOA precursors result from combustion processes and evaporative losses. Further, Yttri et al. (2011a) found higher ASOA concentrations in the Norwegian rural background environment in winter compared to summer, which is opposite of $BSOA_{SRT}$, hence co-variation and/or apportionment to the same factor do not appear likely. ASOA is less abundant than BSOA at Birkenes, as calculated

by Simpson et al. (2007) and Bergström et al. (2012), but the estimates vary substantially and are very uncertain (Spracklen et al., 2011), particularly for ASOA (from 1% to 10–20%). It is difficult to predict which PMF factor(s) accounted for ASOA, but for the sake of separating OC into a natural and an anthropogenic fraction we assume that ASOA is not part of neither $BSOA_{SRT}$ nor the PBAP factor, which we consider as exclusively natural factors. To provide an upper estimate of the natural sources (Figure 8), we neither consider it part of the MIN factor.

With 90% (in $PM_{10}$) and 92% (in $PM_{2.5}$) of the MIN factor's OC content attributed to LRT BSOA ($OC_{BSOA,LRT}$) (See Sect. 2.4.1), the combined contribution of locally formed BSOA ($OC_{BSOA,SRT}$) and $OC_{BSOA,LRT}$ to OC in $PM_{10}$ and $PM_{2.5}$ would be 34–38% on an annual basis, 37–41% in spring and 50–57% in summer. From this we can deduct that 1/3 of BSOA is of local origin, whereas 2/3 are long-range transported. For August 2016–2018, the joint contribution of $OC_{BSOA,SRT}$ and $OC_{BSOA,LRT}$ to OC in $PM_{10}$ is 31%, corresponding better with the LHS estimate (Table 3) but still noticeably lower. Notably, $OC_{BSOA,SRT}$, $OC_{BSOA,LRT}$ and $OC_{PBAP}$ combined contributed 79% to OC in $PM_{10}$ in August 2016–2018, which exactly matches the sum of $OC_{BSOA,LHS}$ and $OC_{PBAP,LHS}$ to OC in $PM_{10}$ in August 2009. This suggests that LHS and PMF apportion an equally large amount of OC to natural sources but that the split between BSOA and PBAP likely differs. It is evident that the LHS-approach provides an upper estimate of BSOA (Gelenscer et al., 2007; Yttri et al. 2011a), whereas the great diversity of PBAP likely is underestimated by just accounting for plant debris and fungal spores. The lower estimate of $OC_{BSOA}$ and the higher estimate of $OC_{PBAP}$ provided by PMF in the present study is in line with this and encourage further effort to apportion these major carbonaceous aerosol sources correctly. Inclusion of monoterpene and sesquiterpene oxidation products (Kleindienst et al., 2007) to PMF would possibly improve our understanding of the SOA apportionment, as would knowledge about their atmospheric lifetime.

## 4. Conclusions

The carbonaceous aerosol time-series at the Birkenes Observatory initiated in 2001 is unique due to its unprecedented length in Europe and because measurements are performed both for $PM_{10}$ and $PM_{2.5}$. Such long-time series are of utmost importance, e.g. for the evaluation of projections, air-quality models, and climate models. The need for concurrent and diverse off-line and on-line carbonaceous aerosol speciation measurements for understanding of carbonaceous aerosol sources, seasonal, annual, and long-term variability has been utterly demonstrated.

Statistically significant and comparably large reductions (~ -4% $yr^{-1}$) were calculated for EC and $PM_{2.5}$ at the Birkenes Observatory for 2001–2018, with EC reductions largely attributed to road transportation. No significant declining trend was calculated for OC, likely because prevailing natural sources masked any reduction in anthropogenic sources. Further reduction of carbonaceous aerosol may be hampered by poorly abated sources such as domestic heating, though more work is needed to assess this. We emphasize the importance of establishing long lasting, high quality carbonaceous aerosol and

organic tracers time series at several sites across Europe for this purpose. The OC fraction of $PM_{10}$ (+2.3% $yr^{-1}$) and $PM_{2.5}$ (+3.2% $yr^{-1}$) increased significantly from 2001–2018, whereas the EC fraction decreased (-4.0 – -4.7% $yr^{-1}$), causing a successive change in the aerosol chemical composition and in the relative source composition.

Source apportionment using PMF identified seven factors, six of which were carbonaceous dominated: Mineral dust dominated (MIN), traffic/industrial-like (TRA/IND), biogenic secondary organic aerosol (BSOA), primary biological aerosol particles (PBAP), biomass burning (BB) and ammonium nitrate dominated ($NH_4NO_3$). Carbonaceous material was negligible in the sea salt (SS) factor. Combustion of fossil fuel (78%) was the major source of EC and TRA/IND (50%) the key factor. Emissions from residential wood burning increased in the heating season but fossil fuel sources dominated EC even in winter (66%). Continental Europe and western parts of Russia were the main source regions of elevated levels of eBC, both for biomass burning and for combustion of fossil fuels. Natural sources dominated both fine (53%) and coarse (78%) fraction OC, thus also OC in $PM_{10}$ (60%). The natural fraction increased substantially in the vegetative season due to biogenic secondary organic aerosol and primary biological aerosol particles, confined to the BSOA, PBAP and MIN factors. 77–91% of OC was attributed to natural sources in summer and 22–37% in winter. The coarse fraction showed the highest share of natural sources regardless of season and was dominated by PBAP, except in winter. Notably, PBAP (26%) made a larger contribution to OC in $PM_{10}$ than BB (14%), and an equally large contribution as BB (17%) in $PM_{2.5}$.

## Author contribution

Conceptualization, Methodology and Writing – Original draft, Visualization: **Wenche Aas, Stephen M. Platt, Xin Wan, Karl Espen Yttri;** Data Curation: **Markus Fiebig, Hans Gundersen, Anne-Gunn Hjellbrekke, Hilde Uggerud, Marit Vadset, Karl Espen Yttri,;** Formal Analysis: **Stephen M. Platt, Sverre Solberg, Xin Wan, Karl Espen Yttri;** Funding acquisition: **Wenche Aas; Kjetil Tørseth;** Resources: **Jason Surratt**; Software: **Francesco Canonaco, Sabine Eckhardt, Nikolaos Evangeliou, Stephen M. Platt, André S. H. Prévôt**; Writing, review and editing: **Wenche Aas, Francesco Canonaco, Sabine Eckhardt, Nikolaos Evangeliou, Markus Fiebig, Hans Gundersen, Anne-Gunn Hjellbrekke, Cathrine Lund Myhre, Stephen M. Platt, André S. H. Prévôt, David Simpson, Sverre Solberg, Jason Surratt, Kjetil Tørseth, Hilde Uggerud, Marit Vadset, Xin Wan**, **Karl Espen Yttri**

## Acknowledgements

Time series used in the present study, except for the organic tracers, were obtained as part of the Norwegian national monitoring program (Aas et al., 2020). The monosaccharide anhydrides, the sugar-alcohols and the 2-methyltetrols (organic tracers) time series were funded by the Norwegian Research Council through the Strategic Institute Projects "*Observation and Modelling Capacities for Northern and Polar Climate and Pollution"* and the "*Studying sources, formation and transport of short-lived*

*climate forcers by advanced high-time resolution measurements".* All data are reported to the EMEP monitoring programme (Tørseth et al., 2012) and are available from the database infrastructure EBAS (http://ebas.nilu.no/) hosted at NILU.

The research leading to these results has benefited from Aerosols, Clouds, and Trace gases Research InfraStructure (ACTRIS), funding from the European Union Seventh Framework Programme (FP7/2007–2013) under ACTRIS-2 and the grant agreement no. 262254, and the COST Action CA16109, Chemical On-Line cOmpoSition and Source Apportionment of fine aerosol-COLOSSAL; i.e., for participation in interlaboratory comparison for thermal-optical analysis and QA/QC of measurements.

OC/EC and mass concentration were measured as part of the Norwegian national monitoring programme (Aas et al., 2020), whereas monosaccharide anhydrides were analysed as part of the SACC (Strategic Aerosol Observation and Modelling Capacities for Northern and Polar Climate and Pollution) and SLCF (Describing sources, formation, and transport of short lived climate forcers using advanced, novel measurement techniques) projects.

**References**

Aas, W., Eckhardt, S., Fiebig, M., Solberg, S., and Yttri, K. E.: Monitoring of long-range transported air pollutants in Norway, annual report 2019. Kjeller, NILU (Miljødirektoratet rapport, M-1710/2020) (NILU OR, 4/2020), 2020.

Alastuey, A., Querol, X., Aas, W., Lucarelli, F., Perez, N., Moreno, T., Cavalli, F., Areskoug, H., Balan, V., Catrambone, M., Ceburnis, D., Cerro, J. C., Conil, S., Gevorgyan, L., Hueglin, C., Imre, K., Jaffrezo, J.-L., Leeson, S. R., Mihalopoulos, N., Mitosinkova, M., O'Dowd, C. D., Pey, J., Putaud, J.-P., Riffault, V., Ripoll, A., Sciare, J., Sellegri, K., Spindler, G., and Yttri, K. E.: Geochemistry of $PM_{10}$ over Europe during the EMEP intensive measurement periods in summer 2012 and winter 2013, Atmos. Chem. Phys., 16, 6107-6129, 10.5194/acp-16-6107-2016, 2016.

Amundsen, C. E., Hanssen, J. E., Semb, A., and Steinnes, E.: Long-range atmospheric transport of trace elements to Southern Norway, Atmos. Environ., Part a-General Topics, 26, 1309-1324, 10.1016/0960-1686(92)90391-w, 1992.

Bauer, H., Claeys, M., Vermeylen, R., Schueller, E., Weinke, G., Berger, A., and Puxbaum, H.: Arabitol and mannitol as tracers for the quantification of airborne fungal spores, Atmos. Environ, 42, 588-593, 10.1016/j.atmosenv.2007.10.013, 2008.

Bauer, H., Kasper-Giebl, A., Loflund, M., Giebl, H., Hitzenberger, R., Zibuschka, F., and Puxbaum, H.: The contribution of bacteria and fungal spores to the organic carbon content of cloud water, precipitation and aerosols, Atmos. Res., 64, 109-119, 10.1016/s0169-8095(02)00084-4, 2002.

737 Bergstrom, R., van der Gon, H. A. C. D., Prevot, A. S. H., Yttri, K. E., and Simpson, D.: Modelling of
738 organic aerosols over Europe (2002-2007) using a volatility basis set (VBS) framework: application of
739 different assumptions regarding the formation of secondary organic aerosol, Atmos. Chem. Phys., 12,
740 8499-8527, 10.5194/acp-12-8499-2012, 2012.

741 Bond, T. C., Doherty, S. J., Fahey, D. W., Forster, P. M., Berntsen, T., DeAngelo, B. J., Flanner, M. G.,
742 Ghan, S., Karcher, B., Koch, D., Kinne, S., Kondo, Y., Quinn, P. K., Sarofim, M. C., Schultz, M. G.,
743 Schulz, M., Venkataraman, C., Zhang, H., Zhang, S., Bellouin, N., Guttikunda, S. K., Hopke, P. K.,
744 Jacobson, M. Z., Kaiser, J. W., Klimont, Z., Lohmann, U., Schwarz, J. P., Shindell, D., Storelvmo, T.,
745 Warren, S. G., and Zender, C. S.: Bounding the role of black carbon in the climate system: A scientific
746 assessment, J. Geophys. Res.-Atmos., 118, 5380-5552, 10.1002/jgrd.50171, 2013.

747 Boucher, O., Randall, D., Artaxo, P., Bretherton, C., Feingold, G., Forster, P., Kerminen, V.-M.,
748 Kondo, Y., Liao, H., Lohmann, U., Rasch, P., Satheesh, S. K., Sherwood, S., Stevens, B., and Zhang,
749 X.Y.: Clouds and Aerosols. In: Climate Change 2013: The Physical Science Basis. Contribution of
750 Working Group I to the Fifth Assessment Report of the Intergovernmental Panel on Climate Change
751 [Stocker, T.F., Qin, D., Plattner, G. K., Tignor, M., Allen, S. K., Boschung, J., Nauels, A., Xia, Y.,
752 Bex, V., and Midgley, P. M. (eds.)]: Cambridge University Press, Cambridge, United Kingdom and
753 New York, NY, USA, 2013.

754 Bougiatioti, A., Stavroulas, I., Kostenidou, E., Zarmpas, P., Theodosi, C., Kouvarakis, G., Canonaco,
755 F., Prevot, A. S. H., Nenes, A., Pandis, S. N., and Mihalopoulos, N.: Processing of biomass-burning
756 aerosol in the eastern Mediterranean during summertime, Atmos. Chem. Phys., 14, 4793-4807,
757 10.5194/acp-14-4793-2014, 2014.

758 Canonaco, F., Crippa, M., Slowik, J. G., Baltensperger, U., and Prevot, A. S. H.: SoFi, an IGOR-based
759 interface for the efficient use of the generalized multilinear engine (ME-2) for the source apportionment:
760 ME-2 application to aerosol mass spectrometer data, Atmos. Meas. Tech., 6, 3649-3661, 10.5194/amt-
761 6-3649-2013, 2013.

762 Carvalho, A., Pio, C., and Santos, C.: Water-soluble hydroxylated organic compounds in German and
763 Finnish aerosols, Atmos. Environ., 37, 1775-1783, 10.1016/s1352-2310(03)00066-9, 2003.

764 Cassiani, M., Stohl, A., and Brioude, J.: Lagrangian Stochastic Modelling of Dispersion in the
765 Convective Boundary Layer with Skewed Turbulence Conditions and a Vertical Density Gradient:
766 Formulation and Implementation in the FLEXPART Model, Bound-Lay Meteorol, 154, 367-390,
767 10.1007/s10546-014-9976-5, 2015.

768 Cavalli, F., Viana, M., Yttri, K. E., Genberg, J., and Putaud, J.-P.: Toward a standardised thermal-optical
769 protocol for measuring atmospheric organic and elemental carbon: the EUSAAR protocol, Atmos.
770 Meas. Tech., 3, 79-89, 2010.

771 Cavalli, C., Putaud, J.P., Yttri, K.E. Availability and quality of the EC and OC measurements within
772 EMEP, including results of the fourth interlaboratory comparison of analytical methods for
773 carbonaceous particulate matter within EMEP (2011). EMEP/CCC-Report 1/2013.

774 Claeys, M., Graham, B., Vas, G., Wang, W., Vermeylen, R., Pashynska, V., Cafmeyer, J., Guyon, P.,
775 Andreae, M. O., Artaxo, P., and Maenhaut, W.: Formation of secondary organic aerosols through
776 photooxidation of isoprene, Science., 303, 1173-1176, 10.1126/science.1092805, 2004.

777 Crippa, M., Canonaco, F., Lanz, V. A., Aijala, M., Allan, J. D., Carbone, S., Capes, G., Ceburnis, D.,
778 Dall'Osto, M., Day, D. A., DeCarlo, P. F., Ehn, M., Eriksson, A., Freney, E., Hildebrandt Ruiz, L.,
779 Hillamo, R., Jimenez, J. L., Junninen, H., Kiendler-Scharr, A., Kortelainen, A. M., Kulmala, M.,
780 Laaksonen, A., Mensah, A., Mohr, C., Nemitz, E., O'Dowd, C., Ovadnevaite, J., Pandis, S. N., Petaja,
781 T., Poulain, L., Saarikoski, S., Sellegri, K., Swietlicki, E., Tiitta, P., Worsnop, D. R., Baltensperger, U.,
782 and Prevot, A. S. H.: Organic aerosol components derived from 25 AMS data sets across Europe using
783 a consistent ME-2 based source apportionment approach, Atmos. Chem. Phys., 14, 6159-6176,
784 10.5194/acp-14-6159-2014, 2014.

785 Donahue, N. M., Robinson, A. L., and Pandis, S. N.: Atmospheric organic particulate matter: From
786 smoke to secondary organic aerosol, Atmos. Environ., 43, 94-106, 10.1016/j.atmosenv.2008.09.055,
787 2009.

788 Dusek, U., Hitzenberger, R., Kasper-Giebl, A., Kistler, M., Meijer, H. A. J., Szidat, S., Wacker, L.,
789 Holzinger, R., and Rockmann, T.: Sources and formation mechanisms of carbonaceous aerosol at a
790 regional background site in the Netherlands: insights from a year-long radiocarbon study, Atmos. Chem.
791 Phys., 17, 3233-3251, 10.5194/acp-17-3233-2017, 2017.

792 Dye, C. and Yttri, K.: Determination of monosaccharide anhydrides in atmospheric aerosols by use of
793 high-performance liquid chromatography combined with high-resolution mass spectrometry, Anal.
794 Chem., 77, 1853-1858, 10.1021/ac049461j, 2005.

795 EEA, 2021: Long term air quality measurements trends in Europe. In prep.

796 Elbert, W., Taylor, P. E., Andreae, M. O., and Poschl, U.: Contribution of fungi to primary biogenic
797 aerosols in the atmosphere: wet and dry discharged spores, carbohydrates, and inorganic ions, Atmos.
798 Chem. Phys., 7, 4569-4588, 10.5194/acp-7-4569-2007, 2007.

799 Fomba, K. W., van Pinxteren, D., Muller, K., Spindler, G., and Herrmann, H.: Assessment of trace metal
800 levels in size-resolved particulate matter in the area of Leipzig, Atmos. Environ., 176, 60-70,
801 10.1016/j.atmosenv.2017.12.024, 2018.

802 Forster, C., Stohl, A., and Seibert, P.: Parameterization of convective transport in a Lagrangian particle
803 dispersion model and its evaluation, J. Appl. Meteorol. Clim., 46, 403-422, 10.1175/jam2470.1, 2007.

804 Frohlich-Nowoisky, J., Kampf, C. J., Weber, B., Huffman, J. A., Pohlker, C., Andreae, M. O., Lang-
805 Yona, N., Burrows, S. M., Gunthe, S. S., Elbert, W., Su, H., Hoor, P., Thines, E., Hoffmann, T., Despres,
806 V. R., and Poschl, U.: Bioaerosols in the Earth system: Climate, health, and ecosystem interactions,
807 Atmos. Res., 182, 346-376, 10.1016/j.atmosres.2016.07.018, 2016.

808 Fuller, G. W., Tremper, A. H., Baker, T. D., Yttri, K. E., and Butterfield, D.: Contribution of wood
809 burning to $PM_{10}$ in London, Atmos. Environ., 87, 87-94, 10.1016/j.atmosenv.2013.12.037, 2014.

810 Gelencser, A., May, B., Simpson, D., Sanchez-Ochoa, A., Kasper-Giebl, A., Puxbaum, H., Caseiro, A.,
811 Pio, C., and Legrand, M.: Source apportionment of $PM_{2.5}$ organic aerosol over Europe:
812 Primary/secondary, natural/anthropogenic, and fossil/biogenic origin, J. Geophys. Res.-Atmos., 112,
813 10.1029/2006jd008094, 2007.

814 Genberg, J., Hyder, M., Stenstrom, K., Bergstrom, R., Simpson, D., Fors, E. O., Jonsson, J. A., and
815 Swietlicki, E.: Source apportionment of carbonaceous aerosol in southern Sweden, Atmos. Chem. Phys.,
816 11, 11387-11400, 10.5194/acp-11-11387-2011, 2011.

817 Gilbert, R. O.: Statistical Methods for Environmental Pollution Monitoring, Wiley, NY, United States,
818 pp. 336, 1987.

819 Gilardoni, S., Vignati, E., Cavalli, F., Putaud, J. P., Larsen, B. R., Karl, M., Stenstrom, K., Genberg, J.,
820 Henne, S., and Dentener, F.: Better constraints on sources of carbonaceous aerosols using a combined
821 C-14 - macro tracer analysis in a European rural background site, Atmos. Chem. Phys., 11, 5685-5700,
822 10.5194/acp-11-5685-2011, 2011.

823 Glasius, M., Hansen, A. M. K., Claeys, M., Henzing, J. S., Jedynska, A. D., Kasper-Giebl, A., Kistler,
824 M., Kristensen, K., Martinsson, J., Maenhaut, W., Nojgaard, J. K., Spindler, G., Stenstrom, K. E.,
825 Swietlicki, E., Szidat, S., Simpson, D., and Yttri, K. E.: Composition and sources of carbonaceous
826 aerosols in Northern Europe during winter, Atmos. Environ., 173, 127-141,
827 10.1016/j.atmosenv.2017.11.005, 2018.

Grythe, H., Kristiansen, N. I., Zwaaftink, C. D. G., Eckhardt, S., Strom, J., Tunved, P., Krejci, R., and Stohl, A.: A new aerosol wet removal scheme for the Lagrangian particle model FLEXPART v10, Geosci. Model Dev., 10, 1447-1466, 10.5194/gmd-10-1447-2017, 2017.

Grythe, H., Lopez-Aparicio, S., Vogt, M., Thanh, D. V., Hak, C., Halse, A. K., Hamer, P., and Santos, G. S.: The MetVed model: development and evaluation of emissions from residential wood combustion at high spatio-temporal resolution in Norway, Atmos. Chem. Phys., 19, 10.5194/acp-19-10217-2019, 2019.

Hallquist, M., Wenger, J. C., Baltensperger, U., Rudich, Y., Simpson, D., Claeys, M., Dommen, J., Donahue, N. M., George, C., Goldstein, A. H., Hamilton, J. F., Herrmann, H., Hoffmann, T., Iinuma, Y., Jang, M., Jenkin, M. E., Jimenez, J. L., Kiendler-Scharr, A., Maenhaut, W., McFiggans, G., Mentel, T. F., Monod, A., Prevot, A. S. H., Seinfeld, J. H., Surratt, J. D., Szmigielski, R., and Wildt, J.: The formation, properties and impact of secondary organic aerosol: current and emerging issues, Atmos. Chem. Phys., 9, 5155-5236, 10.5194/acp-9-5155-2009, 2009.

Herich, H., Gianini, M. F. D., Piot, C., Mocnik, G., Jaffrezo, J. L., Besombes, J. L., Prevot, A. S. H., and Hueglin, C.: Overview of the impact of wood burning emissions on carbonaceous aerosols and PM in large parts of the Alpine region, Atmos. Environ., 89, 64-75, 10.1016/j.atmosenv.2014.02.008, 2014.

Hirdman, D., Sodemann, H., Eckhardt, S., Burkhart, J. F., Jefferson, A., Mefford, T., Quinn, P. K., Sharma, S., Strom, J., and Stohl, A.: Source identification of short-lived air pollutants in the Arctic using statistical analysis of measurement data and particle dispersion model output, Atmos. Chem. Phys., 10, 669-693, 10.5194/acp-10-669-2010, 2010.

Hjellbrekke, A-G.: Data Report 2018. Particulate matter, carbonaceous and inorganic compounds, NILU, Kjeller, EMEP/CCC-Report 1/2020, 2020.

Hodnebrog, O., Myhre, G., and Samset, B. H.: How shorter black carbon lifetime alters its climate effect, Nat. Commun., 5, 10.1038/ncomms6065, 2014.

Hoffmann, D., Tilgner, A., Iinuma, Y., and Herrmann, H.: Atmospheric Stability of Levoglucosan: A Detailed Laboratory and Modeling Study, Environ. Sci. Technol., 44, 694-699, 10.1021/es902476f, 2010a.

Hoffmann, D., Tilgner, A., Iinuma, Y., and Herrmann, H.: Atmospheric Stability of Levoglucosan: A Detailed Laboratory and Modeling Study, Environ. Sci. Technol, 44, 694-699, 10.1021/es902476f, 2010b.

Janssen, N. A. H., Gerlofs-Nijland, M. E., Lanki, T., Salonen, R. O., Cassee, F., Hoek, G., Fischer, P., Brunekreef, B., and Krzyzanowski, M.: Health effects of black carbon. Copenhagen: WHO Regional Office for Europe, 2012.

Jia, Y. L. and Fraser, M.: Characterization of Saccharides in Size-fractionated Ambient Particulate Matter and Aerosol Sources: The Contribution of Primary Biological Aerosol Particles (PBAPs) and Soil to Ambient Particulate Matter, Environ. Sci. Technol., 45, 930-936, 10.1021/es103104e, 2011.

Kahnert, M., Lazaridis, M., Tsyro, S., and Torseth, K.: Requirements for developing a regional monitoring capacity for aerosols in Europe within EMEP, J. Environ. Monitor., 6, 646-655, 10.1039/b315136k, 2004.

Kendall, M. G.: Rank correlation methods, 4th edition, Charles Griffin, London, 1975.

Kleindienst, T. E., Jaoui, M., Lewandowski, M., Offenberg, J. H., Lewis, C. W., Bhave, P. V., and Edney, E. O.: Estimates of the contributions of biogenic and anthropogenic hydrocarbons to secondary organic aerosol at a southeastern US location, Atmos. Environ., 41, 8288-8300, 10.1016/j.atmosenv.2007.06.045, 2007.

Kocbach, A., Li, Y. J., Yttri, K. E., Cassee, F. R., Schwarze, P. E., and Namork, E.: Physicochemical characterisation of combustion particles from vehicle exhaust and residential wood smoke, Part. Fibre Toxicol., 3, 10.1186/1743-8977-3-1, 2006.

Kyllonen, K., Vestenius, M., Anttila, P., Makkonen, U., Aurela, M., Wangberg, I., Mastromonaco, M. N., and Hakola, H.: Trends and source apportionment of atmospheric heavy metals at a subarctic site during 1996-2018, Atmos. Environ., 236, 10.1016/j.atmosenv.2020.117644, 2020.

Lanz, V. A., Prevot, A. S. H., Alfarra, M. R., Weimer, S., Mohr, C., DeCarlo, P. F., Gianini, M. F. D., Hueglin, C., Schneider, J., Favez, O., D'Anna, B., George, C., and Baltensperger, U.: Characterization of aerosol chemical composition with aerosol mass spectrometry in Central Europe: an overview, Atmos. Chem. Phys., 10, 10453-10471, 10.5194/acp-10-10453-2010, 2010.

Lund, M. T., Myhre, G., Haslerud, A. S., Skeie, R. B., Griesfeller, J., Platt, S. M., Kumar, R., Myhre, C. L., and Schulz, M.: Concentrations and radiative forcing of anthropogenic aerosols from 1750 to 2014 simulated with the Oslo CTM3 and CEDS emission inventory, Geosci. Model Dev., 11, 4909-4931, 10.5194/gmd-11-4909-2018, 2018.

Maenhaut, W.: Source apportionment revisited for long-term measurements of fine aerosol trace elements at two locations in southern Norway, Nucl. Instrum. Meth. B., 417, 133-138, 10.1016/j.nimb.2017.07.006, 2018.

Maenhaut, W., Vermeylen, R., Claeys, M., Vercauteren, J., Matheeussen, C., and Roekens, E.: Assessment of the contribution from wood burning to the $PM_{10}$ aerosol in Flanders, Belgium, Sci. Tot. Environ., 437, 226-236, 10.1016/j.scitotenv.2012.08.015, 2012.

Malm, W.C., Sisler, J.F., Huffmann, D., Eldred, R.A., Cahill, T.A.: Spatial and seasonal trends in particles concentrations and optical extinction in the United-States. J. Geophys. Res. 99(D1), 1347-1370, 1994.

Mann, H. B.: Non-parametric tests against trend, Econometrica 13:163-171, 1945.

Matthews, B., Mareckova, K., Schindlbacher, S., Ullrich, B., and Wankmwüller, R.: Emissions for 2018, in: Transboundary particulate matter, photo-oxidants, acidifying and eutrophying components. EMEP Status Report 1/2020, pp. 37-57, The Norwegian Meteorological Institute, Oslo, Norway, 2020.

Myhre, G. and Samset, B. H.: Standard climate models radiation codes underestimate black carbon radiative forcing, Atmos. Chem. Phys., 15, 2883-2888, 10.5194/acp-15-2883-2015, 2015.

Myhre, G., Shindell, D., Bréon, F.-M., Collins, W., Fuglestvedt, J., Huang, J., Koch, D., Lamarque, J.-F., Lee, D., Mendoza, B., Nakajima, T., Robock, A., Stephens, G., Takemura, T., and Zhang, H.: Anthropogenic and Natural Radiative Forcing. In: Climate Change 2013: The Physical Science Basis. Contribution of Working Group I to the Fifth Assessment Report of the Intergovernmental Panel on Climate Change [Stocker, T.F., Qin, D., Plattner, G.-K., Tignor, M., Allen, S.K., Boschung, J., Nauels, A., Xia, Y., Bex, V., and Midgley, P.M. (eds.)], Cambridge University Press, Cambridge, United Kingdom and New York, NY, USA, 2013.

Norris, G., Duvall, R., Brown, S., and Bai, S.: EPA Positive Matrix Factorization (PMF) 5.0 Fundamentals and User Guide, U.S. Environmental Protection Agency, Washington, DC, 20460 (i-124, EPA/600/R-14/108, April), 2014.

O'Dowd, C. D., Facchini, M. C., Cavalli, F., Ceburnis, D., Mircea, M., Decesari, S., Fuzzi, S., Yoon, Y. J., and Putaud, J. P.: Biogenically driven organic contribution to marine aerosol, Nature, 431, 676-680, 10.1038/nature02959, 2004.

Pacyna, J. M., Nriagu, J. O., Davidson, C. I. (Eds.): Toxic Metals in the Atmosphere, Wiley, New York, USA, (1986).

916 Pio, C. A., Legrand, M., Oliveira, T., Afonso, J., Santos, C., Caseiro, A., Fialho, P., Barata, F., Puxbaum,
917 H., Sanchez-Ochoa, A., Kasper-Giebl, A., Gelencser, A., Preunkert, S., and Schock, M.: Climatology
918 of aerosol composition (organic versus inorganic) at nonurban sites on a west-east transect across
919 Europe, J. Geophys. Res.-Atmos., 112, 10.1029/2006jd008038, 2007.

920 Pisso, I., Sollum, E., Grythe, H., Kristiansen, N. I., Cassiani, M., Eckhardt, S., Arnold, D., Morton, D.,
921 Thompson, R. L., Zwaaftink, C. D. G., Evangeliou, N., Sodemann, H., Haimberger, L., Henne, S.,
922 Brunner, D., Burkhart, J. F., Fouilloux, A., Brioude, J., Philipp, A., Seibert, P., and Stohl, A.: The
923 Lagrangian particle dispersion model FLEXPART version 10.4, Geosci. Model Dev., 12, 4955-4997,
924 10.5194/gmd-12-4955-2019, 2019.

925 Polissar, A. V., Hopke, P. K., and Paatero, P.: Atmospheric aerosol over Alaska - 2. Elemental
926 composition and sources, J. Geophys. Res.-Atmos., 103, 19045-19057, 10.1029/98jd01212, 1998.

927 Puxbaum, H., Caseiro, A., Sanchez-Ochoa, A., Kasper-Giebl, A., Claeys, M., Gelencser, A., Legrand,
928 M., Preunkert, S., and Pio, C.: Levoglucosan levels at background sites in Europe for assessing the
929 impact of biomass combustion on the European aerosol background, J. Geophys. Res.-Atmos., 112,
930 10.1029/2006jd008114, 2007.

931 Reis, S., Grennfelt, P., Klimont, Z., Amann, M., ApSimon, H., Hettelingh, J. P., Holland, M., LeGall,
932 A. C., Maas, R., Posch, M., Spranger, T., Sutton, M. A., and Williams, M.: From Acid Rain to Climate
933 Change, Science, 338, 1153-1154, 10.1126/science.1226514, 2012.

934 Ripoll, A., Minguillon, M. C., Pey, J., Perez, N., Querol, X., and Alastuey, A.: Joint analysis of
935 continental and regional background environments in the western Mediterranean: $PM_1$ and $PM_{10}$
936 concentrations and composition, Atmos. Chem. Phys., 15, 1129-1145, 10.5194/acp-15-1129-2015,
937 2015.

938 Rogge, W. F., Hildemann, L. M., Mazurek, M. A., Cass, G. R., and Simonelt, B. R. T.: SOURCES OF
939 FINE ORGANIC AEROSOL .1. CHARBROILERS AND MEAT COOKING OPERATIONS,
940 Environ. Sci. Technol., 25, 1112-1125, 10.1021/es00018a015, 1991.

941 Rotzer, T. and Chmielewski, F. M.: Phenological maps of Europe, Clim. Res., 18, 249-257,
942 10.3354/cr018249, 2001.

943 Saarikoski, S., Timonen, H., Saarnio, K., Aurela, M., Jarvi, L., Keronen, P., Kerminen, V. M., and
944 Hillamo, R.: Sources of organic carbon in fine particulate matter in northern European urban air, Atmos.
945 Chem. Phys., 8, 6281-6295, 10.5194/acp-8-6281-2008, 2008.

946 Saffari, A., Daher, N., Samara, C., Voutsa, D., Kouras, A., Manoli, E., Karagkiozidou, O., Vlachokostas,
947 C., Moussiopoulos, N., Shafer, M. M., Schauer, J. J., and Sioutas, C.: Increased Biomass Burning Due
948 to the Economic Crisis in Greece and Its Adverse Impact on Wintertime Air Quality in Thessaloniki,
949 Environ. Sci. Technol., 47, 13313-13320, 10.1021/es403847h, 2013.

950 Samake, A., Bonin, A., Jaffrezo, J. L., Taberlet, P., Weber, S., Uzu, G., Jacob, V., Conil, S., and Martins,
951 J. M. F.: High levels of primary biogenic organic aerosols are driven by only a few plant-associated
952 microbial taxa, Atmos. Chem. Phys., 20, 5609-5628, 10.5194/acp-20-5609-2020, 2020.

953 Samake, A., Jaffrezo, J. L., Favez, O., Weber, S., Jacob, V., Canete, T., Albinet, A., Charron, A.,
954 Riffault, V., Perdrix, E., Waked, A., Golly, B., Salameh, D., Chevrier, F., Oliveira, D. M., Besombes, J.
955 L., Martins, J. M. F., Bonnaire, N., Conil, S., Guillaud, G., Mesbah, B., Rocq, B., Robic, P. Y., Hulin,
956 A., Le Meur, S., Descheemaecker, M., Chretien, E., Marchand, N., and Uzu, G.: Arabitol, mannitol, and
957 glucose as tracers of primary biogenic organic aerosol: the influence of environmental factors on
958 ambient air concentrations and spatial distribution over France, Atmos. Chem. Phys., 19, 11013-11030,
959 10.5194/acp-19-11013-2019, 2019.

960 Sandradewi, J., Prevot, A. S. H., Szidat, S., Perron, N., Alfarra, M. R., Lanz, V. A., Weingartner, E.,
961 and Baltensperger, U.: Using aerosol light absorption measurements for the quantitative determination
962 of wood burning and traffic emission contributions to particulate matter, Environ. Sci. Technol., 42,
963 3316-3323, 10.1021/es702253m, 2008.

964 Sciare, J., Oikonomou, K., Favez, O., Liakakou, E., Markaki, Z., Cachier, H., and Mihalopoulos, N.:
965 Long-term measurements of carbonaceous aerosols in the Eastern Mediterranean: evidence of long-
966 range transport of biomass burning, Atmos. Chem. Phys., 8, 5551-5563, 10.5194/acp-8-5551-2008,
967 2008.

968 Sen, P. K.: Estimates of the regression coefficient based on Kendall's Tau. J. Am., Stat. Assoc. 63 (324),
969 1379–1389.https://doi.org/10.2307/2285891, 1968.

970 Sillanpaa, M., Frey, A., Hillamo, R., Pennanen, A. S., and Salonen, R. O.: Organic, elemental and
971 inorganic carbon in particulate matter of six urban environments in Europe, Atmos. Chem. Phys., 5,
972 2869-2879, 10.5194/acp-5-2869-2005, 2005.

973 Simpson, D., Yttri, K. E., Klimont, Z., Kupiainen, K., Caseiro, A., Gelencser, A., Pio, C., Puxbaum, H.,
974 and Legrand, M.: Modeling carbonaceous aerosol over Europe: Analysis of the CARBOSOL and EMEP
975 EC/OC campaigns, J. Geophys. Res.-Atmos., 112, 10.1029/2006JD008158, 2007.

976 Simpson, D., Bergström, R., Denier van der Gon, H., Kuenen, J., Schindlbacher, S., and Visschedijk,
977 A.: Condensable organics; issues and implications for EMEP calculations and source-receptor matrices,
978 in: Transboundary particulate matter, photo-oxidants, acidifying and eutrophying components. EMEP
979 Status Report 1/2019, pp. 71-88, The Norwegian Meteorological Institute, Oslo, Norway, 2019.

980 Skjoth, C. A., Sommer, J., Stach, A., Smith, M., and Brandt, J.: The long-range transport of birch
981 (Betula) pollen from Poland and Germany causes significant pre-season concentrations in Denmark,
982 Clin. Exp. Allergy, 37, 1204-1212, 10.1111/j.1365-2222.2007.02771.x, 2007.

983 Sofiev, M., Siljamo, P., Ranta, H., and Rantio-Lehtimaki, A.: Towards numerical forecasting of long-
984 range air transport of birch pollen: theoretical considerations and a feasibility study, Int. J. Biometeorol.,
985 50, 392-402, 10.1007/s00484-006-0027-x, 2006.

986 Spracklen, D. V., Jimenez, J. L., Carslaw, K. S., Worsnop, D. R., Evans, M. J., Mann, G. W., Zhang,
987 Q., Canagaratna, M. R., Allan, J., Coe, H., McFiggans, G., Rap, A., and Forster, P.: Aerosol mass
988 spectrometer constraint on the global secondary organic aerosol budget, Atmos. Chem. Phys., 11,
989 12109-12136, 10.5194/acp-11-12109-2011, 2011.

990 Stohl, A., Forster, C., Frank, A., Seibert, P., and Wotawa, G.: Technical note: The Lagrangian particle
991 dispersion model FLEXPART version 6.2, Atmos. Chem. Phys., 5, 2461-2474, 10.5194/acp-5-2461-
992 2005, 2005.

993 Stohl, A., Andrews, E., Burkhart, J. F., Forster, C., Herber, A., Hoch, S. W., Kowal, D., Lunder, C.,
994 Mefford, T., Ogren, J. A., Sharma, S., Spichtinger, N., Stebel, K., Stone, R., Strom, J., Torseth, K.,
995 Wehrli, C., and Yttri, K. E.: Pan-Arctic enhancements of light absorbing aerosol concentrations due to
996 North American boreal forest fires during summer 2004, J. Geophys. Res.-Atmos., 111,
997 10.1029/2006JD007216, 2006.

998 Stohl, A., Berg, T., Burkhart, J. F., Fjaeraa, A. M., Forster, C., Herber, A., Hov, O., Lunder, C.,
999 McMillan, W. W., Oltmans, S., Shiobara, M., Simpson, D., Solberg, S., Stebel, K., Strom, J., Torseth,
1000 K., Treffeisen, R., Virkkunen, K., and Yttri, K. E.: Arctic smoke - record high air pollution levels in the
1001 European Arctic due to agricultural fires in Eastern Europe in spring 2006, Atmos. Chem. Phys., 7, 511-
1002 534, 2007.

1003 Stumm, W. and Morgan, J. J. (eds.): Aquatic Chemistry: Chemical Equilibria and Rates in Natural
1004 Waters, 3rd Edition, Wiley-Interscience Series of Texts and Monographs, Wiley, New York, 1996.

1005 Szidat, S., Prevot, A. S. H., Sandradewi, J., Alfarra, M. R., Synal, H. A., Wacker, L., and Baltensperger,
1006 U.: Dominant impact of residential wood burning on particulate matter in Alpine valleys during winter,
1007 Geophys. Res. Lett., 34, 10.1029/2006gl028325, 2007.

1008 Szidat, S., Ruff, M., Perron, N., Wacker, L., Synal, H.-A., Hallquist, M., Shannigrahi, A. S., Yttri, K.
1009 E., Dye, C., and Simpson, D.: Fossil and non-fossil sources of organic carbon (OC) and elemental carbon
1010 (EC) in Goteborg, Sweden, Atmos. Chem. Phys., 9, 1521-1535, 10.5194/acp-9-1805-2009, 2009.

1011 Theil, H.: A rank-invariant method of linear and polynomial regression analysis. Proc. R. Netherlands,
1012 Acad. Sci. 53, 386–392, https://doi.org/10.1007/978-94-011-2546-8_20, 1950.

1013 Tørseth, K. and Hov, Ø. (eds.): The EMEP monitoring strategy 2004-2009. Background document with
1014 justification and specification of the EMEP monitoring programme 2004-2009, Kjeller, NILU
1015 (EMEP/CCC, 09/2003), 2003.

1016 Torseth, K., Aas, W., Breivik, K., Fjaeraa, A. M., Fiebig, M., Hjellbrekke, A. G., Myhre, C. L., Solberg,
1017 S., and Yttri, K. E.: Introduction to the European Monitoring and Evaluation Programme (EMEP) and
1018 observed atmospheric composition change during 1972-2009, Atmos. Chem. Phys., 12, 5447-5481,
1019 10.5194/acp-12-5447-2012, 2012.

1020 Trebs, I., Andreae, M. O., Elbert, W., Mayol-Bracero, O. L., Soto-Garcia, L. L., Rudich, Y., Falkovich,
1021 A. H., Maenhaut, W., Artaxo, P., Otjes, R., and Slanina, J.: Aerosol inorganic composition at a tropical
1022 site: Discrepancies between filter-based sampling and a semi-continuous method, Aerosol Sci. Tech,
1023 42, 255-269, 10.1080/02786820801992899, 2008.

1024 UNECE: 1999 Protocol to Abate Acidification, Eutrophication and Ground-level Ozone to the
1025 Convention on Long-range Transboundary Air Pollution, as amended on 4 May 2012, Geneva: UNECE,
1026 2013.

1027 UNECE: Monitoring strategy for the Cooperative Programme for Monitoring and Evaluation of the
1028 Long-range Transmission of Air Pollutants in Europe for the period 2020–2029, UNECE, Geneva,
1029 Decision 2019/1, ECE/EB.AIR/144/Add.1, 2019.

1030 van der Gon, H., Bergstrom, R., Fountoukis, C., Johansson, C., Pandis, S. N., Simpson, D., and
1031 Visschedijk, A. J. H.: Particulate emissions from residential wood combustion in Europe revised
1032 estimates and an evaluation, Atmos. Chem. Phys., 15, 6503-6519, 10.5194/acp-15-6503-2015, 2015.

1033 Viana, M., Kuhlbusch, T. A. J., Querol, X., Alastuey, A., Harrison, R. M., Hopke, P. K., Winiwarter,
1034 W., Vallius, A., Szidat, S., Prevot, A. S. H., Hueglin, C., Bloemen, H., Wahlin, P., Vecchi, R., Miranda,

A. I., Kasper-Giebl, A., Maenhaut, W., and Hitzenberger, R.: Source apportionment of particulate matter in Europe: A review of methods and results, J. Aerosol Sci., 39, 827-849, 10.1016/j.jaerosci.2008.05.007, 2008.

Waked, A., Favez, O., Alleman, L. Y., Piot, C., Petit, J. E., Delaunay, T., Verlinden, E., Golly, B., Besombes, J. L., Jaffrezo, J. L., and Leoz-Garziandia, E.: Source apportionment of $PM_{10}$ in a north-western Europe regional urban background site (Lens, France) using positive matrix factorization and including primary biogenic emissions, Atmos. Chem. Phys., 14, 3325-3346, 10.5194/acp-14-3325-2014, 2014.

Weber, S., Salameh, D., Albinet, A., Alleman, L. Y., Waked, A., Besombes, J. L., Jacob, V., Guillaud, G., Meshbah, B., Rocq, B., Hulin, A., Dominik-Segue, M., Chretien, E., Jaffrezo, J. L., and Favez, O.: Comparison of $PM_{10}$ Sources Profiles at 15 French Sites Using a Harmonized Constrained Positive Matrix Factorization Approach, Atmosphere, 10, 10.3390/atmos10060310, 2019.

WHO: Review of evidence on health aspects of air pollution – REVIHAAP Project, Technical Report, Copenhagen: WHO Regional Office for Europe, 2013.

Yttri, K. E., Aas, W., Bjerke, A., Cape, J. N., Cavalli, F., Ceburnis, D., Dye, C., Emblico, L., Facchini, M. C., Forster, C., Hanssen, J. E., Hansson, H. C., Jennings, S. G., Maenhaut, W., Putaud, J. P., and Torseth, K.: Elemental and organic carbon in $PM_{10}$: a one year measurement campaign within the European Monitoring and Evaluation Programme EMEP, Atmos. Chem. Phys., 7, 5711-5725, 2007a.

Yttri, K. E., Dye, C., and Kiss, G.: Ambient aerosol concentrations of sugars and sugar-alcohols at four different sites in Norway, Atmos. Chem. Phys., 7, 4267-4279, 2007b.

Yttri, K. E., Simpson, D., Nojgaard, J. K., Kristensen, K., Genberg, J., Stenstrom, K., Swietlicki, E., Hillamo, R., Aurela, M., Bauer, H., Offenberg, J. H., Jaoui, M., Dye, C., Eckhardt, S., Burkhart, J. F., Stohl, A., and Glasius, M.: Source apportionment of the summer time carbonaceous aerosol at Nordic rural background sites, Atmos. Chem. Phys., 11, 13339-13357, 10.5194/acp-11-13339-2011, 2011b.

Yttri, K. E., Simpson, D., Stenstrom, K., Puxbaum, H., and Svendby, T.: Source apportionment of the carbonaceous aerosol in Norway - quantitative estimates based on C-14, thermal-optical and organic tracer analysis, Atmos. Chem. Phys., 11, 9375-9394, 10.5194/acp-11-9375-2011, 2011a.

Yttri, K. E., Myhre, C. L., Eckhardt, S., Fiebig, M., Dye, C., Hirdman, D., Stroem, J., Klimont, Z., and Stohl, A.: Quantifying black carbon from biomass burning by means of levoglucosan - a one-year time series at the Arctic observatory Zeppelin, Atmos. Chem. Phys., 14, 6427-6442, 10.5194/acp-14-6427-2014, 2014.

1066 Yttri, K. E., Schnelle-Kreis, J., Maenhaut, W., Abbaszade, G., Alves, C., Bjerke, A., Bonnier, N., Bossi,
1067 R., Claeys, M., Dye, C., Evtyugina, M., Garcia-Gacio, D., Hillamo, R., Hoffer, A., Hyder, M., Iinuma,
1068 Y., Jaffrezo, J.-L., Kasper-Giebl, A., Kiss, G., Lopez-Mahia, P. L., Pio, C., Piot, C., Ramirez-Santa-
1069 Cruz, C., Sciare, J., Teinila, K., Vermeylen, R., Vicente, A., and Zimmermann, R.: An intercomparison
1070 study of analytical methods used for quantification of levoglucosan in ambient aerosol filter samples,
1071 Atmos. Meas. Tech., 8, 125-147, 10.5194/amt-8-125-2015, 2015.

1072 Yttri, K. E., Simpson, D., Bergstrom, R., Kiss, G., Szidat, S., Ceburnis, D., Eckhardt, S., Hueglin, C.,
1073 Nojgaard, J. K., Perrino, C., Pisso, I., Prevot, A. S. H., Putaud, J. P., Spindler, G., Vana, M., Zhang, Y.
1074 L., and Aas, W.: The EMEP Intensive Measurement Period campaign, 2008-2009: characterizing
1075 carbonaceous aerosol at nine rural sites in Europe, Atmos. Chem. Phys., 19, 4211-4233, 10.5194/acp-
1076 19-4211-2019, 2019.

1077 Zotter, P., Ciobanu, V. G., Zhang, Y. L., El-Haddad, I., Macchia, M., Daellenbach, K. R., Salazar, G.
1078 A., Huang, R. J., Wacker, L., Hueglin, C., Piazzalunga, A., Fermo, P., Schwikowski, M., Baltensperger,
1079 U., Szidat, S., and Prevot, A. S. H.: Radiocarbon analysis of elemental and organic carbon in Switzerland
1080 during winter-smog episodes from 2008 to 2012-Part 1: Source apportionment and spatial variability,
1081 Atmos. Chem. Phys., 14, 13551-13570, 10.5194/acp-14-13551-2014, 2014.

1082 Zotter, P., Herich, H., Gysel, M., El-Haddad, I., Zhang, Y. L., Mocnik, G., Huglin, C., Baltensperger,
1083 U., Szidat, S., and Prevot, A. H.: Evaluation of the absorption angstrom exponents for traffic and wood
1084 burning in the Aethalometer-based source apportionment using radiocarbon measurements of ambient
1085 aerosol, Atmos. Chem. Phys., 17, 4229-4249, 10.5194/acp-17-4229-2017, 2017.

1086

## Figures


**Figure 1: The Birkenes Observatory (58°23' N, 8°15' E; 219 m asl) lies in the Boreo-nemoral zone, 20 km from the Skagerrak coastline in Southern Norway.**

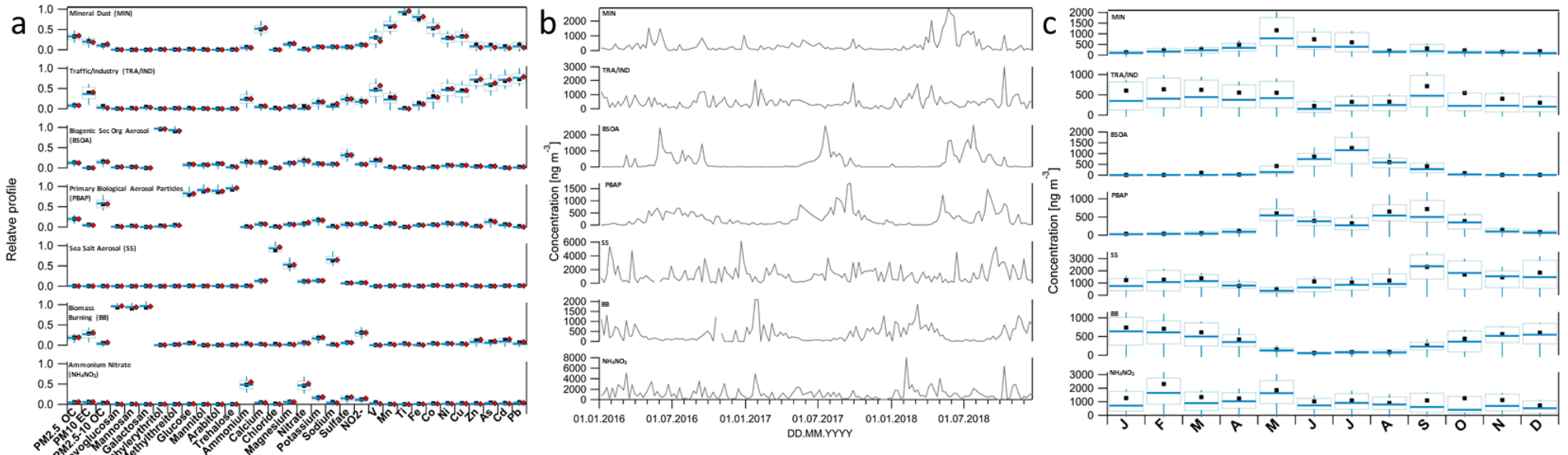
a
Mineral Dust (MIN)
Traffic/Industry (TRA/IND)
Biogenic Sec Org Aerosol (BSOA)
Primary Biological Aerosol Particles (PBAP)
Sea Salt Aerosol (SS)
Biomass Burning (BB)
Ammonium Nitrate (NH4NO3)
Relative profile
PM2.5 OC
PM10 EC
PM2.5-10 OC
Levoglucosan
Mannosan
Galactosan
2-Methylerythritol
2-Methylthreitol
Glucose
Mannitol
Arabitol
Trehalose
Ammonium
Calcium
Chloride
Magnesium
Nitrate
Potassium
Sodium
Sulfate
NO2-
V
Mn
Ti
Fe
Co
Ni
Cu
Zn
As
Cd
Pb
b
MIN
TRA/IND
BSOA
PBAP
SS
BB
NH4NO3
Concentration [ng m-3]
01.01.2016
01.07.2016
01.01.2017
01.07.2017
01.01.2018
01.07.2018
DD.MM.YYYY
c
MIN
TRA/IND
BSOA
PBAP
SS
BB
NH4NO3
Concentration [ng m-3]
J
F
M
A
M
J
J
A
S
O
N
D

1092

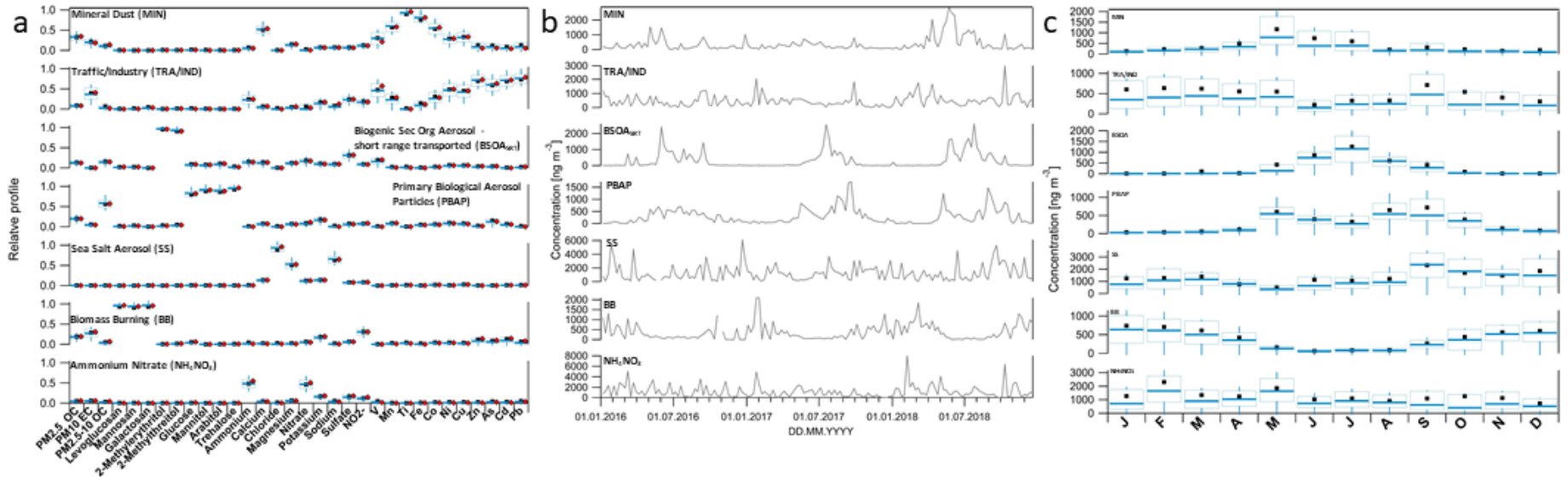


**Figure 2: Results from PMF for Birkenes 2016–2018. a) Factor profiles b) Factor time series c) aggregated monthly data. Boxes in a), c) show statistics from bootstrapped solutions (n=5000): percentiles 25/75 (box), median (horizontal line) and 10/90 (whiskers). Black markers are the means. Red markers in a) show the base factor profiles.**

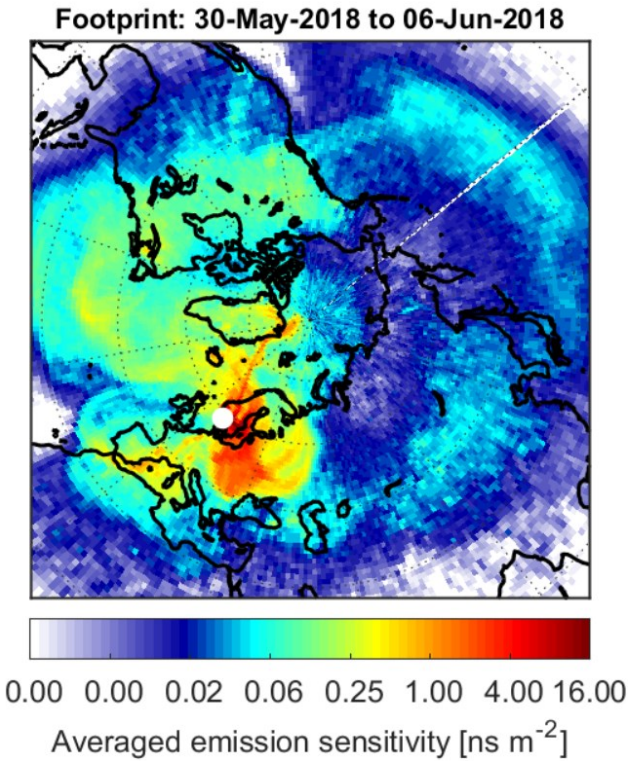


**Figure 3: Footprint emission sensitivities calculated using the FLEXPART model for the period 30 May–6 June 2018 at the Birkenes Observatory.**

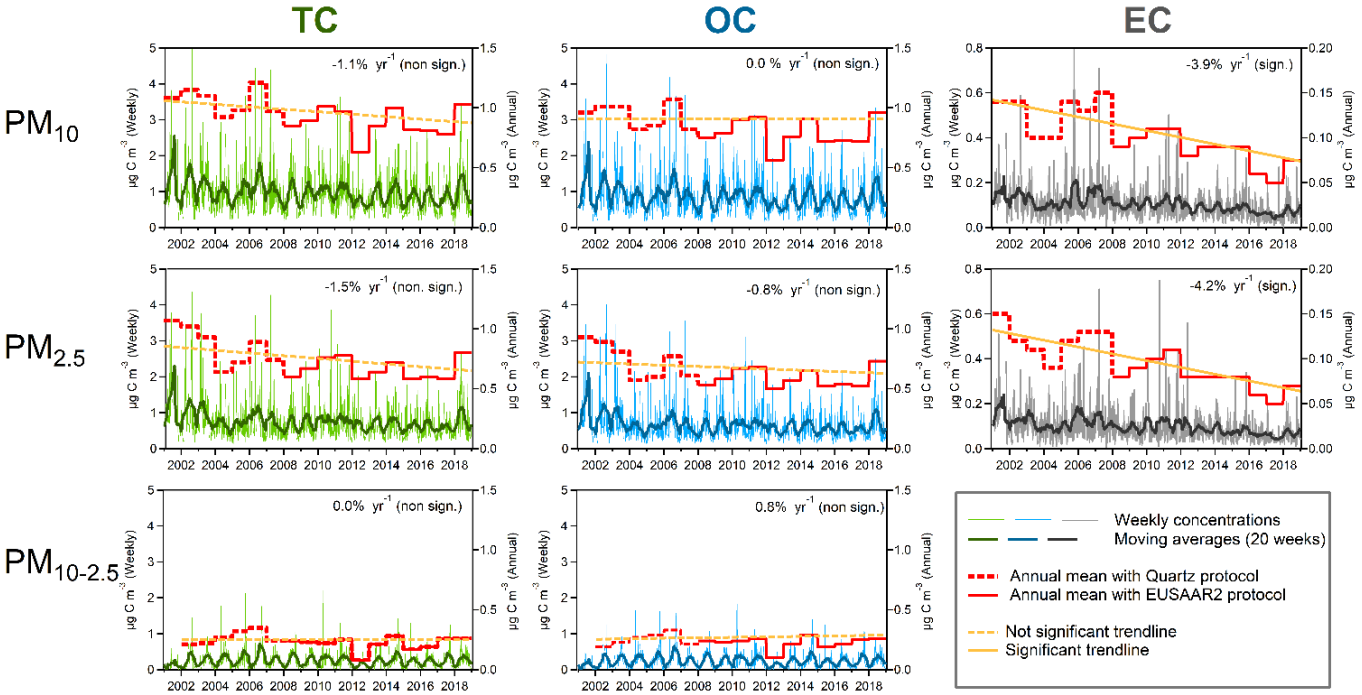


**Figure 4: Ambient aerosol concentrations of TC, OC and EC in $PM_{10}$ (Upper panels), in $PM_{2.5}$ (Mid-Panels), and TC and OC in $PM_{10-2.5}$ (Lower panels), presented as weekly (168 h) and annual mean concentrations for the Birkenes Observatory for 2001–2018. The trendlines account for the protocol shift.**

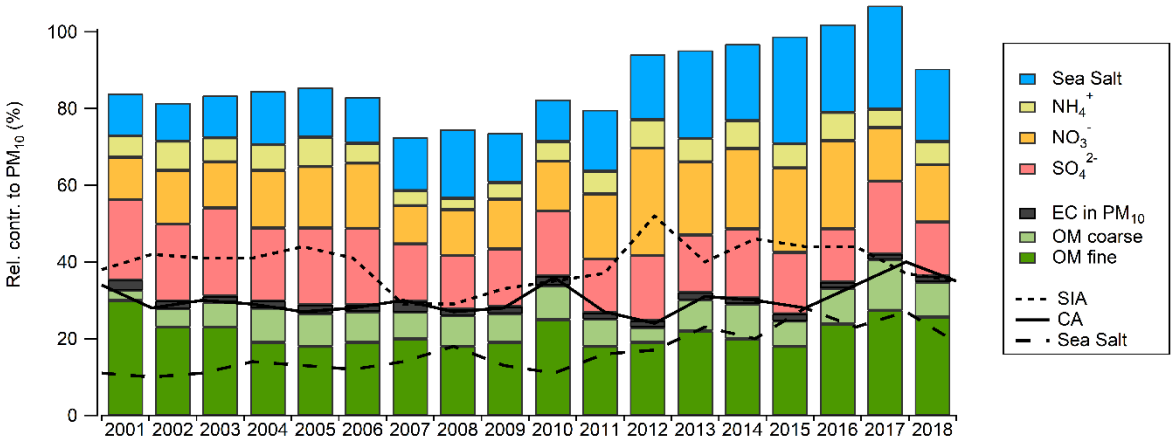


**Figure 5: Mass closure of $PM_{10}$ for Birkenes for the period 2001–2018 (Unit: %). Notation: Sea salt = Sum of $Na^+$, $Mg^{2+}$, $Cl^-$; SIA = Secondary inorganic aerosol (SIA) = Sum of $SO_4^{2-}$, $NO_3^-$; $NH_4^+$; CA = Carbonaceous aerosol; OM = Organic matter. OM is calculated using OC:OM=1.9 (Yttri et al., 2011a).**

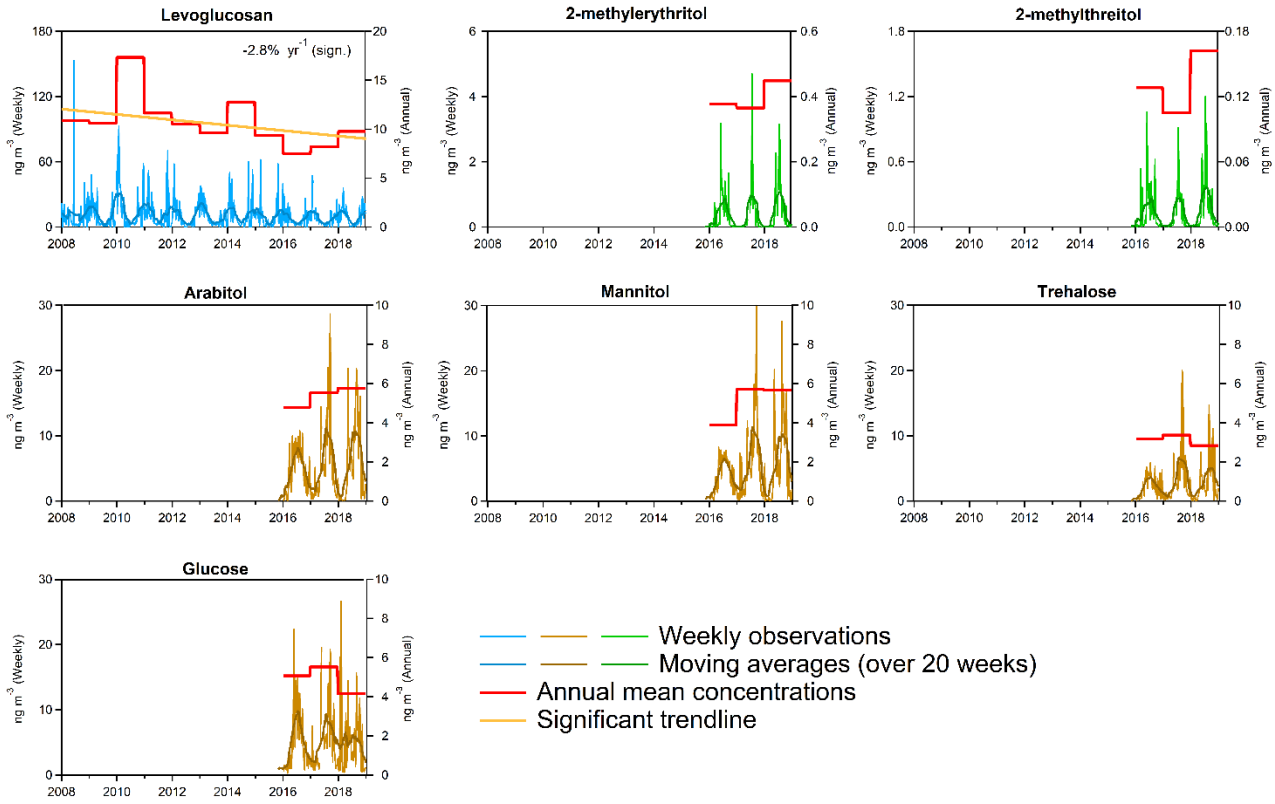


**Figure 6: Ambient aerosol concentrations of organic tracers in $PM_{10}$. Levoglucosan, 2-methylerythritol and 2-methylthreitol (Upper panels), arabitol, mannitol, trehalose (Mid-Panels), and glucose (Lower panel), presented as weekly (168 h) and annual mean concentrations for the Birkenes Observatory for the period 2008–2018.**

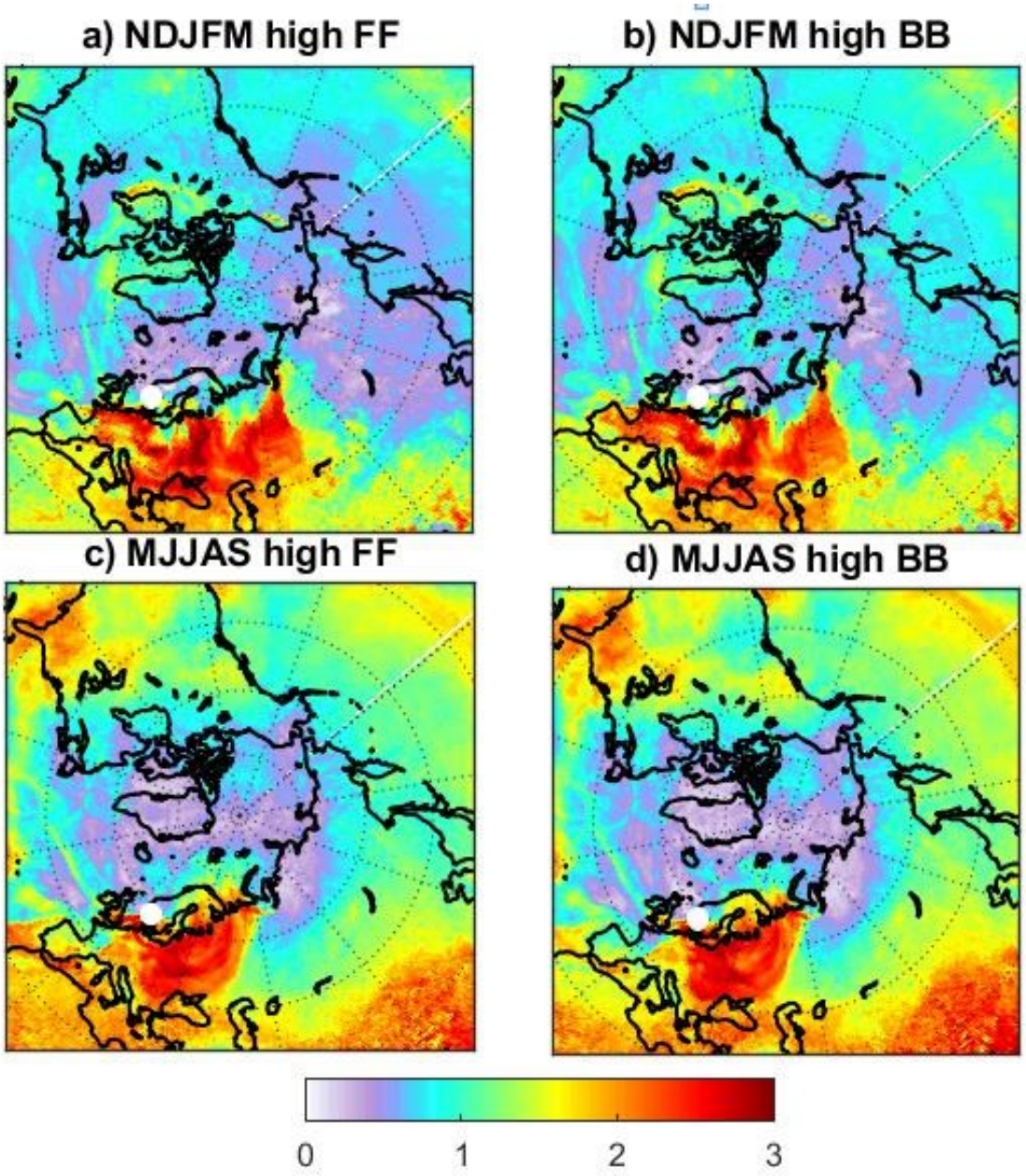


**Figure 7: 70th percentiles of $eBC_{ff}$ (left panels, a and c) and $eBC_{bb}$ (right panels, b and d) for winter (NDJFM) and summer (MJJAS). The color-coding shows the ratio of residence times for footprint sensitivities during measurements exceeding the 70th percentile and the average footprint sensitivity.**

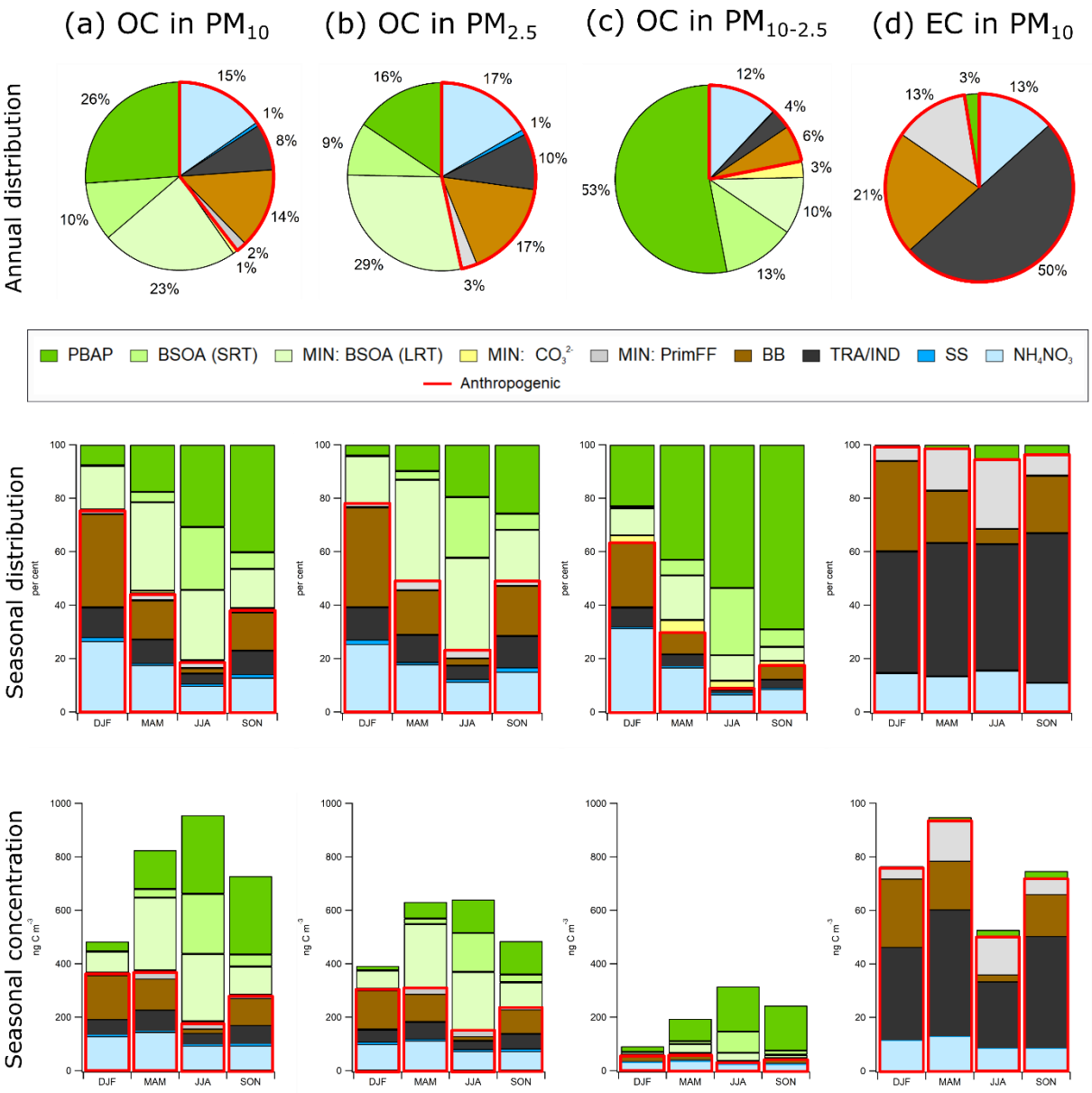


**Figure 8: Factor contributions to OC in $PM_{10}$ (a), $PM_{2.5}$ (b), $PM_{10-2.5}$ (c), and EC in $PM_{10}$ (d) at Birkenes (2016–2018) (upper panels), and divided into seasons (middle and lower panels), as determined by positive matrix factorization. The factors enclosed by the full red line represents anthropogenic sources. The OC content of the MIN factor is divided into long range transported BSOA ($OC_{BSOA,LRT}$) and primary OC from fossil fuel combustion ($OC_{PrimFF}$) following Eq. (1), and carbonate carbon ($OC_{CO32-}$) (Sect. 2.4.1).**

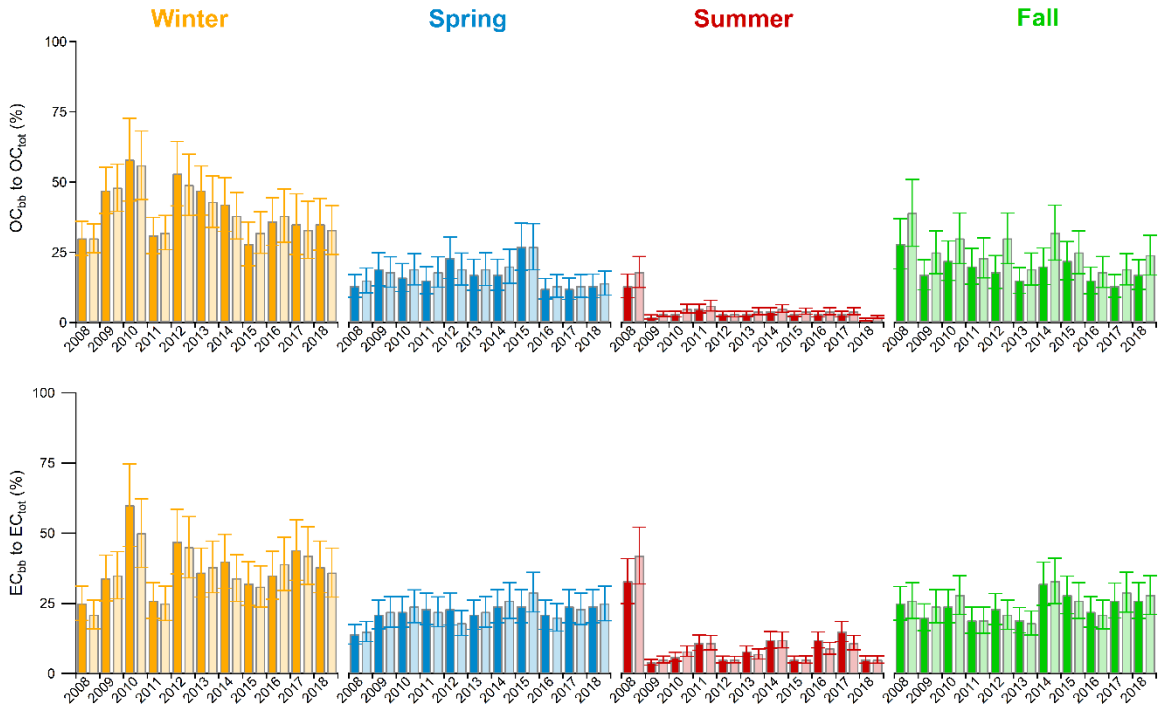


**Figure 9: Relative contribution of $OC_{bb}$ to $OC_{tot}$ (upper panel) and $EC_{bb}$ to $EC_{tot}$ (lower panel) in $PM_{10}$ (dark colors) and in $PM_{2.5}$ (light colors), as a function of season at Birkenes for 2008–2018 (DJF = Winter; MAM = Spring; JJA = Summer; SON = Fall).**

## Tables

**Table 1: Variables describing the biomass burning source derived from the PMF BB factor in the present study, and comparable variables obtained by $^{14}C$-analysis reported by Zotter et al. (2014).**

| Present study | Zotter et al. (2014)[1] |
|---|---|
| OC/Levoglucosan (in $PM_{10}$) = 12.7 | $OC_{NF}$/Levoglucosan (in $PM_{10}$) = 12.6 ± 3.1 |
| OC/Levoglucosan (in $PM_{2.5}$) = 11.1 | |
| EC/Levoglucosan (in $PM_{10}$) = 1.96 | $EC_{NF}$/Levoglucosan (in $PM_{10}$) = 1.72 ± 0.59 |
| OC/EC (in $PM_{10}$) = 6.5 | $OC/_{NF}EC_{NF}$ (in $PM_{10}$) = 7.7 ± 2.1 |
| OC/EC (in $PM_{2.5}$) = 5.7 | |

[1]North of the Alps
Notation: $OC_{NF}$ = Non-fossil OC; $EC_{NF}$ = Non-fossil EC

**Table 2: Biomass burning fraction derived from the PMF and the aethalometer model. Aethalometer model 1 shows the biomass burning fraction obtained by the default pair of Absorption Ångstrøm Exponents (AAE) suggested by Zotter et al. (2014), whereas Aethalometer model 2 show the biomass burning fraction obtained using the pair of AAEs derived from PMF.**

| | PMF | Aethalometer model 1 | Aethalometer model 2 |
|---|---|---|---|
| Biomass burning fraction | 0.27 | 0.48 | 0.28 |
| Fossil AAE | 0.93 | 0.9 (Zotter et al., 2014) | 0.93 (from PMF) |
| Biomass burning AAE | 2.04 | 1.68 (Zotter et al., 2014) | 2.04 (from PMF) |

**Table 3: $OC_{BSOA}$, short-range transported (SRT) and long-range transported (LRT), and $OC_{PBAP}$ concentrations and their relative contribution to OC in $PM_{10}$ at Birkenes in August, as obtained by Latin Hypercube Sampling (Yttri et al., 2011b) and by PMF (present study).**

| | Reference | Approach | $OC_{BSOA,SRT}$ (ng C $m^{-3}$) | $OC_{BSOA,SRT}$/OC | $OC_{BSOA,SRT+LRT}$ (ng C $m^{-3}$) | $OC_{BSOA,SRT+LRT}$/OC | $OC_{PBAP}$ (ng C $m^{-3}$) | $OC_{PBAP}$/OC |
|---|---|---|---|---|---|---|---|---|
| August 2009 | Yttri et al. (2011b) | LHS[3] | | | 505[1] (408–598)[2,3] | 0.48[1] (0.38–0.58)[2,3] | 290[1] (213–380)[2] | 0.31[1] (0.22–0.40)[2] |
| August 2016 | Present study | PMF | 115 | 0.19 | 173 | 0.28 | 318 | 0.52 |
| August 2017 | Present study | PMF | 183 | 0.19 | 252 | 0.26 | 553 | 0.57 |
| August 2018 | Present study | PMF | 159 | 0.20 | 316 | 0.40 | 287 | 0.36 |
| August 2016–2018 | Present study | PMF | 152 | 0.19 | 247 | 0.31 | 386 | 0.48 |

1. $50^{th}$ percentile
2. $10^{th}$–$90^{th}$ percentile
3. LHS-approach includes both $OC_{BSOA,SRT}$ and $OC_{BSOA,LRT}$

**SUPPLEMENT TO**

**Trends, composition and sources of carbonaceous aerosol in the last 18 years at the Birkenes Observatory, Northern Europe, by K. E. Yttri et al.**

## S1. Quality assurance

The OC/EC data are not field blank corrected, in accordance with the standard operating procedure provided by EMEP (Yttri et al., 2007a; EMEP, 2014). The positive sampling artefact of OC for weekly samples collected at Birkenes has been quantified on a campaign basis using the QBQ (Quartz fibre filter Behind Quartz fibre filter) approach (McDow and Huntzicker, 1990; Turpin et al., 1994) in summer (18±4%; Yttri et al., 2011b), fall (19±7%; Yttri et al., 2019), and winter/spring (24±13%; Yttri et al., 2019) but only for $PM_{10}$. For OC in $PM_{2.5}$, which at Birkenes is obtained from an identical and co-located sampler, operating at the same filter face velocity as the $PM_{10}$ sampler, the positive sampling artefact is considered equally large, whereas its relative importance is slightly higher. The negative sampling artefact has not been addressed.

OC/EC analysis was performed within 2 months after the filter samples were collected and according to the Quartz (2001–2008) and the EUSAAR-2 (from 2008) temperature programs. EUSAAR-2 is designed to reduce the inherited uncertainties associated with splitting of OC and EC, e.g. by preventing premature burn-off of EC (Cavalli et al., 2010). The uncertainty associated with repeated OC/EC analyzes of a filter sample is typically <10%, which includes both analytical uncertainty and heterogenic distribution of the deposited aerosol particles on the filter sample.

The laser´s ability to detect changes in the transmittance of a filter sample high in initial EC is crucial to obtain a correct value for EC (and OC). 15 µg EC $cm^{-2}$ has been suggested as an upper limit (Subramanian et al., 2004; Wallén et al., 2010) but this value is likely to vary. The nine filter samples (out of nearly 1800) with an EC content exceeding 15 µg C $cm^{-2}$ in the current dataset were considered valid. Further, a non-biased separation between OC and EC requires that either pyrolytic carbon (PC) evolves before EC during analysis or that PC and EC have the same light absorption coefficient. It is well known that this is not always the case (Yang and Yu, 2002) and there is a lack of information on the magnitude of this imperfection.

Deviation from the protocol-defined temperature steps will affect the analysis results of the TOA instrument (Chow et al., 2005; Panteliadis et al., 2015) and temperature offsets ranging from -93 °C to +100 °C per temperature step have been reported (Panteliadis et al., 2015). Thus, calibration by the temperature calibration kit available from the instrument manufacturer (Sunset laboratory Inc) since 2012 is strongly recommended. Temperature calibration was implemented as part of the regular QA/QC procedures for thermal-optical analysis in 2013.

A comparison of the two temperature programmes used for the Birkenes time series was performed for $PM_{2.5}$ filter samples collected at Birkenes in 2014, using temperature calibrated versions of both Quartz and EUSAAR-2. There was a good agreement between the two temperature programs

for TC and OC, i.e. close to the expected uncertainty associated with analysis and sampling, whereas for EC the difference was pronounced (Table S 17), although in close correspondence with that previously reported by Panteliadis et al. (2015). Note that OC and EC data for the period 2001–2007 discussed in the main are text not corrected according to Eq. (S 18–20) (Table S 17), except for the purpose of trend calculations.

Field blanks did not contain monosaccharide anhydrides, sugars, sugar-alcohols or 2-methyltetrols in noticeable amounts. Filter samples for which the content was below the limit of detection (LOD) but > 0, were considered valid and included when calculating the annual and seasonal means. Organic tracers were analyzed within 1 year after collection of the aerosol filter samples. The uncertainty (analytical and sampling uncertainty) associated with measurements of monosaccharide anhydrides is within 10 – 15 % (Yttri et al., 2015). A similar range of uncertainty is expected for the other organic tracers.

Mass concentrations of $PM_{10}$ and $PM_{2.5}$ were field blank corrected. The overall uncertainty associated with determination of the $PM_{10}$ and $PM_{2.5}$ mass concentration is < 5%. The monitoring of major ions and trace elements follows the guidelines by EMEP (EMEP, 2014) and are within the data quality objective of the network: 15–25% uncertainty for the combined sampling and analysis of major ions and 30% for heavy metals.

## S2. Calculation of trends - Statistical approach

The Mann-Kendall test (Mann, 1945; Kendall, 1975; Gilbert, 1987) was used for calculating the significance of the trend and if a significant trend was found, the Theil-Sen slope (Theil, 1950; Sen, 1968; Gilbert, 1987) was calculated. This procedure has been widely used in atmospheric science, like in the recent TOAR project analysing global surface ozone trends (e.g. Fleming et al., 2018; Lefohn et al., 2018), in the review of the EMEP observations (Tørseth et al., 2012) and in numerous other observation based papers (Aas et al. 2019; Ciarelli et al., 2019; Theobald et al., 2019; Masiol et al., 2019; Collaud Coen et al., 2020).

The Mann-Kendall test is a non-parametric test that does not rely on any assumptions of distribution and is therefore well suited for atmospheric data that often deviate from normality and contain outliers that would hamper a standard linear regression. The basics of the Mann-Kendall test is to count the signs of all forward concentration differences in time, and if there is a sufficient overweight of positive or negative differences, the 0-hypothesis ($H_0$) of no trend could be rejected. The S statistic given below contains the sum of all the signs based on the observed values $y_i$ at time *i*:

$$S = \sum_{1=1}^{n-1} \sum_{j=i+1}^{n} sign\left(y_j - y_i\right) \qquad Eq.S1$$

This statistic together with the number of samples and the number of ties in the data were used to calculate the $p$ value as given by Gilbert (1987). In our work, we assumed significant trends when $p < 0.05$.

With $p < 0.05$ $H_0$ was rejected and the value of the trend was estimated by the Theil-Sen slope estimator:

$$\beta = median\left(\frac{y_j - y_i}{t_j - t_i}\right), \qquad j > i \qquad Eq.S2$$

where $t_i$ denotes the time $i$ of the observed value $y_i$.

The Theil-Sen slope is simply the median of all the forward concentration gradients. In addition to the slope, the 2σ confidence intervals were calculated according to Gilbert (1987), providing the 95 % confidence range of the slopes.

The Mann-Kendall test and Theil-Sen slope estimation were applied to all species and ratios discussed in this work. These calculations were based on the seasonal and annual mean values, separately, as presented below. For the ratios, r = x/y (e.g. the fraction of $NO_3^-$ in $PM_{10}$), we based the calculations on the ratios of the seasonal means and not on the seasonal means of the ratios, i.e.:

$$r = \frac{x}{y}, where\ x = \frac{1}{n}\sum(x_i)\ and\ y = \frac{1}{n}\sum(y_i) \qquad Eq.S3$$

For all cases where the 0-hypothesis ($H_0$) could be rejected, the Theil-Sen slopes were calculated, and this slope was further transferred into the relative trend by dividing the trend (β) by the mean of the observed values:

$$\beta_{rel} = \frac{\beta}{\left[\frac{1}{n}\sum(y_i)\right]}, where\ y_i = observed\ concentration\ or\ ratio\ at\ time\ i \qquad Eq.S4$$

## S3. Absorption coefficent measurements and source apportionment

The absorption coefficient ($B_{Abs}$) was measured using the multi wavelength (λ=370; 470; 520; 590; 660; 880; 950 nm) aethalometer (AE33, Magee Scientific), operating behind a $PM_{10}$ inlet. We calculate absorption coefficients ($B_{Abs}$) according to Drinovec et al. (2015):

$$B_{Abs}(\lambda) = \frac{A\cdot\left(\frac{ATN_{t2}(\lambda) - ATN_{t1}(\lambda)}{100}\right)}{Q\cdot C\cdot(1-\zeta)\cdot\left(1-k(\lambda)\cdot\left(ATN_{t2}(\lambda) - ATN_{ref}(\lambda)\right)\right)\cdot(t_2 - t_1)} \qquad Eq.\ S5$$

where $ATN$ = attenuation at time $t$ =1 and $t$ =2, and of the reference spot *ref*, $Q$ is the instrument flow rate on spot 1, $A$ is the filter spot area, $k$ is the loading compensation parameter from the 2 spot compensation algorithm. Here we neglect lateral air flow losses (ζ) and the scattering compensation $C$

since these are not wavelength dependent in Eq. (S5) and hence do not affect source apportionment based on wavelength dependence, while conversion to eBC via co-located filter measurements of EC also results in compensation of these parameters using:

$$\mathrm{eBC}(\lambda) = B_{Abs}(\lambda) / \alpha_{\mathrm{effective}}(\lambda) \qquad Eq.S6$$

where $\alpha_{\mathrm{effective}}$ is an effective mass absorption cross section (α) incorporating scattering and lateral flow losses:

$$\alpha_{effective}(\lambda) = \alpha(\lambda) \times c \times (1 - \zeta) \qquad Eq.S7$$

Hence $\alpha_{effective}$ is a conversion factor between $B_{Abs}$ and eBC and has no physical meaning beyond this.

The AE33 of this study automatically generates $B_{Abs}(\lambda)$ at 1-minute resolution. However, as discussed by Springston et al. (2007) and Backman et al. (2017), the time interval $(t_2 - t_1)$ Eq.(S5) can be adjusted to any integer multiple of the base resolution in post-processing. Here we adopt the approach of Backman et al. (2017), fixing the time interval to 1 hour and calculating $B_{Abs}(\lambda)$ according to Eq. (S5). In case one or more filter advances occurred within the one-hour interval, data from each individual filter spot falling within the interval were treated separately and a time-weighted average recorded for that hour. The advantage of this technique is enhanced noise reduction, i.e. using the one-hour interval approach the noise reduction is proportional to as much as *1/n* (where *n* are the measurement points), rather than *1/sqrt(n),* attainable via signal averaging.

Here we performed source apportionment of aethalometer data using the *aethalometer model* (Sandradewi et al., 2008). Assuming two sources contribute to total Babs ($B_{Abs,Tot}$), i.e. fossil fuel combustion ($B_{Abs,ff}$) and biomass burning ($B_{Abs,bb}$):

$$B_{Abs,Tot} = B_{Abs,ff} + B_{Abs,bb} \qquad Eq.\ S8$$

Then, using a wavelength pair, here $\lambda_1$=470 nm and $\lambda_2$=880 nm,

$$B_{Abs,bb}(\lambda_2) = \frac{B_{Abs}(\lambda_1) - B_{Abs}(\lambda_2) \cdot \left(\frac{\lambda_1}{\lambda_2}\right)^{-\alpha_{ff}}}{\left(\frac{\lambda_1}{\lambda_2}\right)^{-\alpha_{bb}} - \left(\frac{\lambda_1}{\lambda_2}\right)^{-\alpha_{ff}}} \qquad Eq.\ S9 \text{ and}$$

$$B_{Abs,ff}(\lambda_2) = \frac{B_{Abs}(\lambda_1) - B_{Abs}(\lambda_2) \cdot \left(\frac{\lambda_1}{\lambda_2}\right)^{-\alpha_{bb}}}{\left(\frac{\lambda_1}{\lambda_2}\right)^{-\alpha_{ff}} - \left(\frac{\lambda_1}{\lambda_2}\right)^{-\alpha_{bb}}} \qquad Eq.\ S10$$

where $\alpha_{ff}$ and $\alpha_{bb}$ are the absorption Ångstrøm exponents (AAE) for fossil fuel and biomass burning, respectively. Note that when using this approach, the AAEs must be assumed *a priori,* while the data are not fitted or error weighted, which can lead to negative values in the resulting time series of the factors due to uncertainty in the AAEs e.g. Grange et al. (2020).

Here we also used positive matrix factorisation (PMF) to distinguish between the two sources in Eq. (S8). The theory of PMF is detailed elsewhere (Paatero and Tapper, 1994) Briefly, a matrix of measurement data $X$ is represented by a bilinear model comprising factor profiles $F$ (rows), factor time

series $G$ (columns) and a residual matrix $E$:

$$X = G \cdot F + E \qquad Eq.\ S11$$

In PMF factors are found using a least-squares fitting routine in which the object function $Q$, i.e. the square of residuals $e$ weighted to uncertainty $\sigma$, is mimimised across all cells (rows $i$-$m$, columns $j$-$n$)

$$Q^m = \sum_{i=1}^{m} \sum_{j=1}^{n} \left(\frac{e_{ij}}{\sigma_{ij}}\right)^2 \qquad Eq.\ \text{S12}$$

Here, we use the source finder (SoFi, (Canonaco et al., 2013)) toolkit ref, to call PMF (To model the error matrix $\sigma_{ij}$ we use the clean air test function of the AE33 to determine the standard deviation of the attenuation of the blank $\delta_{ATN_{air}}$, calculating $\sigma_{ij}$, using:

$$\sigma_{ij} = \sqrt{f_A^2 + f_Q^2 + 2\left(\frac{\delta_{ATN_{air}}(\lambda_j)}{ATN_i(\lambda_j)}\right)^2 + \left(\frac{\delta_{ATN_{air}}(\lambda_j)}{ATN_{i-1}(\lambda_j)}\right)^2 + \left(\frac{\delta_{ATN_{air}}(\lambda_j)}{ATN_{ref}(\lambda_J)}\right)^2} \cdot B_{Abs,i}(\lambda_j) \qquad Eq.S13$$

where $f_A$ and $f_Q$ are the fractional uncertainties in the spot area and the flow rate, respectively (both 0.015 according to Backman et al., 2017). Clean air tests were performed only periodically. Therefore, to generate an error estimate for all time points, we interpolated (bilinear interpolation) between the clean air tests to generate the full error matrix, accounting for drift in $\delta_{ATN_{air}}$. Points before and after the last clean air test were calculated using the first and last values of $\delta_{ATN_{air}}$, respectively.

According to Eq. (S11), $X$ could be represented by any combination of $G$ and $F$, i.e. the PMF model has *rotational ambiguity.* In practice, many rotations produce negative values and are thus forbidden. Nevertheless, many rotations and local minima in Eq. (S11) are likely to exist. To assess this, we generated multiple ($n$=2000) bootstrap replacement matrices (block size 24 to conserve diurnal variation if present), running PMF on each matrix 5 times for a total of 10000 runs. PMF settings are shown in Table S 2.

We import all 2000 files generated using SoFi for each factor solution. To map the factors, we calculated an effective AAE from the factor profiles $\alpha_F$, using

$$\alpha_F = -\frac{\log\left(F_{j=2} / F_{j=6}\right)}{\log\left(470/880\right)} \qquad Eq.S14$$

sorting factors and time series from each run from low to high with respect to $\alpha_F$. Binning the effective AAEs from each factor also provides a convenient means to investigate the solution space for rotational

ambiguity.

## S4. Positive matrix factorisation applied to filter data

We performed PMF for samples collected in 2016-2018 (151 samples), with the following as input data: OC (in $PM_{2.5}$ and $PM_{10-2.5}$), EC (in $PM_{10}$), levoglucosan, mannosan, galactosan, arabitol, mannitol, trehalose, glucose, V, Mn, Ti, Fe, Co, Ni, Cu, Zn, As, Cd, and Pb (all in $PM_{10}$), $SO_4^{2}$, $NO_3^{-}$, $NH_4^{+}$, $Ca^{2+}$, $Mg^{2+}$, $K^{+}$, $Na^{+}$, $Cl^{-}$ (open filter face).

Table S 3 shows miscellaneous settings of the PMF analysis of these data. The input data and error estimates were prepared using the procedure suggested by Polissar et al. (1998) and Norris et al. (2014), see also Table S 3 for miscellaneous settings including missing data treatment and assessment of the PMF performance.

If the concentration was greater than the LOD, the calculation was based on a user provided fraction of the concentration and LOD:

$$Unc = \sqrt{(Error\ Fraction \times Concentration)^2 + (\frac{1}{2} \times LOD)^2} \qquad Eq.S15$$

The analytical uncertainties (20%) as error fraction of OC, EC, organic tracers, ions, and elements were used to determine the corresponding error estimates. Based on given understanding of OC sources, 2–10 factors with random seeds were examined, and 7 factors were determined based on: 1) The decrease in Q/Qexp was larger than the relative change in number of factors up to 7; 2) All factors could be interpreted; 3) All factors were distinct.

To assess the statistical uncertainty in the model we performed repeated analyses on bootstrap-resampled matrices. A base profile was generated from a manually mapped average of 50 runs. From each bootstrap run, we fitted all 7 bootstrap factors vs all 7 factors from the base run profile (representing a 7×7 matrix of $r^2$ values). We then mapped the bootstrap factors in order of the $r^2$ value: The highest value was assumed to be a match, then then the next highest value excluding both previously mapped factors to any other factor (representing a 6×6 matrix of $r^2$ values), and so on. This was to avoid any factors being mapped twice.

The minimal robust and true Q values of the base run were 5507.9 and 5580.8, respectively. All the (error) scaled residuals were within ±5 and > 97.8% within ± 3, normally distributed and centred around zero. The average Q/Qexp was 1.2. We also observe no structure in the residuals, which were evenly distributed between measurements from different instruments (i.e. we did not observe factors representing groups of compounds by instrument type, Figure S 3).

## S5. Emission ratios used to calculate OC and EC from biomass burning

Emission ratios derived from ambient data are a good alternative to direct emission measurements, accounting for the aggregate effects of fuel type and combustion conditions, but results will nevertheless vary from region to region (e.g. Zotter et al., 2014). Here, we used ratios from our PMF analysis (Table 1) to calculate carbonaceous aerosol from biomass burning for 2008–2018. The levoglucosan to mannosan ratio is rather consistent between seasons, with the values for summer (5.1±0.9) and fall (5.2±0.7) being slightly lower than for winter (5.4±0.8) and spring (6.0±0.7). This might indicate that emissions from one source of biomass burning (wood burning for residential heating) dominate for all seasons, supporting the use of one levoglucosan to OC (and EC) ratio for calculations. The lower levoglucosan to mannosan ratio observed in summer and fall might indicate increased influence of wild and agricultural fires, but the magnitude of these sources remains speculative, except during severe episodes, e.g. in August 2002, May and September 2006, and June 2008.

## S6. Levels of PBAP and BSOA organic tracers

The annual mean concentration of the PBAP tracers ranged from 2.8–3.4 ng $m^{-3}$ (trehalose) to 4.8–5.8 ng $m^{-3}$ (arabitol) (2016–2018) (Figure 6, Table S 15). Levels were elevated in the vegetative season, particularly in summer and fall. Mannitol and arabitol were highly correlated ($R^2$=0.85), underlining their common origin, and the mannitol to arabitol ratio (0.9±0.2) corresponds well with previously reported results for these fungal spore tracers (e.g. Bauer et al., 2008; Yttri et al., 2007b; Yttri et al. 2011 a, b).

The annual mean concentration of 2-methylerythritol (0.365–0.441 ng $m^{-3}$) (2016–2018) was higher than that of 2-methylthreitol (0.105–162 ng $m^{-3}$), and the two isomers were highly correlated ($R^2$=0.915), which is consistent with other studies (e.g., Ion et al., 2005; Kourtchev et al., 2005; Edney et al., 2005; El Haddad et al., 2011; Alier et al., 2013). 2-methyltetrols were elevated in the period when deciduous trees have leaves (transition May/June to early October).

## References Supplementary


Aas, W., Mortier, A., Bowersox, V., Cherian, R., Faluvegi, G., Fagerli, H., Hand, J., Klimont, Z., Galy-Lacaux, C., Lehmann, C. M. B., Myhre, C. L., Myhre, G., Olivie, D., Sato, K., Quaas, J., Rao, P. S. P., Schulz, M., Shindell, D., Skeie, R. B., Stein, A., Takemura, T., Tsyro, S., Vet, R., and Xu, X. B.: Global and regional trends of atmospheric sulfur (vol 9, 953, 2019), Sci. Rep., 10, 10.1038/s41598-020-62441-w, 2020.

Alier, M., van Drooge, B. L., Dall'Osto, M., Querol, X., Grimalt, J. O., and Tauler, R.: Source apportionment of submicron organic aerosol at an urban background and a road site in Barcelona (Spain) during SAPUSS, Atmos. Chem. Phys., 13, 10353-10371, 10.5194/acp-13-10353-2013, 2013.

Backman, J., Schmeisser, L., Virkkula, A., Ogren, J. A., Asmi, E., Starkweather, S., Sharma, S.,

241 Eleftheriadis, K., Uttal, T., Jefferson, A., Bergin, M., Makshtas, A., Tunved, P., and Fiebig, M.: On
242 Aethalometer measurement uncertainties and an instrument correction factor for the Arctic, Atmos.
243 Meas. Techn., 10, 5039-5062, 10.5194/amt-10-5039-2017, 2017.

244 Bauer, H., Claeys, M., Vermeylen, R., Schueller, E., Weinke, G., Berger, A., and Puxbaum, H.: Arabitol
245 and mannitol as tracers for the quantification of airborne fungal spores, Atmos. Environ., 42, 588-593,
246 10.1016/j.atmosenv.2007.10.013, 2008.

247 Canonaco, F., Crippa, M., Slowik, J. G., Baltensperger, U., and Prevot, A. S. H.: SoFi, an IGOR-based
248 interface for the efficient use of the generalized multilinear engine (ME-2) for the source apportionment:
249 ME-2 application to aerosol mass spectrometer data, Atmos. Meas.Tech., 6, 3649-3661, 10.5194/amt-
250 6-3649-2013, 2013.

251 Cavalli, F., Viana, M., Yttri, K. E., Genberg, J., and Putaud, J.-P.: Toward a standardised thermal-optical
252 protocol for measuring atmospheric organic and elemental carbon: the EUSAAR protocol, Atmos.
253 Meas. Tech., 3, 79-89, 2010.

254 Chow, J. C., Watson, J. G., Chen, L. W. A., Paredes-Miranda, G., Chang, M. C. O., Trimble, D., Fung,
255 K. K., Zhang, H., and Yu, J. Z.: Refining temperature measures in thermal/optical carbon analysis,
256 Atmos. Chem. Phys., 5, 2961-2972, 10.5194/acp-5-2961-2005, 2005.

257 Ciarelli, G., Theobald, M. R., Vivanco, M. G., Beekmann, M., Aas, W., Andersson, C., Bergstrom, R.,
258 Manders-Groot, A., Couvidat, F., Mircea, M., Tsyro, S., Fagerli, H., Mar, K., Raffort, V., Roustan, Y.,
259 Pay, M. T., Schaap, M., Kranenburg, R., Adani, M., Briganti, G., Cappelletti, A., D'Isidoro, M.,
260 Cuvelier, C., Cholakian, A., Bessagnet, B., Wind, P., and Colette, A.: Trends of inorganic and organic
261 aerosols and precursor gases in Europe: insights from the EURODELTA multi-model experiment over
262 the 1990-2010 period, Geosci. Model Dev., 12, 4923-4954, 10.5194/gmd-12-4923-2019, 2019.

263 Coen, M. C., Andrews, E., Alastuey, A., Arsov, T. P., Backman, J., Brem, B. T., Bukowiecki, N., Couret,
264 C., Eleftheriadis, K., Flentje, H., Fiebig, M., Gysel-Beer, M., Hand, J. L., Hoffer, A., Hooda, R.,
265 Hueglin, C., Joubert, W., Keywood, M., Kim, J. E., Kim, S. W., Labuschagne, C., Lin, N. H., Lin, Y.,
266 Myhre, C. L., Luoma, K., Lyamani, H., Marinoni, A., Mayol-Bracero, O. L., Mihalopoulos, N., Pandolfi,
267 M., Prats, N., Prenni, A. J., Putaud, J. P., Ries, L., Reisen, F., Sellegri, K., Sharma, S., Sheridan, P.,
268 Sherman, J. P., Sun, J. Y., Titos, G., Torres, E., Tuch, T., Weller, R., Wiedensohler, A., Zieger, P., and
269 Laj, P.: Multidecadal trend analysis of in situ aerosol radiative properties around the world, Atmos.
270 Chem. Phys., 20, 8867-8908, 10.5194/acp-20-8867-2020, 2020.

271 Drinovec, L., Mocnik, G., Zotter, P., Prevot, A. S. H., Ruckstuhl, C., Coz, E., Rupakheti, M., Sciare, J.,
272 Muller, T., Wiedensohler, A., and Hansen, A. D. A.: The "dual-spot" Aethalometer: an improved

measurement of aerosol black carbon with real-time loading compensation, Atmos. Meas. Tech., 8, 1965-1979, 10.5194/amt-8-1965-2015, 2015.

Edney, E. O., Kleindienst, T. E., Jaoui, M., Lewandowski, M., Offenberg, J. H., Wang, W., and Claeys, M.: Formation of 2-methyl tetrols and 2-methylglyceric acid in secondary organic aerosol from laboratory irradiated isoprene/NOX/SO2/air mixtures and their detection in ambient PM2.5 samples collected in the eastern United States, Atmos. Environ., 39, 5281-5289, 10.1016/j.atmosenv.2005.05.031, 2005.

El Haddad, I., Marchand, N., Temime-Roussel, B., Wortham, H., Piot, C., Besombes, J. L., Baduel, C., Voisin, D., Armengaud, A., and Jaffrezo, J. L.: Insights into the secondary fraction of the organic aerosol in a Mediterranean urban area: Marseille, Atmos. Chem. Phys., 11, 2059-2079, 10.5194/acp-11-2059-2011, 2011.

EMEP: Standard Operating Procedures for thermal-optical analysis of atmospheric particulate organic and elemental carbon, in: EMEP manual for sampling and chemical analysis, EMEP/CCC 01/2014, NILU, Kjeller, Norway, chapter 4.22, 2014.

Fleming, Z. L., Doherty, R. M., von Schneidemesser, E., Malley, C. S., Cooper, O. R., Pinto, J. P., Colette, A., Xu, X. B., Simpson, D., Schultz, M. G., Lefohn, A. S., Hamad, S., Moolla, R., Solberg, S., and Feng, Z. Z.: Tropospheric Ozone Assessment Report: Present-day ozone distribution and trends relevant to human health, Elem. Sci. Anth., 6, 10.1525/elementa.273, 2018.

Grange, S. K., Lotscher, H., Fischer, A., Emmenegger, L., and Hueglin, C.: Evaluation of equivalent black carbon source apportionment using observations from Switzerland between 2008 and 2018, Atmos. Meas. Tech., 13, 1867-1885, 10.5194/amt-13-1867-2020, 2020.

Gilbert, R. O.: Statistical Methods for Environmental Pollution Monitoring, Wiley, NY, United States, pp. 336, 1987.

Ion, A. C., Vermeylen, R., Kourtchev, I., Cafmeyer, J., Chi, X., Gelencser, A., Maenhaut, W., and Claeys, M.: Polar organic compounds in rural $PM_{2.5}$ aerosols from K-puszta, Hungary, during a 2003 summer field campaign: Sources and diel variations, Atmos. Chem. Phys., 5, 1805-1814, 10.5194/acp-5-1805-2005, 2005.

Kendall, M. G.: Rank correlation methods, 4th edition, Charles Griffin, London, 1975.

Kourtchev, I., Ruuskanen, T., Maenhaut, W., Kulmala, M., and Claeys, M.: Observation of 2-methyltetrols and related photo-oxidation products of isoprene in boreal forest aerosols from Hyytiala,

303 Finland, Atmos. Chem. Phys., 5, 2761-2770, 10.5194/acp-5-2761-2005, 2005.

304 Lefohn, A. S., Malley, C. S., Smith, L., Wells, B., Hazucha, M., Simon, H., Naik, V., Mills, G., Schultz,
305 M. G., Paoletti, E., De Marco, A., Xu, X. B., Zhang, L., Wang, T., Neufeld, H. S., Musselman, R. C.,
306 Tarasick, D., Brauer, M., Feng, Z. Z., Tang, H. Y., Kobayashi, K., Sicard, P., Solberg, S., and Gerosa,
307 G.: Tropospheric ozone assessment report: Global ozone metrics for climate change, human health, and
308 crop/ecosystem research, Elem. Sci. Anth., 6, 10.1525/elementa.279, 2018.

309 Mann, H. B.: Non-parametric tests against trend, Econometrica 13:163-171, 1945.

310 Masiol, M., Squizzato, S., Rich, D. Q., and Hopke, P. K.: Long-term trends (2005-2016) of source
311 apportioned PM2.5 across New York State, Atmos. Environ., 201, 110-120,
312 10.1016/j.atmosenv.2018.12.038, 2019.

313 McDow, S. R. and Huntzicker, J. J.: Vapor adsorption artifact in the sampling of organic aerosol: face
314 velocity effects, Atmos. Environ., 24A, 2563–2571, 10.1016/0960-1686(90)90134-9, 1990.

315 Norris, G., Duvall, R., Brown, S., and Bai, S.: EPA Positive Matrix Factorization (PMF) 5.0
316 Fundamentals and User Guide, U.S. Environmental Protection Agency, Washington, DC, 20460 (i-124,
317 EPA/600/R-14/108, April), 2014.

318 Paatero, P. and Tapper, U.: Positive Matrix Factorization – A nonnegative factor model with optimal
319 utilization of error-estimates of data values. Environmetrics, 5, 111-126, DOI:
320 10.1002/env.3170050203, 1994.

321 Panteliadis, P., Hafkenscheid, T., Cary, B., Diapouli, E., Fischer, A., Favez, O., Quincey, P., Viana, M.,
322 Hitzenberger, R., Vecchi, R., Saraga, D., Sciare, J., Jaffrezo, J. L., John, A., Schwarz, J., Giannoni, M.,
323 Novak, J., Karanasiou, A., Fermo, P., and Maenhaut, W.: ECOC comparison exercise with identical
324 thermal protocols after temperature offset correction - instrument diagnostics by in-depth evaluation of
325 operational parameters, Atmos. Meas. Tech., 8, 779-792, 10.5194/amt-8-779-2015, 2015.

326 Pio, C. A., Legrand, M., Oliveira, T., Afonso, J., Santos, C., Caseiro, A., Fialho, P., Barata, F., Puxbaum,
327 H., Sanchez-Ochoa, A., Kasper-Giebl, A., Gelencser, A., Preunkert, S., and Schock, M.: Climatology
328 of aerosol composition (organic versus inorganic) at nonurban sites on a west-east transect across
329 Europe, J. Geophys. Res.-Atmos., 112, 10.1029/2006jd008038, 2007.

330 Polissar, A. V., Hopke, P. K., and Paatero, P.: Atmospheric aerosol over Alaska - 2. Elemental
331 composition and sources, J. Geophys. Res.-Atmos., 103, 19045-19057, 10.1029/98jd01212, 1998.

Sandradewi, J., Prevot, A. S. H., Szidat, S., Perron, N., Alfarra, M. R., Lanz, V. A., Weingartner, E., and Baltensperger, U.: Using aerosol light absorption measurements for the quantitative determination of wood burning and traffic emission contributions to particulate matter, Environ. Sci. Technol., 42, 3316-3323, 10.1021/es702253m, 2008.

Sen, P. K.: Estimates of the regression coefficient based on Kendall's Tau. J. Am., Stat. Assoc. 63 (324), 1379–1389, https://doi.org/10.2307/2285891, 1968.

Springston, S. R. and Sedlacek, A. J.: Noise characteristics of an instrumental particle absorbance technique, Aerosol Sci. and Techn.., 41, 1110-1116, 10.1080/02786820701777457, 2007.

Subramanian, R., Khlystov, A. Y., Cabada, J. C., and Robinson, A. L.: Positive and negative artifacts in particulate organic carbon measurements with denuded and undenuded sampler configurations, Aerosol Sci. Techn., 38, 27-48, 10.1080/02786820390229354, 2004.

Theil, H.: A rank-invariant method of linear and polynomial regression analysis. Proc. R. Netherlands, Acad. Sci. 53, 386–392, https://doi.org/10.1007/978-94-011-2546-8_20, 1950.

Theobald, M. R., Vivanco, M. G., Aas, W., Andersson, C., Ciarelli, G., Couvidat, F., Cuvelier, K., Manders, A., Mircea, M., Pay, M. T., Tsyro, S., Adani, M., Bergstrom, R., Bessagnet, B., Briganti, G., Cappelletti, A., D'Isidoro, M., Fagerli, H., Mar, K., Otero, N., Raffort, V., Roustan, Y., Schaap, M., Wind, P., and Colette, A.: An evaluation of European nitrogen and sulfur wet deposition and their trends estimated by six chemistry transport models for the period 1990-2010, Atmos. Chem. Phys., 19, 379-405, 10.5194/acp-19-379-2019, 2019.

Torseth, K., Aas, W., Breivik, K., Fjaeraa, A. M., Fiebig, M., Hjellbrekke, A. G., Myhre, C. L., Solberg, S., and Yttri, K. E.: Introduction to the European Monitoring and Evaluation Programme (EMEP) and observed atmospheric composition change during 1972-2009, Atmos. Chem. Phys., 12, 5447-5481, 10.5194/acp-12-5447-2012, 2012.

Turpin, B. J., Huntzicker, J. J., and Hering, S. V.: Investigation of organic aerosol sampling artifacts in the Los-Angeles basin, Atmos. Environ., 28, 3061-3071, 10.1016/1352-2310(94)00133-6, 1994.

Wallen, A., Liden, G., and Hansson, H. C.: Measured Elemental Carbon by Thermo-Optical Transmittance Analysis in Water-Soluble Extracts from Diesel Exhaust, Woodsmoke, and Ambient Particulate Samples, J. Occup. Environ. Hyg., 7, 35-45, 10.1080/15459620903368859, 2010.

Yang, H. and Yu, J. Z.: Uncertainties in charring correction in the analysis of elemental and organic carbon in atmospheric particles by thermal/optical methods, Environ. Sci. Technol., 36, 5199-5204,

10.1021/es025672z, 2002.

Yttri, K. E., Dye, C., and Kiss, G.: Ambient aerosol concentrations of sugars and sugar-alcohols at four different sites in Norway, Atmos. Chem. Phys., 7, 4267-4279, 2007b.

Yttri, K. E., Aas, W., Bjerke, A., Cape, J. N., Cavalli, F., Ceburnis, D., Dye, C., Emblico, L., Facchini, M. C., Forster, C., Hanssen, J. E., Hansson, H. C., Jennings, S. G., Maenhaut, W., Putaud, J. P., and Torseth, K.: Elemental and organic carbon in $PM_{10}$: a one year measurement campaign within the European Monitoring and Evaluation Programme EMEP, Atmos. Chem. Phys., 7, 5711-5725, 2007a.

Yttri, K. E., Simpson, D., Bergstrom, R., Kiss, G., Szidat, S., Ceburnis, D., Eckhardt, S., Hueglin, C., Nojgaard, J. K., Perrino, C., Pisso, I., Prevot, A. S. H., Putaud, J. P., Spindler, G., Vana, M., Zhang, Y. L., and Aas, W.: The EMEP Intensive Measurement Period campaign, 2008-2009: characterizing carbonaceous aerosol at nine rural sites in Europe, Atmos. Chem. Phys., 19, 4211-4233, 10.5194/acp-19-4211-2019, 2019.

Yttri, K. E., Simpson, D., Nojgaard, J. K., Kristensen, K., Genberg, J., Stenstrom, K., Swietlicki, E., Hillamo, R., Aurela, M., Bauer, H., Offenberg, J. H., Jaoui, M., Dye, C., Eckhardt, S., Burkhart, J. F., Stohl, A., and Glasius, M.: Source apportionment of the summer time carbonaceous aerosol at Nordic rural background sites, Atmos. Chem. Phys., 11, 13339-13357, 10.5194/acp-11-13339-2011, 2011b.

Yttri, K. E., Simpson, D., Stenstrom, K., Puxbaum, H., and Svendby, T.: Source apportionment of the carbonaceous aerosol in Norway - quantitative estimates based on C-14, thermal-optical and organic tracer analysis, Atmos. Chem. Phys., 11, 9375-9394, 10.5194/acp-11-9375-2011, 2011a.

Yttri, K. E., Schnelle-Kreis, J., Maenhaut, W., Abbaszade, G., Alves, C., Bjerke, A., Bonnier, N., Bossi, R., Claeys, M., Dye, C., Evtyugina, M., Garcia-Gacio, D., Hillamo, R., Hoffer, A., Hyder, M., Iinuma, Y., Jaffrezo, J.-L., Kasper-Giebl, A., Kiss, G., Lopez-Mahia, P. L., Pio, C., Piot, C., Ramirez-Santa-Cruz, C., Sciare, J., Teinila, K., Vermeylen, R., Vicente, A., and Zimmermann, R.: An intercomparison study of analytical methods used for quantification of levoglucosan in ambient aerosol filter samples, Atmos. Meas. Tech., 8, 125-147, 10.5194/amt-8-125-2015, 2015.

Zotter, P., Ciobanu, V. G., Zhang, Y. L., El-Haddad, I., Macchia, M., Daellenbach, K. R., Salazar, G. A., Huang, R. J., Wacker, L., Hueglin, C., Piazzalunga, A., Fermo, P., Schwikowski, M., Baltensperger, U., Szidat, S., and Prevot, A. S. H.: Radiocarbon analysis of elemental and organic carbon in Switzerland during winter-smog episodes from 2008 to 2012-Part 1: Source apportionment and spatial variability, Atmos. Chem. Phys., 14, 13551-13570, 10.5194/acp-14-13551-2014, 2014.

## Supplementary Figures

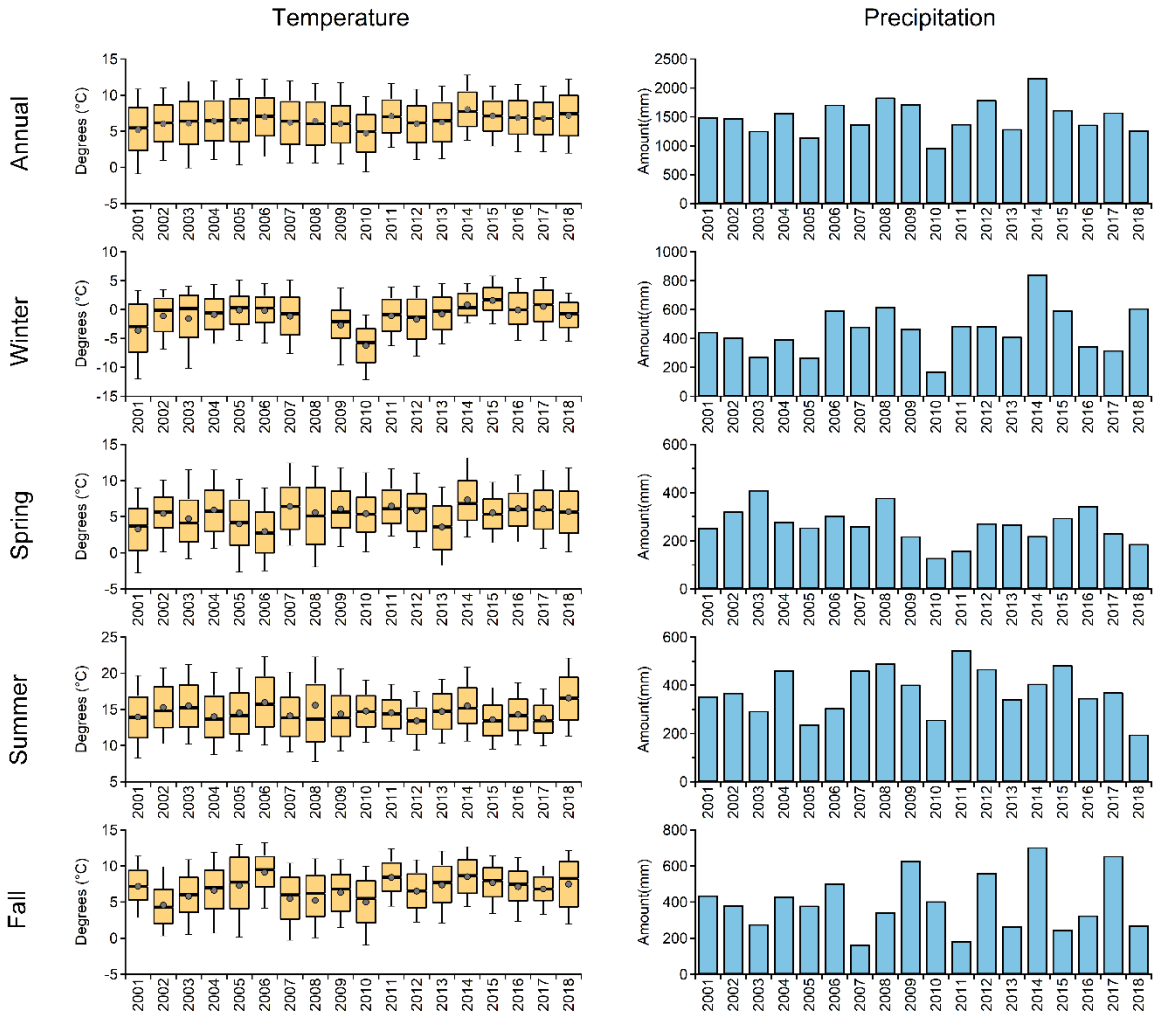


**Figure S 1: Annual and seasonal ambient mean (point), 10th to 25th percentile (bar), 50th percentile (line), 75th to 90th percentile (whisker) temperature (left panel) and precipitation (right panel) at the Birkenes Observatory, 2001–2018.**

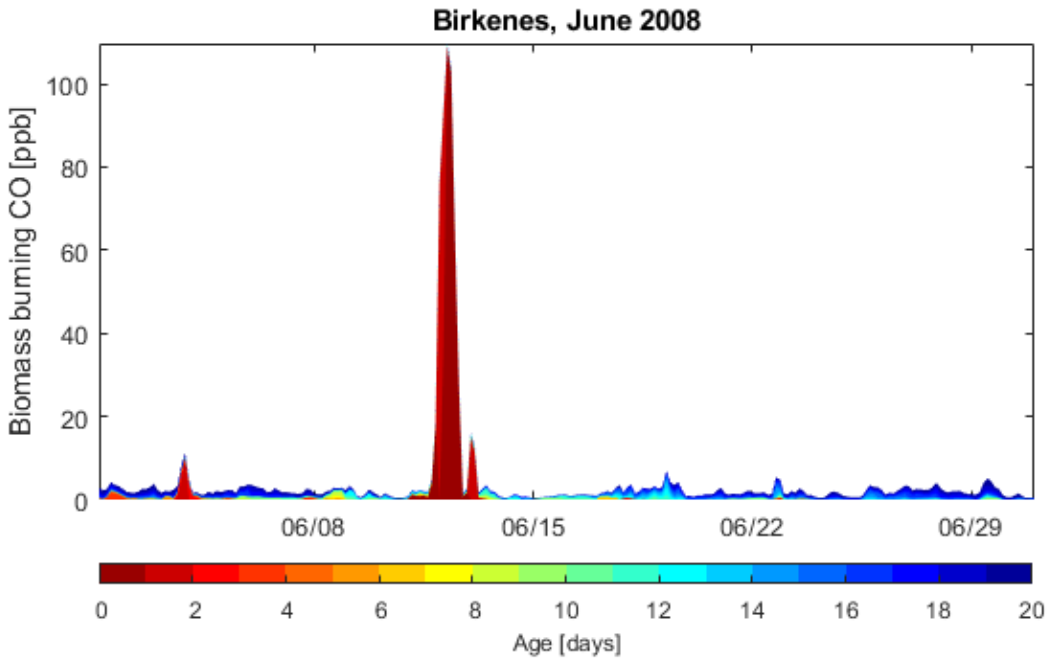


**Figure S 2: Age spectra for June 2008 for the CO tracer originating from wildfires calculated for the Birkenes Observatory. We ran a 20 days FLEXPART simulation backwards in time, releasing 40 000 particles for the Birkenes Observatory on a 3-hourly basis, using ECMWF meteorology. With daily MODIS information of burned area we constructed a CO emission inventory, which we combined with the model simulation. With this approach we achieved a time series of CO from wildfires with a 3-hourly time resolution. Additionally, we split the modeled CO concentrations by age. The spectrum goes from 1 to 20 days after release according to the bar. This approach is described in more detail in Stohl et al. (2007). For most of June 2008, concentrations of a few ppb were calculated for the Birkenes Observatory, except for 11–12 of June (100 ppb). The age of the airmasses were only 1 day, which means that the CO was released on a location less than 24 hours before it reached the site.**

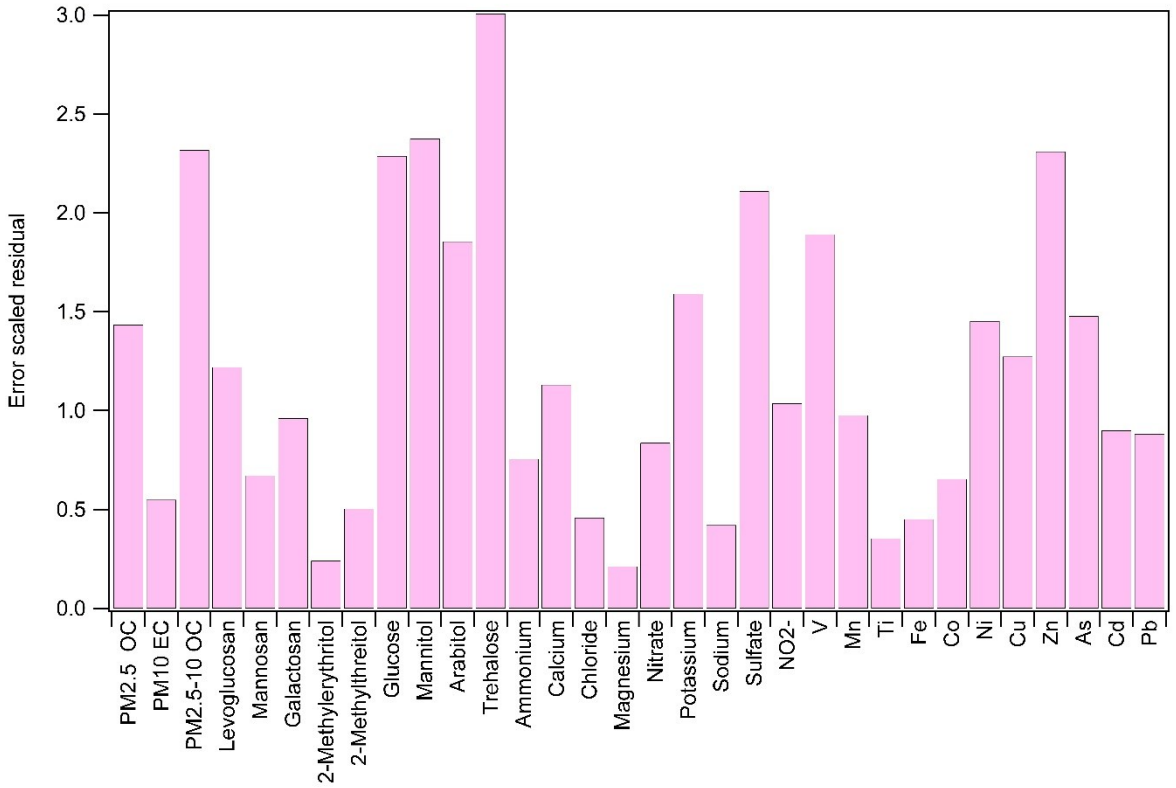


**Figure S 3: Average error scaled residuals for each of the variables in the PMF solution presented in this paper**

## Supplementary Tables

**Table S 1: Species quantification ion, molecular weight and formula, and internal/recovery and quantification standards used for identification and quantification.**

| Species | Quantitation ion M-H(+) | Molecular weight | Molecular formula | Internal/ Recovery standard | Quantification standard |
|---|---|---|---|---|---|
| ***Monosaccharide anhydrides*** | | | | | |
| Galactosan | 161.046 | 162.141 | $C_6H_{10}O_5$ | $^{13}C_6$-Galactosan (CIL; 98%; Andover, MA) | Galactosan (Sigma; purity not given; Product of England) |
| Mannosan | 161.046 | 162.141 | $C_6H_{10}O_5$ | $^{13}C_6$-Levoglucosan[1] $^{13}C_6$-Galactosan[1] | Mannosan (Sigma; Approx 98%; Product of England) |
| Levoglucosan | 161.046 | 162.141 | $C_6H_{10}O_5$ | $^{13}C_6$-Levoglucosan (CIL; 98%; city not given) | Levoglucosan (Aldrich; 99%; Product of Switzerland) |
| ***Sugar-alcohols*** | | | | | |
| Mannitol | 181.072 | 182.172 | $C_6H_{14}O_6$ | $^{13}C_6$-Mannitol (Omnicron Biochemicals Inc; 99.70%; South Bend, Indiana) | Mannitol (ICN Biochemicals; ACS reagent grade; Aurora, Ohio) |
| Arabitol | 151.061 | 152.15 | $C_5H_{12}O_6$ | $^{13}C_5$-Arabitol (Omnicron Biochemicals Inc; 99.60%; South Bend, Indiana) | Arabitol (ICN Biochemicals; purity not given; Aurora, Ohio) |
| ***2-methyltetrols*** | | | | | |
| 2-Methylerythritol | 135.066 | 136.147 | $C_5H_{12}O_4$ | $^{13}C_6$-Galactosan (CIL; 98%; Andover, MA) | 2-Methylerythritol, Produced at UNC[2] |
| 2-Methylthreitol | 135.066 | 136.147 | $C_5H_{12}O_4$ | $^{13}C_6$-Galactosan (Brand; purity; city) | 2-Methylthreitol, Produced at UNC[2] |
| ***Dimeric sugars*** | | | | | |
| Trehalose | 341.109 | 342.296 | $C_{12}H_{22}O_{11}$ | $^{13}C_{12}$-Trehaose (Omnicron Biochemicals Inc; 99.70%; South Bend, Indiana) | Trehalose (Fluka; <99.5%; Packed in Switzerland) |
| ***Monomeric sugars*** | | | | | |
| Glucose | 179.0561 | 180.16 | $C_6H_{12}O_6$ | $^{13}C_1$-Glucose (CIL; 99%; Andover, MA) | Glucose (Sigma; purity not given; city not given) |

1.C-labelled mannosan is not commersially available, hence we used the average of $^{13}C_6$-Levoglucosan $^{13}C_6$-Galactosan to calculate the recovery of mannosan.

2.Standard produced by University of North Carolina (UNC)

**Table S 2: Settings used for absorption coefficient PMF analysis.**

| **Parameter** | **Setting** |
|---|---|
| Data matrix dimensions i×j | 5240×7 |
| Missing data treatment | Rows removed |
| Number of factors | 2 |
| Factor constraints | None |
| Robust mode setting | 4 |
| Seed | Random |
| Bootstrap replacement runs | 2000 |
| Block size | 24 |
| Repeat runs (per bootstrap) | 5 |

**Table S 3: Miscellaneous settings of PMF analysis.**

| Parameter | Setting |
|---|---|
| Data matrix dimensions i×j | 151×34 |
| Missing data and below detection limit data | Replaced with geometric mean concentration |
| Missing data error estimate | Replaced with 4 × geometric mean concentration |
| Missing data error estimate | 5/6 × limit of detection |
| Number of factors | 7 |
| Factor contsraints | None |
| Robust mode setting | 4 |
| Seed | Random |
| Bootstrap replacement runs | 5000 |
| Block size | 1 row |
| Repeat runs (per bootstrap) | 5 |

12 **Table S 4: Contribution weighted relative profiles for PMF–derived factors (%).**

| | Mineral Dust (MIN) | Traffic/Industry (TRA/IND) | Biogenic Secondary Organic Aerosol ($BSOA_{SRT}$) | Primary Biological Aerosol Particle (PBAP) | Sea salt aerosol (SS) | Biomass burning (BB) | Ammonium Nitrate ($NH_4NO_3$) |
|---|---|---|---|---|---|---|---|
| **$PM_{2.5}$ OC** | 31.3 | 9.7 | 9.1 | 15.6 | 0.9 | 16.7 | 16.6 |
| **$PM_{10}$ EC** | 12.8 | 50.0 | 0.0 | 2.6 | 0.0 | 21.2 | 13.4 |
| **$PM_{10-2.5}$ OC** | 12.6 | 3.5 | 12.5 | 53.0 | 0.1 | 6.3 | 12.0 |
| **Levoglucosan** | 0.2 | 0.0 | 1.5 | 0.5 | 0.0 | 97.8 | 0.0 |
| **Mannosan** | 0.0 | 0.5 | 1.5 | 1.5 | 0.0 | 95.6 | 0.9 |
| **Galactosan** | 0.0 | 3.5 | 0.0 | 0.0 | 1.1 | 95.5 | 0.0 |
| **2-methylerythritol** | 0.5 | 0.7 | 95.9 | 1.8 | 0.0 | 0.4 | 0.7 |
| **2-methylthreitol** | 0.6 | 1.3 | 91.5 | 3.2 | 0.7 | 1.5 | 1.2 |
| **Glucose** | 1.0 | 0.6 | 6.5 | 81.6 | 2.0 | 5.2 | 3.1 |
| **Mannitol** | 0.1 | 0.3 | 6.1 | 91.3 | 1.7 | 0.0 | 0.5 |
| **Arabitol** | 0.0 | 0.0 | 8.6 | 89.5 | 1.3 | 0.5 | 0.0 |
| **Trehalose** | 0.5 | 0.0 | 3.3 | 93.5 | 1.1 | 0.7 | 0.9 |
| **Ammonium** | 2.1 | 13.9 | 4.8 | 0.0 | 1.5 | 1.0 | 76.7 |
| **Calcium** | 39.0 | 6.0 | 7.7 | 3.9 | 34.9 | 1.0 | 7.6 |
| **Chloride** | 0.0 | 0.0 | 0.0 | 0.0 | 96.2 | 0.2 | 3.5 |
| **Magnesium** | 5.8 | 2.7 | 3.9 | 1.8 | 79.0 | 0.6 | 6.2 |
| **Nitrate** | 0.8 | 3.6 | 5.7 | 3.4 | 17.1 | 1.7 | 67.8 |
| **Potassium** | 3.6 | 12.7 | 4.6 | 8.3 | 28.4 | 10.4 | 32.0 |
| **Sodium** | 2.2 | 5.1 | 2.7 | 0.0 | 86.8 | 0.3 | 3.0 |
| **Sulfate** | 3.9 | 19.6 | 17.2 | 3.3 | 17.4 | 3.4 | 35.2 |
| **$NO_2^-$** | 7.2 | 15.0 | 4.6 | 4.6 | 20.0 | 19.0 | 29.7 |
| **V** | 14.1 | 70.1 | 10.1 | 0.0 | 0.0 | 0.0 | 5.8 |
| **Mn** | 51.9 | 38.6 | 0.6 | 5.7 | 2.4 | 0.8 | 0.0 |
| **Ti** | 93.4 | 0.5 | 0.6 | 0.0 | 3.7 | 1.8 | 0.0 |
| **Fe** | 74.5 | 18.4 | 0.0 | 3.2 | 0.7 | 1.0 | 2.1 |
| **Co** | 42.6 | 42.1 | 1.3 | 3.3 | 5.0 | 2.4 | 3.4 |
| **Ni** | 17.1 | 68.6 | 3.0 | 4.5 | 1.7 | 2.1 | 2.9 |

| | Mineral Dust (MIN) | Traffic/Industry (TRA/IND) | Biogenic Secondary Organic Aerosol ($BSOA_{SRT}$) | Primary Biological Aerosol Particle (PBAP) | Sea salt aerosol (SS) | Biomass burning (BB) | Ammonium Nitrate ($NH_4NO_3$) |
|---|---|---|---|---|---|---|---|
| **Cu** | 19.9 | 61.9 | 3.3 | 3.7 | 5.7 | 1.3 | 4.2 |
| **Zn** | 4.3 | 81.5 | 1.4 | 0.6 | 0.0 | 5.8 | 6.4 |
| **As** | 3.2 | 78.4 | 1.7 | 6.2 | 0.0 | 4.8 | 5.7 |
| **Cd** | 5.4 | 80.5 | 0.1 | 2.3 | 1.6 | 6.4 | 3.8 |
| **Pb** | 4.5 | 83.9 | 0.8 | 0.0 | 1.5 | 2.8 | 6.4 |

13

**Table S 5: Annual and seasonal mean concentrations of EC and OC in $PM_{10}$, $PM_{2.5}$ and $PM_{10-2.5}$ at Birkenes for 2001–2018 (Unit: $\mu g\ C\ m^{-3}$).**

| | $PM_{10}$ | | | | $PM_{10-2.5}$ | | $PM_{2.5}$ | | | |
|---|---|---|---|---|---|---|---|---|---|---|
| | OC | Capture | EC | Capture | OC | Capture | OC | Capture | EC | Capture |
| ***2001*** | ***0.96*** | ***56*** | ***0.14*** | ***56*** | ***0.08*** | ***45*** | ***0.93*** | ***56*** | ***0.15*** | ***56*** |
| DJF | 0.60 | 59 | 0.12 | 59 | NA | 34 | 0.64 | 59 | 0.12 | 59 |
| MAM | 0.98 | 92 | 0.16 | 92 | 0.03 | 73 | 1.00 | 92 | 0.18 | 92 |
| JJA | 2.34 | 26 | 0.16 | 26 | 0.24 | 26 | 2.1 | 26 | 0.20 | 26 |
| SON | 0.58 | 48 | 0.10 | 48 | 0.09 | 48 | 0.49 | 48 | 0.11 | 48 |
| ***2002*** | ***1.01*** | ***85*** | ***0.14*** | ***85*** | ***0.190*** | ***80*** | ***0.89*** | ***91*** | ***0.12*** | ***91*** |
| DJF | 0.53 | 95 | 0.12 | 95 | 0.05 | 88 | 0.49 | 95 | 0.12 | 95 |
| MAM | 1.30 | 92 | 0.17 | 92 | 0.12 | 92 | 1.19 | 92 | 0.14 | 92 |
| JJA | 1.77 | 68 | 0.20 | 68 | 0.48 | 68 | 1.4 | 91 | 0.14 | 91 |
| SON | 0.59 | 86 | 0.10 | 86 | 0.16 | 73 | 0.49 | 85 | 0.09 | 85 |
| ***2003*** | ***1.01*** | ***82*** | ***0.10*** | ***82*** | ***0.23*** | ***77*** | ***0.81*** | ***81*** | ***0.11*** | ***81*** |
| DJF | 0.83 | 85 | 0.11 | 85 | 0.06 | 76 | 0.84 | 85 | 0.12 | 85 |
| MAM | 1.13 | 86 | 0.13 | 86 | 0.21 | 76 | 1.02 | 86 | 0.15 | 86 |
| JJA | 1.26 | 85 | 0.08 | 85 | 0.44 | 85 | 0.82 | 85 | 0.09 | 85 |
| SON | 0.75 | 70 | 0.09 | 70 | 0.22 | 70 | 0.53 | 70 | 0.09 | 70 |
| ***2004*** | ***0.82*** | ***85*** | ***0.10*** | ***85*** | ***0.27*** | ***81*** | ***0.57*** | ***84*** | ***0.09*** | ***84*** |
| DJF | 0.57 | 86 | 0.08 | 86 | 0.09 | 86 | 0.48 | 86 | 0.08 | 86 |
| MAM | 1.13 | 86 | 0.12 | 86 | 0.28 | 73 | 0.79 | 86 | 0.12 | 86 |
| JJA | 0.99 | 79 | 0.10 | 79 | 0.38 | 79 | 0.61 | 79 | 0.08 | 79 |
| SON | 0.71 | 86 | 0.08 | 86 | 0.32 | 86 | 0.39 | 86 | 0.08 | 80 |
| ***2005*** | ***0.85*** | ***79*** | ***0.14*** | ***79*** | ***0.29*** | ***75*** | ***0.60*** | ***80*** | ***0.12*** | ***80*** |
| DJF | 0.46 | 64 | 0.10 | 64 | 0.06 | 51 | 0.53 | 71 | 0.11 | 71 |
| MAM | 0.78 | 85 | 0.13 | 86 | 0.15 | 85 | 0.63 | 85 | 0.12 | 85 |
| JJA | 0.92 | 86 | 0.09 | 85 | 0.33 | 86 | 0.59 | 86 | 0.08 | 86 |
| SON | 1.16 | 79 | 0.25 | 79 | 0.53 | 79 | 0.62 | 79 | 0.16 | 79 |
| ***2006*** | ***1.07*** | ***78*** | ***0.13*** | ***78*** | ***0.33*** | ***75*** | ***0.77*** | ***78*** | ***0.13*** | ***78*** |
| DJF | 0.79 | 86 | 0.12 | 86 | 0.08 | 79 | 0.71 | 86 | 0.17 | 86 |
| MAM | 0.95 | 85 | 0.08 | 85 | 0.16 | 78 | 0.82 | 85 | 0.14 | 85 |
| JJA | 1.43 | 57 | 0.12 | 57 | 0.48 | 57 | 0.96 | 57 | 0.10 | 57 |
| SON | 1.24 | 86 | 0.19 | 86 | 0.60 | 86 | 0.64 | 86 | 0.11 | 86 |
| ***2007*** | ***0.82*** | ***79*** | ***0.15*** | ***77*** | ***0.21*** | ***77*** | ***0.61*** | ***77*** | ***0.13*** | ***77*** |
| DJF | 0.58 | 58 | 0.17 | 58 | 0.08 | 58 | 0.50 | 58 | 0.17 | 58 |
| MAM | 0.99 | 86 | 0.18 | 85 | 0.17 | 86 | 0.82 | 86 | 0.15 | 86 |
| JJA | 1.03 | 86 | 0.13 | 86 | 0.39 | 79 | 0.66 | 79 | 0.10 | 79 |
| SON | 0.60 | 86 | 0.13 | 79 | 0.18 | 86 | 0.41 | 86 | 0.10 | 86 |
| ***2008*** | ***0.75*** | ***87*** | ***0.09*** | ***84*** | ***0.24*** | ***75*** | ***0.53*** | ***88*** | ***0.08*** | ***88*** |
| DJF | 0.44 | 90 | 0.08 | 83 | 0.07 | 82 | 0.38 | 90 | 0.09 | 84 |
| MAM | 0.79 | 86 | 0.11 | 92 | 0.20 | 79 | 0.61 | 86 | 0.10 | 86 |
| JJA | 1.27 | 86 | 0.08 | 86 | 0.46 | 86 | 0.81 | 86 | 0.06 | 86 |
| SON | 0.51 | 90 | 0.09 | 82 | 0.23 | 82 | 0.32 | 90 | 0.08 | 97 |
| ***2009*** | ***0.79*** | ***98*** | ***0.10*** | ***98*** | ***0.23*** | ***77*** | ***0.58*** | ***96*** | ***0.09*** | ***96*** |
| DJF | 0.56 | 100 | 0.12 | 100 | 0.06 | 69 | 0.47 | 92 | 0.11 | 92 |
| MAM | 0.81 | 92 | 0.11 | 85 | 0.11 | 85 | 0.74 | 92 | 0.10 | 92 |
| JJA | 1.1 | 100 | 0.09 | 100 | 0.40 | 100 | 0.71 | 100 | 0.07 | 100 |
| SON | 0.68 | 100 | 0.09 | 100 | 0.28 | 100 | 0.40 | 100 | 0.07 | 100 |
| ***2010*** | ***0.90*** | ***94*** | ***0.11*** | ***94*** | ***0.24*** | ***79*** | ***0.67*** | ***96*** | ***0.10*** | ***96*** |
| DJF | 0.95 | 92 | 0.14 | 92 | 0.09 | 40 | 0.86 | 92 | 0.16 | 92 |
| MAM | 0.82 | 85 | 0.09 | 85 | 0.18 | 82 | 0.61 | 100 | 0.08 | 100 |
| JJA | 1.02 | 100 | 0.09 | 100 | 0.34 | 100 | 0.68 | 100 | 0.07 | 100 |
| SON | 0.79 | 100 | 0.11 | 100 | 0.24 | 100 | 0.51 | 92 | 0.09 | 92 |
| ***2011*** | ***0.92*** | ***98*** | ***0.11*** | ***92*** | ***0.26*** | ***94*** | ***0.68*** | ***98*** | ***0.11*** | ***96*** |
| DJF | 0.60 | 100 | 0.11 | 100 | 0.09 | 92 | 0.51 | 92 | 0.11 | 100 |
| MAM | 0.99 | 93 | 0.10 | 70 | 0.27 | 93 | 0.73 | 100 | 0.10 | 85 |
| JJA | 1.07 | 100 | 0.07 | 100 | 0.37 | 100 | 0.69 | 100 | 0.07 | 100 |
| SON | 1.04 | 100 | 0.17 | 100 | 0.30 | 92 | 0.77 | 100 | 0.16 | 100 |
| ***2012*** | ***0.56*** | ***89*** | ***0.08*** | ***86*** | ***0.10*** | ***79*** | ***0.50*** | ***90*** | ***0.08*** | ***90*** |

| | $PM_{10}$ | | | | $PM_{10-2.5}$ | | $PM_{2.5}$ | | | |
|---|---|---|---|---|---|---|---|---|---|---|
| | **OC** | **Capture** | **EC** | **Capture** | **OC** | **Capture** | **OC** | **Capture** | **EC** | **Capture** |
| DJF | 0.52 | 100 | 0.09 | 100 | 0.04 | 84 | 0.49 | 100 | 0.09 | 100 |
| MAM | 0.58 | 85 | 0.09 | 85 | 0.03 | 70 | 0.63 | 70 | 0.11 | 70 |
| JJA | 0.78 | 70 | 0.07 | 70 | 0.18 | 70 | 0.59 | 100 | 0.07 | 100 |
| SON | 0.56 | 100 | 0.07 | 92 | 0.14 | 92 | 0.30 | 92 | 0.07 | 92 |
| ***2013*** | ***0.76*** | ***92*** | ***0.09*** | ***96*** | ***0.21*** | ***90*** | ***0.57*** | ***98*** | ***0.08*** | ***96*** |
| DJF | 0.49 | 92 | 0.10 | 92 | 0.05 | 68 | 0.47 | 91 | 0.09 | 91 |
| MAM | 0.79 | 100 | 0.10 | 100 | 0.15 | 100 | 0.63 | 100 | 0.09 | 100 |
| JJA | 1.16 | 100 | 0.07 | 92 | 0.37 | 100 | 0.79 | 100 | 0.07 | 92 |
| SON | 0.58 | 100 | 0.07 | 100 | 0.22 | 92 | 0.39 | 100 | 0.07 | 100 |
| ***2014*** | ***0.91*** | ***98*** | ***0.09*** | ***100*** | ***0.29*** | ***94*** | ***0.65*** | ***96*** | ***0.08*** | ***96*** |
| DJF | 0.61 | 100 | 0.10 | 100 | 0.08 | 76 | 0.59 | 84 | 0.11 | 84 |
| MAM | 0.91 | 100 | 0.10 | 100 | 0.23 | 100 | 0.69 | 100 | 0.09 | 100 |
| JJA | 1.10 | 100 | 0.05 | 100 | 0.35 | 100 | 0.75 | 100 | 0.05 | 100 |
| SON | 1.20 | 100 | 0.10 | 100 | 0.47 | 100 | 0.55 | 100 | 0.09 | 100 |
| ***2015*** | ***0.72*** | ***98*** | ***0.09*** | ***98*** | ***0.19*** | ***85*** | ***0.52*** | ***88*** | ***0.08*** | ***88*** |
| DJF | 0.44 | 100 | 0.06 | 100 | 0.11 | 100 | 0.34 | 100 | 0.06 | 100 |
| MAM | 0.59 | 92 | 0.10 | 92 | 0.11 | 79 | 0.50 | 92 | 0.08 | 92 |
| JJA | 1.01 | 100 | 0.09 | 100 | 0.35 | 63 | 0.66 | 63 | 0.08 | 63 |
| SON | 0.83 | 100 | 0.10 | 100 | 0.22 | 99 | 0.62 | 99 | 0.10 | 99 |
| ***2016*** | ***0.73*** | ***100*** | ***0.06*** | ***100*** | ***0.21*** | ***95*** | ***0.54*** | ***100*** | ***0.06*** | ***100*** |
| DJF | 0.44 | 100 | 0.07 | 100 | 0.07 | 86 | 0.37 | 100 | 0.06 | 100 |
| MAM | 0.83 | 100 | 0.07 | 100 | 0.21 | 92 | 0.64 | 100 | 0.07 | 100 |
| JJA | 0.98 | 100 | 0.04 | 100 | 0.33 | 100 | 0.65 | 100 | 0.05 | 100 |
| SON | 0.68 | 100 | 0.07 | 100 | 0.20 | 100 | 0.48 | 100 | 0.07 | 100 |
| ***2017*** | ***0.72*** | ***94*** | ***0.05*** | ***94*** | ***0.25*** | ***79*** | ***0.52*** | ***94*** | ***0.05*** | ***94*** |
| DJF | 0.57 | 100 | 0.07 | 100 | 0.11 | 63 | 0.53 | 100 | 0.07 | 100 |
| MAM | 0.65 | 92 | 0.05 | 92 | 0.14 | 84 | 0.52 | 92 | 0.05 | 92 |
| JJA | 0.92 | 86 | 0.03 | 86 | 0.34 | 86 | 0.58 | 86 | 0.04 | 86 |
| SON | 0.77 | 100 | 0.06 | 100 | 0.38 | 83 | 0.47 | 100 | 0.05 | 100 |
| ***2018*** | ***0.96*** | ***100*** | ***0.08*** | ***100*** | ***0.26*** | ***90*** | ***0.73*** | ***100*** | ***0.07*** | ***100*** |
| DJF | 0.49 | 100 | 0.07 | 100 | 0.08 | 77 | 0.45 | 100 | 0.07 | 100 |
| MAM | 1.32 | 100 | 0.11 | 100 | 0.28 | 92 | 1.06 | 100 | 0.10 | 100 |
| JJA | 1.20 | 100 | 0.05 | 100 | 0.32 | 100 | 0.90 | 100 | 0.05 | 100 |
| SON | 0.81 | 100 | 0.08 | 100 | 0.31 | 100 | 0.50 | 100 | 0.07 | 100 |

Notation: Red numbers indicate annual or seasonal means based on < 50% data capture.

19 **Table S 6: $R^2$-values for OC versus EC as a function of size fraction and season.**

| | Winter | Spring | Summer | Fall |
|---|---|---|---|---|
| **$PM_{10}$** | 0.66 | 0.58 | 0.51 | 0.64 |
| **$PM_{2.5}$** | 0.75 | 0.69 | 0.58 | 0.76 |

20

**Table S 7: Annual mean (±SD) relative chemical composition for the period 2001–2018. Unit (%)**[1]

| | $OM/PM_{10}$ | $EC/PM_{10}$ | $SO_4^{2-}/PM_{10}$ | $NO_3^-/PM_{10}$ | $NH_4^+/PM_{10}$ | $SS/PM_{10}$ | $OM/PM_{2.5}$ | $EC/PM_{2.5}$ | $OM/PM_{10-2.5}$ |
|---|---|---|---|---|---|---|---|---|---|
| **2001** | 31±4 | 2.7±0.4 | 21 | 11 | 6 | 11 | 38±5 | 3.6±0.5 | 8.9±1.8[1)] |
| **2002** | 26±4 | 2.1±0.3 | 20 | 14 | 8 | 10 | 30±4 | 2.3±0.3 | 16±3 |
| **2003** | 29±4 | 1.6±0.2 | 23 | 12 | 6 | 11 | 32±5 | 2.5±0.4 | 18±4 |
| **2004** | 27±4 | 1.9±0.3 | 19 | 15 | 7 | 14 | 32±5 | 2.9±0.4 | 21±4 |
| **2005** | 25±4 | 2.4±0.3 | 20 | 16 | 8 | 13 | 29±4 | 3.3±0.5 | 21±4 |
| **2006** | 26±4 | 1.8±0.3 | 20 | 17 | 5 | 12 | 31±4 | 3.0±0.4 | 18±4 |
| **2007** | 27±4 | 2.9±0.4 | 15 | 10 | 4 | 14 | 35±5 | 4.3±0.6 | 16±3 |
| **2008** | 25±4 | 1.7±0.2 | 14 | 12 | 3 | 18 | 36±5 | 3.1±0.4 | 17±3 |
| **2009** | 26±4 | 3.7±1.9 | 15 | 13 | 4 | 13 | 31±4 | 2.8±0.4 | 19±4 |
| **2010** | 34±5 | 2.4±0.3 | 17 | 13 | 5 | 11 | 37±5 | 3.2±0.5 | 21±4 |
| **2011** | 25±4 | 1.7±0.2 | 14 | 17 | 6 | 16 | 32±4 | 3.0±0.4 | 15±3 |
| **2012** | 22±3 | 1.8±0.3 | 17 | 28 | 7 | 17 | 33±5 | 3.0±0.4 | 10±2 |
| **2013** | 29±4 | 2.0±0.3 | 15 | 19 | 6 | 23 | 37±5 | 3.0±0.4 | 18±4 |
| **2014** | 28±4 | 1.6±0.2 | 18 | 21 | 7 | 20 | 36±5 | 2.6±0.4 | 20±4 |
| **2015** | 26±4 | 1.9±0.3 | 16 | 22 | 6 | 28 | 36±5 | 3.3±0.5 | 20±3 |
| **2016** | 32±5 | 1.5±0.2 | 14 | 23 | 7 | 23 | 41±6 | 2.6±0.4 | 21±4 |
| **2017** | 38±5 | 1.5±0.2 | 19 | 14 | 5 | 27 | 49±7 | 2.8±0.4 | 28±6 |
| **2018** | 34±5 | 1.6±0.2 | 14 | 15 | 6 | 19 | 46±7 | 2.6±0.4 | 20±4 |

[1] 1) Data capture below 50%.
2) Notation: Conversion factors applied OM = OC x 1.9; EC = EC x 1.1

**Table S 8: Mean (±SD) relative chemical composition of the 3 weekly samples with the highest PM mass concentration ($PM_{MAX}$) per year for the period 2001–2018.**[2]

| | $PM_{10\ MAX}$ | | OM | EC | $SO_4^{2-}$ | $NO_3^-$ | $NH_4^+$ | SS | $PM_{2.5\ MAX}$ | | OM | EC |
|---|---|---|---|---|---|---|---|---|---|---|---|---|
| | µg m$^{-3}$ | Season[1)] | % | % | % | % | % | % | µg m$^{-3}$ | Season[1)] | % | % |
| **2001** | 12.4±1.6 | 234 | 43±16 | 3±1 | 14±10 | 4±3 | 4±3 | 3±3 | 12.2±2.4 | 234 | 50±10 | 5±2 |
| **2002** | 23.8±3.6 | 223 | 26±11 | 1.8±0.7 | 14±9 | 13±14 | 8±4 | 2±2 | 18.8±2.9 | 223 | 29±12 | 1.7±0.5 |
| **2003** | 17.9±2.7 | 222 | 16±3 | 1.3±0.4 | 17±3 | 18±8 | 11±2 | 8±3 | 12.0±1.9 | 222 | 19±3 | 1.6±0.3 |
| **2004** | 17.0±6.8 | 222 | 23±9 | 1.5±0.4 | 21±3 | 11±10 | 8±4 | 14±18 | 11.6±6.5 | 222 | 27±9 | 2.4±0.8 |
| **2005** | 16.9±2.8 | 244 | 26±6 | 3.4±1.6 | 15±3 | 20±3 | 2±0 | 5±3 | 12.4±3.1 | 224 | 27±10 | 2.9±0.4 |
| **2006** | 26.5±3.0 | 144 | 23±8 | 4.1±1.6 | 19±7 | 17±4 | 8±2 | 7±5 | 15.5±0.9 | 124 | 30±10 | 2.3±0.7 |
| **2007** | 13.8±3.5 | 223 | 40±2 | 4.2±1.5 | 12±0 | 6±2 | 4±1 | 1±0 | 10.7±3.4 | 223 | 48±2 | 4.1±1.5 |
| **2008** | 12.5±3.0 | 222 | 12±5 | 1.5±0.5 | 12±3 | 20±7 | 5±3 | 15±15 | 7.0±2.7 | 223 | 16±3 | 1.9±0.6 |
| **2009** | 14.8±5.7 | 222 | 21±1 | 1.8±0.0 | 12±5 | 13±9 | 5±3 | 3±2 | 10.6±4.1 | 122 | 28±3 | 2.5±0.5 |
| **2010** | 12.0±2.4 | 344 | 21±6 | 1.9±0.6 | 14±3 | 13±2 | 3±1 | 23±11 | 10.7±3.7 | 144 | 42±9 | 5.0±0.6 |
| **2011** | 16.7±1.2 | 224 | 23±13 | 2.0±1.3 | 23±2 | 17±4 | 12±0 | 2±1 | 12.1±1.5 | 224 | 27±13 | 3.0±1.9 |
| **2012** | 11.9±1.7 | 122 | 29±21 | 3.9±3.4 | 10±9 | 24±25 | 3±2 | 1±0 | 7.2±1.4 | 123 | 30±26 | 3.0±2.7 |
| **2013** | 9.4±0.6 | 222 | 12±4 | 1.4±0.5 | 9±2 | 7±2 | 8±0 | 13±5 | 5.7±0.6 | 223 | 30±9 | 2.6±1.0 |
| **2014** | 17.7±3.3 | 224 | 18±8 | 1.5±0.2 | 15±5 | 25±6 | 10±1 | 14±8 | 8.1±0.9 | 122 | 21±6 | 2.5±0.5 |
| **2015** | 12.0±4.0 | 122 | 21±10 | 2.2±1.3 | 12±7 | 23±10 | 11±2 | 12±12 | 6.9±1.7 | 122 | 31±20 | 3.3±2.0 |
| **2016** | 9.2.±0.2 | 223 | 30±22 | 1.3±0.3 | 6±5 | 18±17 | 7±7 | 6±1 | 6.7±1.5 | 223 | 37±25 | 1.9±0.3 |
| **2017** | 9.8.±2.7 | 114 | 33±8 | 2.3±1.1 | 19±3 | 14±7 | 7±1 | 13±13 | 6.3±2.0 | 112 | 29±8 | 2.7±0.3 |
| **2018** | 12.8.±3.1 | 124 | 32±24 | 1.3±0.5 | 11±3 | 20±15 | 8±5 | 5±1 | 9.0±1.0 | 144 | 21±11 | 1.7±1.2 |

[2] 1 = DJF; 2 = MAM; 3 = JJA; 4 = SON

**Table S 9: Annual and seasonal mean concentrations of TC in $PM_{10}$, $PM_{2.5}$ and $PM_{10-2.5}$ at Birkenes for 2001–2018 (Unit: *µg C m$^{-3}$*).**

| | $PM_{10}$ | | $PM_{10-2.5}$ | | $PM_{2.5}$ | |
|---|---|---|---|---|---|---|
| | TC | Capture | TC | Capture | TC | Capture |
| ***2001*** | ***1.09*** | ***63*** | ***0.07*** | ***48*** | ***1.08*** | ***63*** |
| DJF | 0.72 | 59 | 0 | 34 | 0.75 | 59 |
| MAM | 1.14 | 92 | 0.02 | 65 | 1.19 | 92 |
| JJA | 2.50 | 26 | 0.20 | 26 | 2.30 | 26 |
| SON | 0.68 | 48 | 0.08 | 48 | 0.60 | 48 |
| ***2002*** | ***1.15*** | ***85*** | ***0.21*** | ***80*** | ***1.01*** | ***91*** |
| DJF | 0.65 | 95 | 0.05 | 88 | 0.60 | 95 |
| MAM | 1.47 | 92 | 0.14 | 92 | 1.33 | 92 |
| JJA | 1.96 | 68 | 0.53 | 68 | 1.50 | 91 |
| SON | 0.68 | 86 | 0.18 | 73 | 0.59 | 86 |
| ***2003*** | ***1,12*** | ***82*** | ***0,23*** | ***78*** | ***0,93*** | ***82*** |
| DJF | 0.94 | 85 | 0.05 | 82 | 0.95 | 85 |
| MAM | 1.26 | 86 | 0.20 | 76 | 1.16 | 86 |
| JJA | 1.34 | 85 | 0.43 | 85 | 0.91 | 85 |
| SON | 0.84 | 70 | 0.22 | 70 | 0.62 | 70 |
| ***2004*** | ***0.91*** | ***84*** | ***0.28*** | ***79*** | ***0.65*** | ***84*** |
| DJF | 0.65 | 86 | 0.09 | 86 | 0.56 | 86 |
| MAM | 1.13 | 86 | 0.32 | 66 | 0.91 | 86 |
| JJA | 1.09 | 79 | 0.41 | 79 | 0.68 | 79 |
| SON | 0.79 | 86 | 0.33 | 86 | 0.47 | 86 |
| ***2005*** | ***0.99*** | ***79*** | ***0.32*** | ***75*** | ***0.71*** | ***80*** |
| DJF | 0.56 | 64 | 0.06 | 51 | 0.64 | 71 |
| MAM | 0.91 | 85 | 0.16 | 85 | 0.75 | 85 |
| JJA | 1.01 | 86 | 0.34 | 86 | 0.67 | 86 |
| SON | 1.41 | 79 | 0.62 | 79 | 0.79 | 79 |
| ***2006*** | ***1.20*** | ***78*** | ***0.35*** | ***70*** | ***0.90*** | ***78*** |
| DJF | 0.91 | 86 | 0.08 | 66 | 0.88 | 86 |
| MAM | 1.03 | 85 | 0.10 | 72 | 0.96 | 85 |
| JJA | 1.55 | 57 | 0.49 | 57 | 1.06 | 57 |
| SON | 1.43 | 86 | 0.68 | 86 | 0.75 | 86 |
| ***2007*** | ***0.99*** | ***77*** | ***0.24*** | ***76*** | ***0.74*** | ***77*** |
| DJF | 0.76 | 58 | 0.09 | 58 | 0.67 | 58 |
| MAM | 1.17 | 86 | 0.20 | 86 | 0.97 | 86 |
| JJA | 1.16 | 86 | 0.41 | 79 | 0.77 | 79 |
| SON | 0.76 | 79 | 0.21 | 79 | 0.52 | 86 |
| ***2008*** | ***0.85*** | ***84*** | ***0.25*** | ***81*** | ***0.60*** | ***86*** |
| DJF | 0.47 | 84 | 0.05 | 76 | 0.43 | 84 |
| MAM | 0.90 | 86 | 0.21 | 79 | 0.71 | 86 |
| JJA | 1.35 | 86 | 0.47 | 86 | 0.87 | 86 |
| SON | 0.65 | 82 | 0.24 | 82 | 0.39 | 90 |
| ***2009*** | ***0.89*** | ***98*** | ***0.23*** | ***92*** | ***0.67*** | ***96*** |
| DJF | 0.68 | 100 | 0.05 | 84 | 0.58 | 92 |
| MAM | 0.92 | 92 | 0.12 | 85 | 0.85 | 92 |
| JJA | 1.19 | 100 | 0.41 | 100 | 0.78 | 100 |
| SON | 0.76 | 100 | 0.29 | 100 | 0.47 | 100 |
| ***2010*** | ***1.00*** | ***94*** | ***0.21*** | ***87*** | ***0.77*** | ***96*** |
| DJF | 1.09 | 92 | 0.06 | 69 | 1.03 | 92 |
| MAM | 0.91 | 85 | 0.17 | 85 | 0.69 | 100 |
| JJA | 1.11 | 100 | 0.36 | 100 | 0.75 | 100 |
| SON | 0.90 | 100 | 0.26 | 92 | 0.61 | 92 |
| ***2011*** | ***0.99*** | ***98*** | ***0.25*** | ***92*** | ***0.80*** | ***100*** |
| DJF | 0.71 | 100 | 0.09 | 92 | 0.64 | 100 |
| MAM | 0.88 | 92 | 0.20 | 85 | 0.84 | 100 |
| JJA | 1.13 | 100 | 0.37 | 100 | 0.76 | 100 |
| SON | 1.21 | 100 | 0.32 | 92 | 0.93 | 100 |
| ***2012*** | ***0.64*** | ***89*** | ***0.10*** | ***79*** | ***0.58*** | ***92*** |

| | $PM_{10}$ | | $PM_{10-2.5}$ | | $PM_{2.5}$ | |
|---|---|---|---|---|---|---|
| | **TC** | **Capture** | **TC** | **Capture** | **TC** | **Capture** |
| DJF | 0.61 | 100 | 0.03 | 92 | 0.58 | 100 |
| MAM | 0.67 | 85 | 0 | 68 | 0.73 | 77 |
| JJA | 0.85 | 70 | 0.25 | 56 | 0.66 | 100 |
| SON | 0.51 | 100 | 0.14 | 92 | 0.37 | 92 |
| ***2013*** | ***0.84*** | ***98*** | ***0.21*** | ***92*** | ***0.65*** | ***98*** |
| DJF | 0.59 | 92 | 0.04 | 76 | 0.56 | 91 |
| MAM | 0.89 | 100 | 0.17 | 100 | 0.72 | 100 |
| JJA | 1.22 | 100 | 0.37 | 100 | 0.86 | 100 |
| SON | 0.66 | 100 | 0.23 | 92 | 0.46 | 100 |
| ***2014*** | ***1.00*** | ***100*** | ***0.30*** | ***94*** | ***0.73*** | ***96*** |
| DJF | 0.71 | 100 | 0.07 | 76 | 0.70 | 84 |
| MAM | 1.02 | 100 | 0.24 | 100 | 0.78 | 100 |
| JJA | 1.16 | 100 | 0.35 | 100 | 0.80 | 100 |
| SON | 1.12 | 100 | 0.48 | 100 | 0.64 | 100 |
| ***2015*** | **0.81** | ***98*** | ***0.19*** | ***88*** | ***0.60*** | ***88*** |
| DJF | 0.50 | 100 | 0.11 | 100 | 0.39 | 100 |
| MAM | 0.70 | 92 | 0.10 | 92 | 0.60 | 92 |
| JJA | 1.10 | 100 | 0.36 | 63 | 0.74 | 63 |
| SON | 0.94 | 100 | 0.23 | 96 | 0.71 | 96 |
| ***2016*** | ***0.80*** | ***100*** | ***0.21*** | ***94*** | ***0.6*** | ***100*** |
| DJF | 0.51 | 100 | 0.08 | 82 | 0.43 | 100 |
| MAM | 0.90 | 100 | 0.22 | 92 | 0.71 | 100 |
| JJA | 1.02 | 100 | 0.32 | 100 | 0.70 | 100 |
| SON | 0.76 | 100 | 0.21 | 100 | 0.55 | 100 |
| ***2017*** | ***0.78*** | ***94*** | ***0.26*** | ***78*** | ***0.58*** | ***94*** |
| DJF | 0.63 | 100 | 0.11 | 59 | 0.60 | 100 |
| MAM | 0.70 | 92 | 0.14 | 84 | 0.58 | 92 |
| JJA | 0.95 | 86 | 0.34 | 86 | 0.61 | 86 |
| SON | 0.84 | 100 | 0.40 | 83 | 0.51 | 100 |
| ***2018*** | ***1.03*** | ***100*** | ***0.26*** | ***90*** | ***0.8*** | ***100*** |
| DJF | 0.56 | 100 | 0.08 | 77 | 0.52 | 100 |
| MAM | 1.43 | 100 | 0.30 | 92 | 1.06 | 100 |
| JJA | 1.25 | 100 | 0.32 | 92 | 0.95 | 100 |
| SON | 0.88 | 100 | 0.32 | 100 | 0.56 | 100 |

Notation: Red numbers indicate annual or seasonal means based on < 50% data capture.

**Table S 10: Annual and seasonal mean mass concentrations of $PM_{10}$, $PM_{2.5}$ and $PM_{10-2.5}$ at Birkenes for 2001–2018 (Unit: $\mu g\ m^{-3}$).**

| | $PM_{10}$ | Capture | $PM_{2.5}$ | Capture | $PM_{10-2.5}$ | Capture |
|---|---|---|---|---|---|---|
| ***2001*** | ***5.8*** | ***56*** | ***4.6*** | ***58*** | ***1.7*** | ***54*** |
| DJF | 4.5 | 59 | 3.2 | 59 | 1.3 | 59 |
| MAM | 6.6 | 92 | 5.5 | 100 | 1.8 | 92 |
| JJA | 7.9 | 26 | 7.3 | 26 | 1.3 | 19 |
| SON | 4.9 | 48 | 2.9 | 48 | 1.9 | 48 |
| ***2002*** | ***7.5*** | ***83*** | ***5.7*** | ***91*** | ***2.2*** | ***80*** |
| DJF | 5.6 | 88 | 3.8 | 95 | 1.8 | 88 |
| MAM | 11.0 | 92 | 8.5 | 92 | 2.4 | 92 |
| JJA | 10.0 | 68 | 7.3 | 95 | 2.9 | 68 |
| SON | 3.9 | 86 | 2.8 | 86 | 1.5 | 73 |
| ***2003*** | ***6.7*** | ***78*** | ***4.8*** | ***82*** | ***2.4*** | ***74*** |
| DJF | 5.9 | 76 | 4.4 | 85 | 2.2 | 76 |
| MAM | 9.3 | 82 | 6.7 | 86 | 3.4 | 76 |
| JJA | 5.9 | 85 | 4.4 | 81 | 1.7 | 79 |
| SON | 5.4 | 70 | 3.5 | 70 | 2.3 | 64 |
| ***2004*** | ***5.7*** | ***84*** | ***3.4*** | ***84*** | ***2.4*** | ***83*** |
| DJF | 4.5 | 86 | 2.8 | 86 | 1.7 | 86 |
| MAM | 8.2 | 86 | 5.4 | 85 | 3.1 | 79 |
| JJA | 5.7 | 79 | 3.3 | 79 | 2.4 | 79 |
| SON | 4.3 | 86 | 2.0 | 86 | 2.3 | 86 |
| ***2005*** | ***6.5*** | ***79*** | ***4.0*** | ***80*** | ***2.6*** | ***75*** |
| DJF | 5.2 | 64 | 3.1 | 71 | 2.8 | 51 |
| MAM | 6.9 | 85 | 4.9 | 85 | 1.9 | 85 |
| JJA | 5.5 | 86 | 3.4 | 86 | 2.1 | 86 |
| SON | 8.0 | 79 | 4.4 | 79 | 3.6 | 79 |
| ***2006*** | ***7.8*** | ***78*** | ***4.7*** | ***77*** | ***3.4*** | ***73*** |
| DJF | 7.4 | 86 | 4.5 | 79 | 3.0 | 79 |
| MAM | 6.2 | 85 | 4.6 | 86 | 2.1 | 72 |
| JJA | 8.3 | 57 | 5.4 | 57 | 3.0 | 57 |
| SON | 9.5 | 86 | 4.5 | 86 | 5.0 | 86 |
| ***2007*** | ***5.8*** | ***72*** | ***3.3*** | ***74*** | ***2.5*** | ***72*** |
| DJF | 4.2 | 38 | 2.0 | 38 | 2.2 | 38 |
| MAM | 7.5 | 86 | 4.4 | 86 | 3.1 | 86 |
| JJA | 6.1 | 79 | 3.5 | 86 | 2.5 | 79 |
| SON | 4.4 | 86 | 2.4 | 86 | 2.0 | 86 |
| ***2008*** | ***5.7*** | ***77*** | ***2.8*** | ***86*** | ***2.7*** | ***75*** |
| DJF | 5.1 | 84 | 2.5 | 90 | 2.8 | 84 |
| MAM | 7.1 | 79 | 4.1 | 73 | 2.7 | 73 |
| JJA | 6.1 | 86 | 3.1 | 86 | 2.9 | 86 |
| SON | 4.0 | 58 | 1.9 | 97 | 2.1 | 58 |
| ***2009*** | ***5.8*** | ***85*** | ***3.6*** | ***94*** | ***2.3*** | ***76*** |
| DJF | 4.4 | 96 | 3 | 92 | 1.4 | 88 |
| MAM | 9.4 | 74 | 5.3 | 100 | 3.4 | 74 |
| JJA | 6.1 | 71 | 3.8 | 92 | 2.2 | 63 |
| SON | 4.3 | 99 | 2.2 | 92 | 2.3 | 83 |

| | $PM_{10}$ | Capture | $PM_{2.5}$ | Capture | $PM_{10-2.5}$ | Capture |
|---|---|---|---|---|---|---|
| ***2010*** | ***5.1*** | ***88*** | ***3.4*** | ***94*** | ***2.2*** | *77* |
| DJF | 3.8 | 100 | 3.4 | 87 | 0.55 | 64 |
| MAM | 5.4 | 71 | 3 | 98 | 2.3 | 68 |
| JJA | 6.7 | 90 | 3.7 | 100 | 3.1 | 91 |
| SON | 4.8 | 92 | 3.5 | 92 | 2.5 | 85 |
| ***2011*** | ***7.0*** | ***98*** | ***4.1*** | ***100*** | ***3.2*** | ***96*** |
| DJF | 5.6 | 100 | 3.1 | 100 | 2.5 | 100 |
| MAM | 8.2 | 93 | 5.5 | 100 | 3.9 | 85 |
| JJA | 5.2 | 100 | 3.5 | 100 | 1.7 | 100 |
| SON | 9.0 | 100 | 4.4 | 100 | 4.6 | 100 |
| ***2012*** | ***4.9*** | ***89*** | ***2.9*** | ***92*** | ***2.0*** | ***85*** |
| DJF | 4.4 | 100 | 2.7 | 100 | 1.7 | 99 |
| MAM | 6.7 | 85 | 3.2 | 100 | 3.3 | 70 |
| JJA | 4.6 | 70 | 3.8 | 70 | 1.4 | 70 |
| SON | 4.0 | 100 | 2.0 | 100 | 2.0 | 100 |
| ***2013*** | ***4.9*** | ***92*** | ***2.9*** | ***86*** | ***2.2*** | ***84*** |
| DJF | 3.8 | 69 | 2.6 | 44 | 1.7 | 44 |
| MAM | 6.4 | 100 | 3.7 | 100 | 2.8 | 100 |
| JJA | 5.4 | 100 | 3.4 | 100 | 2.0 | 100 |
| SON | 3.6 | 100 | 1.8 | 100 | 2.0 | 92 |
| ***2014*** | ***6.1*** | ***98*** | ***3.4*** | ***96*** | ***2.7*** | ***94*** |
| DJF | 5.7 | 100 | 3.5 | 84 | 2.4 | 84 |
| MAM | 7.2 | 92 | 3.7 | 100 | 3.3 | 92 |
| JJA | 5.2 | 100 | 3.2 | 100 | 2.0 | 100 |
| SON | 6.3 | 100 | 3.3 | 100 | 3.0 | 100 |
| ***2015*** | ***5.3*** | ***98*** | ***2.7*** | ***88*** | ***2.5*** | ***88*** |
| DJF | 5.5 | 100 | 2.5 | 100 | 31 | 100 |
| MAM | 5.2 | 100 | 2.8 | 100 | 2.5 | 100 |
| JJA | 5.5 | 92 | 2.9 | 63 | 1.9 | 63 |
| SON | 5.0 | 100 | 2.8 | 99 | 2.4 | 99 |
| ***2016*** | **4.3** | **100** | **2.5** | **100** | **1.9** | **100** |
| DJF | 4.1 | 100 | 2.1 | 100 | 2.0 | 100 |
| MAM | 4.8 | 100 | 3.1 | 100 | 1.7 | 100 |
| JJA | 4.3 | 100 | 2.6 | 100 | 1.7 | 100 |
| SON | 4.1 | 100 | 2.1 | 100 | 2.1 | 100 |
| ***2017*** | **3.8** | **90** | **2.0** | **94** | **1.7** | **90** |
| DJF | 3.7 | 100 | 2.2 | 100 | 1.4 | 100 |
| MAM | 3.8 | 92 | 2.3 | 92 | 1.5 | 92 |
| JJA | 3.9 | 86 | 2.1 | 86 | 1.8 | 86 |
| SON | 3.8 | 85 | 1.4 | 100 | 2.4 | 85 |
| ***2018*** | **5.4** | **100** | **3.0** | **98** | **2.5** | **98** |
| DJF | 3.8 | 100 | 2.4 | 92 | 1.4 | 92 |
| MAM | 6.5 | 100 | 4.2 | 100 | 2.3 | 100 |
| JJA | 5.4 | 100 | 3.1 | 100 | 2.3 | 100 |
| SON | 6.2 | 100 | 2.2 | 100 | 3.9 | 100 |

Red numbers indicate annual or seasonal means based on < 50% data capture.

**Table S 11: Sen slope of annual means and corresponding confidence intervals for significant slopes (*p=0.05*), as well as change in annual mean presented as percentage change per year and as percentage change for the period 2001–2018. Non-significant values in red.**

| | Slope (% $yr^{-1}$) | CI-1 | CI-2 | Change 2001-2018 (%) |
|---|---|---|---|---|
| **$PM_{10}$** | -2.2 | -3.7 | -0.7 | -38 |
| **$PM_{2.5}$** | -4.0 | -5.7 | -2.2 | -69 |
| **$PM_{10-2.5}$** | -0.1 | -2.2 | 1.4 | -2.4 |
| **OC in $PM_{10}$** | 0 | -1.4 | 0.9 | 0 |
| **OC in $PM_{2.5}$** | -0.8 | -2.8 | 0.7 | -13 |
| **OC in $PM_{10-2.5}$** | 0.8 | -1.7 | 3.4 | 13 |
| **EC in $PM_{10}$** | -3.9 | -5.8 | -1.9 | -66 |
| **EC in $PM_{2.5}$** | -4.2 | -6.2 | -2.6 | -71 |
| **TC in $PM_{10}$** | -1.1 | -2.0 | 0.0 | -19 |
| **TC in $PM_{2.5}$** | -1.5 | -3.5 | 0.0 | -26 |
| **TC in $PM_{10-2.5}$** | 0.0 | -2.4 | 1.9 | 0 |
| **$SO_4^{2-}$** | -3.8 | -6.1 | -1.8 | -65 |
| **$NO_3^-$** | 0.8 | -2.5 | 4.3 | 14 |
| **$NH_4^+$** | -2.7 | -5.8 | 0.5 | -47 |
| **SS** | 2.2 | 0.6 | 4.5 | 38 |
| **Levoglucosan[1)]** | -2.8 | -8.8 | -0.2 | -28 |

Notation: Trends for levoglucosan are calculated for the period 2008–2018.

**Table S 12: Sen slope of seasonal means in % $yr^{-1}$ and corresponding confidence intervals for significant slopes ($p=0.05$) for 2001–2018. Non-significant values in red.**

| | DJF | | | MAM | | | JJA | | | SON | | |
|---|---|---|---|---|---|---|---|---|---|---|---|---|
| | Slope (% $yr^{-1}$) | CI-1 | CI-2 | Slope (% $yr^{-1}$) | CI-1 | CI-2 | Slope (% $yr^{-1}$) | CI-1 | CI-2 | Slope (% $yr^{-1}$) | CI-1 | CI-2 |
| $PM_{10}$ | -1.6 | -3.3 | -0.1 | -3.3 | -5.6 | -0.9 | -2.4 | -5.1 | -0.9 | -0.5 | -3.3 | 2.2 |
| $PM_{2.5}$ | -2.4 | -4.6 | -0.8 | -4.4 | -7.0 | -3.0 | -3.0 | -7.1 | -1.4 | -2.9 | -6.5 | 0.6 |
| $PM_{10-2.5}$ | 0.0 | -2.6 | 3.0 | -0.4 | -4.2 | 2.3 | -2.3 | -4.5 | 0.6 | 0.8 | -1.2 | 4.3 |
| OC in $PM_{10}$ | -0.2 | -2.8 | 1.4 | -1.0 | -3.1 | 1.2 | -0.7 | -3.2 | 1.4 | 1.7 | -1.3 | 4.0 |
| OC in $PM_{2.5}$ | -0.8 | -3.7 | 1.4 | -1.9 | -3.7 | 0.5 | -0.6 | -2.8 | 2.1 | 1.5 | -1.2 | 4.3 |
| OC in $PM_{10-2.5}$ | 3.2 | 0.0 | 6.7 | 3.7 | -1.7 | 7.2 | -1.4 | -2.5 | 0.1 | 1.2 | -2.4 | 5.4 |
| EC in $PM_{10}$ | -2.8 | -4.9 | -0.7 | -4.0 | -6.0 | -1.6 | -5.9 | -9.8 | -3.3 | -2.3 | -9.2 | 0.0 |
| EC in $PM_{2.5}$ | -3.1 | -5.4 | -0.7 | -4.6 | -6.7 | -3.0 | -4.1 | -6.7 | -2.2 | -2.0 | -5.5 | 0.0 |
| TC in $PM_{10}$ | -1.0 | -3.5 | 0.7 | -2.0 | -3.4 | -0.1 | -1.2 | -3.6 | 0.9 | 0.9 | -2.8 | 3.5 |
| TC in $PM_{2.5}$ | -1.4 | -3.5 | 0.7 | -2.6 | -4.2 | -0.9 | -1.0 | -3.6 | 1.3 | 0.5 | -2.5 | 2.7 |
| TC in $PM_{10-2.5}$ | 3.4 | -0.3 | 6.7 | 3.1 | -2.6 | 7.9 | -1.7 | -3.2 | -0.7 | 1.1 | -3.3 | 4.9 |
| $SO_4^{2-}$ | -3.0 | -6.1 | -0.2 | -6.4 | -9.0 | -3.8 | -4.2 | -5.9 | -2.9 | -2.4 | -5.3 | 0.7 |
| SS | 2.9 | -1.4 | 7.4 | 1.0 | -1.6 | 3.9 | 3.7 | 2.3 | 5.6 | 3.1 | 0.0 | 4.8 |
| Levoglucosan[1)] | -3.3 | -15.9 | 6.7 | 1.9 | -6.7 | 5.3 | -5.7 | -18.1 | 1.4 | -1.4 | -12.3 | 7.2 |

Notation: Trends for levoglucosan are calculated for the period 2008–2018

.

**Table S 13: Sen slope of annual mean ratios and corresponding confidence intervals for significant slopes (*p=0.05*), as well as change in annual mean presented as percentage change per year and as percentage change for the period 2001–2018 (2008–2018 for levoglucosan). Non-significant values in red.**

| | Slope (% $yr^{-1}$) | CI-1 | CI-2 | Change 2001-2018 (%) |
|---|---|---|---|---|
| **$OC_{PM10}$ to $PM_{10}$** | 2.4 | 0.7 | 3.4 | 41 |
| **$OC_{PM2.5}$ to $PM_{2.5}$** | 3.2 | 1.7 | 4.4 | 55 |
| **$OC_{PM10-2.5}$ to $PM_{10-2.5}$** | 1.1 | -1.3 | 2.5 | 17 |
| **$EC_{PM10}$ to $PM_{10}$** | -4.5 | -7.1 | -2.8 | -77 |
| **$EC_{PM2.5}$ to $PM_{2.5}$** | -3.9 | -5.8 | -1.9 | -66 |
| **$TC_{PM10}$ to $PM_{10}$** | 1.8 | 0.3 | 2.6 | 30 |
| **$TC_{PM2.5}$ to $PM_{2.5}$** | 2.6 | 1.4 | 3.7 | 44 |
| **$TC_{PM10-2.5}$ to $PM_{10-2.5}$** | 0.4 | -1.8 | 1.8 | 7.1 |
| **$SO_4^{2-}$ to $PM_{10}$** | -2.1 | -3.4 | -0.4 | -35 |
| **$NO_3^-$ to $PM_{10}$** | 3.8 | 0.8 | 6.3 | 64 |
| **$NH_4^+$ to $PM_{10}$** | -0.7 | -3.1 | 2.4 | -12 |
| **SS to $PM_{10}$** | 4.4 | 3.0 | 6.7 | 75 |
| **Levoglucosan to $OC_{PM10}$** | -1.8 | -10.6 | 1.8 | -18 |
| **Levoglucosan to $OC_{PM2.5}$** | -3.6 | -9.8 | 1.3 | -36 |
| **Levoglucosan to $EC_{PM10}$** | 2.8 | -3.5 | 6.5 | 28 |
| **Levoglucosan to $EC_{PM2.5}$** | 2.3 | -2.2 | 5.0 | 24 |
| **Levoglucosan to $TC_{PM10}$** | -1.1 | -9.0 | 2.7 | -11 |
| **Levoglucosan to $TC_{PM2.5}$** | -3.1 | -8.1 | 2.0 | -31 |

Notation: Trends for levoglucosan are calculated for the period 2008–2018.

**Table S 14:Sen slope of seasonal mean ratios and corresponding confidence intervals for significant slopes (*p=0.05*), as well as change in annual mean presented as percentage change per year and as percentage change for the period 2001 – 2018 (2008 – 2018 for levoglucosan). Non-significant values in red.**

| | DJF | | | MAM | | | JJA | | | SON | | |
|---|---|---|---|---|---|---|---|---|---|---|---|---|
| | Slope (% yr$^{-1}$) | CI-1 | CI-2 | Slope (% yr$^{-1}$) | CI-1 | CI-2 | Slope (% yr$^{-1}$) | CI-1 | CI-2 | Slope (% yr$^{-1}$) | CI-1 | CI-2 |
| **$OC_{PM10}$ to $PM_{10}$** | 1.8 | -0.6 | 3.7 | 1.7 | 0.4 | 3.7 | 2.3 | 1.0 | 3.6 | 1.7 | 0.4 | 3.7 |
| **$OC_{PM2.5}$ to $PM_{2.5}$** | 1.8 | -0.4 | 3.9 | 3.1 | 0.9 | 5.8 | 3.9 | 2.4 | 5.1 | 3.1 | 0.9 | 5.8 |
| **$OC_{PM10-2.5}$ to $PM_{10-2.5}$** | 2.8 | -0.9 | 5.8 | -0.3 | -2.5 | 2.6 | 1.6 | -1.2 | 3.1 | -0.3 | -2.5 | 2.6 |
| **$EC_{PM10}$ to $PM_{10}$** | -4.6 | -7.2 | -2.7 | -4.7 | -7.9 | -2.5 | -7.1 | -10.7 | -3.4 | -4.7 | -7.9 | -2.5 |
| **$EC_{PM2.5}$ to $PM_{2.5}$** | -3.9 | -5.4 | -2.5 | -3.6 | -5.3 | -1.2 | -4.3 | -7.5 | -1.7 | -3.6 | -5.3 | -1.2 |
| **$TC_{PM10}$ to $PM_{10}$** | 0.9 | -1.2 | 3.2 | 1.1 | -0.2 | 2.7 | 1.7 | 0.6 | 2.8 | 1.1 | -0.2 | 2.7 |
| **$TC_{PM2.5}$ to $PM_{2.5}$** | 1.2 | -0.6 | 3.3 | -0.7 | -3.6 | 1.6 | 0.7 | -1.4 | 1.9 | -0.7 | -3.6 | 1.6 |
| **$TC_{PM10-2.5}$ to $PM_{10-2.5}$** | 2.2 | -1.6 | 4.4 | 2.4 | 0.5 | 4.6 | 3.2 | 2.1 | 4.1 | 2.4 | 0.5 | 4.6 |
| **$SO_4^{2-}$ to $PM_{10}$** | -2.2 | -4.0 | 0.1 | -1.3 | -3.4 | -0.4 | -1.3 | -3.1 | 0.0 | -1.3 | -3.4 | -0.4 |
| **$NO_3^-$ to $PM_{10}$** | 7.3 | 3.2 | 11.1 | 1.2 | -2.4 | 4.1 | 4.4 | -0.4 | 7.1 | 1.2 | -2.4 | 4.1 |
| **$NH_4^+$ to $PM_{10}$** | 2.6 | -1.7 | 5.4 | -1.4 | -6.5 | 3.0 | -0.6 | -4.8 | 3.6 | -1.4 | -6.5 | 3.0 |
| **SS to $PM_{10}$** | 4.1 | -0.3 | 7.4 | 4.8 | 1.8 | 7.6 | 6.2 | 4.3 | 8.0 | 4.8 | 1.8 | 7.6 |
| **Levoglucosan to $OC_{PM10}$** | -5.9 | -7.9 | 2.5 | -4.9 | -9.2 | 0.0 | 0.0 | -13.6 | 0.0 | -4.9 | -9.2 | 0.0 |
| **Levoglucosan to $OC_{PM2.5}$** | -2.7 | -6.5 | 1.8 | -4.2 | -10.8 | 0.0 | 0.0 | -8.7 | 3.7 | -4.2 | -10.8 | 0.0 |
| **Levoglucosan to $EC_{PM10}$** | 3.1 | -6.9 | 8.6 | 1.1 | -6.5 | 5.1 | 8.2 | -2.6 | 13.6 | 1.1 | -6.5 | 5.1 |
| **Levoglucosan to $EC_{PM2.5}$** | 2.5 | -3.7 | 6.4 | -0.4 | -8.7 | 5.6 | 3.5 | -5.1 | 10.7 | -0.4 | -8.7 | 5.6 |
| **Levoglucosan to $TC_{PM10}$** | -3.5 | -7.4 | 3.5 | -5.6 | -8.7 | 0.0 | 0.0 | -13.6 | 0.0 | -5.6 | -8.7 | 0.0 |
| **Levoglucosan to $TC_{PM2.5}$** | -3.2 | -6.4 | 2.1 | -2.1 | -6.6 | 1.8 | 0.0 | -11.9 | 7.4 | -2.1 | -6.6 | 1.8 |

Notation: Trends for levoglucosan are calculated for the period 2008–2018

**Table S 15: Annual and seasonal mean mass concentrations of levoglucosan, mannosan and galactosan (2008–2018), arabitol, mannitol, trehalose, glucose, 2-methylerythritol and 2-methyltreitol (2016–2018) in $PM_{10}$ at Birkenes. (Unit: $ng\ m^{-3}$).**

| | Levo-glucosan | Cap | Man-nosan | Cap | Galact-osan | Cap | Levo/ Mann | Cap | Ara-bitol | Cap | Man-nitol | Cap | 2-methyl-erythritol | Cap | 2-methyl-threitol | Cap | Tre-halose | Cap | Glu-cose | Cap |
|---|---|---|---|---|---|---|---|---|---|---|---|---|---|---|---|---|---|---|---|---|
| **2008** | **10.90** | **90** | **2.68** | **90** | **0.91** | **90** | **4.7** | **75** | | | | | | | | | | | | |
| DJF | 10.24 | 90 | 2.32 | 90 | 0.69 | 90 | 4.7 | 69 | | | | | | | | | | | | |
| MAM | 8.00 | 86 | 1.37 | 86 | 0.40 | 86 | 5.5 | 82 | | | | | | | | | | | | |
| JJA | 13.40 | 86 | 4.48 | 86 | 2.00 | 90 | 3.4 | 58 | | | | | | | | | | | | |
| SON | 11.34 | 97 | 2.63 | 100 | 0.53 | 97 | 4.5 | 89 | | | | | | | | | | | | |
| **2009** | **10.62** | **98** | **1.73** | **98** | **0.57** | **98** | **5.9** | **90** | | | | | | | | | | | | |
| DJF | 20.53 | 92 | 3.40 | 92 | 1.05 | 92 | 5.6 | 83 | | | | | | | | | | | | |
| MAM | 11.84 | 100 | 1.84 | 100 | 0.69 | 100 | 6.6 | 100 | | | | | | | | | | | | |
| JJA | 1.91 | 100 | 0.35 | 100 | 0.09 | 100 | 5.4 | 94 | | | | | | | | | | | | |
| SON | 9.08 | 100 | 1.49 | 100 | 0.50 | 100 | 5.4 | 85 | | | | | | | | | | | | |
| **2010** | **17.33** | 100 | **3.89** | **100** | **1.11** | **100** | **5.2** | **85** | | | | | | | | | | | | |
| DJF | 43.04 | 100 | 9.39 | 100 | 2.85 | 100 | 4.9 | 92 | | | | | | | | | | | | |
| MAM | 10.22 | 100 | 2.69 | 100 | 0.79 | 100 | 4.6 | 71 | | | | | | | | | | | | |
| JJA | 2.96 | 100 | 1.06 | 100 | 0.11 | 100 | 5.2 | 84 | | | | | | | | | | | | |
| SON | 13.71 | 100 | 2.52 | 100 | 0.73 | 100 | 5.7 | 92 | | | | | | | | | | | | |
| **2011** | **11.64** | 100 | **2.33** | **100** | **0.83** | **100** | **4.7** | **90** | | | | | | | | | | | | |
| DJF | 14.74 | 100 | 3.25 | 100 | 1.13 | 100 | 4,4 | 84 | | | | | | | | | | | | |
| MAM | 11.79 | 100 | 2.16 | 100 | 0.94 | 100 | 5.3 | 92 | | | | | | | | | | | | |
| JJA | 4.00 | 100 | 0.81 | 100 | 0.16 | 100 | 4.8 | 100 | | | | | | | | | | | | |
| SON | 16.23 | 100 | 3.11 | 100 | 1.12 | 100 | 4.5 | 85 | | | | | | | | | | | | |
| **2012** | **10.54** | 100 | **2.34** | **100** | **0.73** | **100** | **4.4** | **90** | | | | | | | | | | | | |
| DJF | 21.75 | 100 | 4.95 | 100 | 1.43 | 100 | 4.8 | 100 | | | | | | | | | | | | |
| MAM | 10.67 | 100 | 1.96 | 100 | 0.61 | 100 | 5.5 | 100 | | | | | | | | | | | | |
| JJA | 1.75 | 100 | 0.65 | 100 | 0.20 | 100 | 3.2 | 70 | | | | | | | | | | | | |
| SON | 8.07 | 100 | 1.82 | 100 | 0.69 | 100 | 3.8 | 92 | | | | | | | | | | | | |
| **2013** | **9.62** | 100 | **1.57** | **100** | **0.50** | **100** | **5.6** | **92** | | | | | | | | | | | | |
| DJF | 18.21 | 100 | 2.88 | 100 | 0.85 | 100 | 5,3 | 92 | | | | | | | | | | | | |
| MAM | 10.88 | 100 | 1.81 | 100 | 0.62 | 100 | 6.7 | 100 | | | | | | | | | | | | |
| JJA | 2.74 | 100 | 0.49 | 100 | 0.15 | 100 | 5.8 | 92 | | | | | | | | | | | | |
| SON | 6.66 | 100 | 1.13 | 100 | 0.36 | 100 | 5.5 | 85 | | | | | | | | | | | | |
| **2014** | **12.78** | 100 | **2.99** | **100** | **0.60** | **100** | **5** | **96** | | | | | | | | | | | | |
| DJF | 20.14 | 100 | 4.72 | 100 | 0.92 | 100 | 4.2 | 92 | | | | | | | | | | | | |
| MAM | 12.44 | 100 | 2.42 | 100 | 0.62 | 100 | 5.8 | 92 | | | | | | | | | | | | |
| JJA | 3.15 | 100 | 0.56 | 100 | 0.14 | 100 | 5.8 | 100 | | | | | | | | | | | | |
| SON | 16.10 | 100 | 4.47 | 100 | 0.89 | 100 | 4.1 | 100 | | | | | | | | | | | | |
| **2015** | **9.36** | **88** | **1.36** | **98** | **0.43** | **98** | **6.4** | **80** | | | | | | | | | | | | |
| DJF | 9.84 | 100 | 1.53 | 98 | 0.45 | 98 | 6.9 | 80 | | | | | | | | | | | | |
| MAM | 12.31 | 92 | 1.45 | 92 | 0.63 | 92 | 6.6 | 61 | | | | | | | | | | | | |
| JJA | 2.26 | 100 | 0.44 | 100 | 0.07 | 100 | 5.6 | 84 | | | | | | | | | | | | |
| SON | 14.04 | 100 | 2.16 | 100 | 0.61 | 100 | 6.1 | 97 | | | | | | | | | | | | |

| | Levo-glucosan | Cap | Man-nosan | Cap | Galact-osan | Cap | Levo/ Mann | Cap | Ara-bitol | Cap | Man-nitol | Cap | 2-methyl-erythritol | Cap | 2-methyl-threitol | Cap | Tre-halose | Cap | Glu-cose | Cap |
|---|---|---|---|---|---|---|---|---|---|---|---|---|---|---|---|---|---|---|---|---|
| **2016** | **7.52** | **97** | **1.21** | **97** | **0.30** | **94** | **5.7** | **92** | **4.78** | **99** | **3.89** | **99** | **0.38** | **99** | **0.13** | **99** | **3.17** | **99** | **5.07** | **99** |
| DJF | 12.54 | 94 | 1.87 | 94 | 0.47 | 94 | 6.4 | 93 | 1.70 | 94 | 1.09 | 94 | 0.02 | 94 | 0.01 | 94 | 0.76 | 94 | 1.47 | 94 |
| MAM | 7.62 | 100 | 1.25 | 100 | 0.31 | 100 | 5.9 | 100 | 4.67 | 100 | 3.40 | 100 | 0.21 | 100 | 0.11 | 100 | 5.82 | 100 | 4.60 | 100 |
| JJA | 2.37 | 100 | 0.47 | 100 | 0.09 | 77 | 5.3 | 100 | 8.29 | 100 | 6.69 | 100 | 1.01 | 100 | 0.29 | 100 | 3.73 | 100 | 9.93 | 100 |
| SON | 7.92 | 92 | 1.30 | 92 | 0.28 | 100 | 5.5 | 76 | 4.26 | 100 | 4.17 | 100 | 0.24 | 100 | 0.09 | 100 | 2.19 | 100 | 4.04 | 100 |
| **2017** | ***8.24*** | ***94*** | ***1.35*** | **95** | ***0.32*** | **94** | **5.6** | **92** | **5.52** | **94** | **5.70** | **94** | **0.37** | **94** | **0.10** | **94** | **3.37** | **94** | **5.17** | **94** |
| DJF | 15.77 | 100 | 2.49 | 100 | 0.65 | 100 | 5.6 | 100 | 1.16 | 100 | 1.40 | 100 | 0.01 | 100 | 0.01 | 100 | 1.03 | 100 | 2.03 | 100 |
| MAM | 6.22 | 92 | 0.98 | 92 | 0.23 | 92 | 6.6 | 84 | 3.90 | 92 | 3.65 | 92 | 0.05 | 92 | 0.02 | 92 | 1.58 | 92 | 4.11 | 92 |
| JJA | 2.27 | 86 | 0.48 | 86 | 0.06 | 86 | 4,8 | 86 | 9.15 | 86 | 8.45 | 86 | 1.32 | 86 | 0.35 | 86 | 4.21 | 86 | 7.09 | 86 |
| SON | 7.84 | 100 | 1.31 | 100 | 0.29 | 100 | 5.5 | 100 | 8.18 | 100 | 9.49 | 100 | 0.17 | 100 | 0.06 | 100 | 6.61 | 100 | 7.58 | 100 |
| **2018** | **9.77** | **100** | **1.62** | **100** | **0.39** | **100** | **6.1** | **98** | **5.76** | **100** | **5.65** | **100** | **0.45** | **98** | **0.16** | **98** | **2.83** | **100** | **4.16** | **100** |
| DJF | 13.50 | 100 | 2.21 | 100 | 0.60 | 100 | 5.9 | 100 | 0.72 | 100 | 0.94 | 100 | 0.01 | 92 | 0.01 | 92 | 0.60 | 100 | 2.74 | 100 |
| MAM | 13.64 | 100 | 2.04 | 100 | 0.54 | 100 | 6.8 | 100 | 4.18 | 100 | 4.21 | 100 | 0.24 | 100 | 0.08 | 100 | 1.91 | 100 | 3.59 | 100 |
| JJA | 1.38 | 100 | 0.25 | 100 | 0.04 | 100 | 5.8 | 100 | 8.66 | 100 | 7.94 | 100 | 1.24 | 100 | 0.42 | 100 | 2.90 | 100 | 4.52 | 100 |
| SON | 10.64 | 100 | 2.01 | 100 | 0.41 | 100 | 5.5 | 92 | 9.38 | 100 | 9.47 | 100 | 0.25 | 100 | 0.12 | 100 | 5.91 | 100 | 5.79 | 100 |

**Table S 16: Seasonal mean (±SD) concentrations of $TC_{bb}$, $OC_{bb}$ and $EC_{bb}$ in $PM_{10}$ and $PM_{2.5}$ at Birkenes 2008–2018. (Unit: µg C $m^{-3}$).**

| | $TC_{bb}$ $PM_{10}$ | $OC_{bb}$ $PM_{10}$ | $EC_{bb}$ $PM_{10}$ | $TC_{bb}$ $PM_{2.5}$ | $OC_{bb}$ $PM_{2.5}$ | $EC_{bb}$ $PM_{2.5}$ |
|---|---|---|---|---|---|---|
| | $TC_{bb}$ $PM_{10}$ | $OC_{bb}$ $PM_{10}$ | $EC_{bb}$ $PM_{10}$ | $TC_{bb}$ $PM_{2.5}$ | $OC_{bb}$ $PM_{2.5}$ | $EC_{bb}$ $PM_{2.5}$ |
| **2008** | **0.160±0.042** | **0.138±0.042** | **0.021±0.005** | **0.141 ± 0.034** | **0.121 ± 0.034** | **0.020 ± 0.004** |
| DJF | 0.150±0.039 | 0.130±0.039 | 0.020±0.004 | 0.133±0.032 | 0.114±0.032 | 0.019±0.004 |
| MAM | 0.117±0.031 | 0.102±0.030 | 0.016±0.003 | 0.104±0.025 | 0.089±0.025 | 0.015±0.003 |
| JJA | 0.196±0.05 | 0.170±0.051 | 0.026±0.006 | 0.174±0.042 | 0.149±0.042 | 0.025±0.006 |
| SON | 0.166±0.043 | 0.144±0.043 | 0.022±0.005 | 0.147±0.036 | 0.126±0.036 | 0.021±0.005 |
| **2009** | **0.156±0.041** | **0.135±0.040** | **0.021±0.005** | **0.138±0.034** | **0.118±0.034** | **0.020±0.004** |
| DJF | 0.301±0.078 | 0.261±0.078 | 0.040±0.009 | 0.266±0.065 | 0.228±0.065 | 0.038±0.008 |
| MAM | 0.174±0.045 | 0.150±0.045 | 0.023±0.005 | 0.154±0.037 | 0.131±0.037 | 0.022±0.005 |
| JJA | 0.028±0.007 | 0.024±0.007 | 0.004±0.001 | 0.025±0.006 | 0.021±0.006 | 0.004±0.001 |
| SON | 0.133±0.035 | 0.115±0.035 | 0.018±0.004 | 0.118±0.029 | 0.101±0.029 | 0.017±0.004 |
| **2010** | **0.254±0.066** | **0.220±0.066** | **0.034±0.008** | **0.225±0.055** | **0.192±0.055** | **0.032±0.007** |
| DJF | 0.631±0.164 | 0.547±0.164 | 0.084±0.019 | 0.558±0.136 | 0.478±0.136 | 0.080±0.018 |
| MAM | 0.150±0.039 | 0.130±0.039 | 0.020±0.004 | 0.132±0.032 | 0.113±0.032 | 0.019±0.004 |
| JJA | 0.043±0.011 | 0.038±0.011 | 0.006±0.001 | 0.038±0.009 | 0.033±0.009 | 0.006±0.001 |
| SON | 0.201±0.052 | 0.174±0.052 | 0.027±0.006 | 0.178±0.043 | 0.152±0.043 | 0.026±0.006 |
| **2011** | **0.171±0.044** | **0.148±0.044** | **0.023±0.005** | **0.151±0.037** | **0.129±0.037** | **0.022±0.005** |
| DJF | 0.216±0.056 | 0.187±0.056 | 0.029±0.006 | 0.191±0.047 | 0.164±0.047 | 0.027±0.006 |
| MAM | 0.173±0.045 | 0.150±0.045 | 0.023±0.005 | 0.153±0.037 | 0.131±0.037 | 0.022±0.005 |
| JJA | 0.059±0.015 | 0.051±0.015 | 0.008±0.002 | 0.052±0.013 | 0.044±0.013 | 0.007±0.002 |
| SON | 0.238±0.062 | 0.206±0.062 | 0.032±0.007 | 0.210±0.051 | 0.180±0.051 | 0.030±0.007 |
| **2012** | **0.155±0.040** | **0.134±0.040** | **0.021±0.005** | **0.137±0.033** | **0.117±0.033** | **0.020±0.004** |
| DJF | 0.319±0.083 | 0.276±0.083 | 0.043±0.009 | 0.282±0.069 | 0.241±0.069 | 0.040±0.009 |
| MAM | 0.156±0.041 | 0.136±0.041 | 0.021±0.005 | 0.138±0.034 | 0.118±0.034 | 0.020±0.004 |
| JJA | 0.026±0.007 | 0.022±0.007 | 0.003±0.001 | 0.023±0.006 | 0.019±0.006 | 0.003±0.001 |
| SON | 0.118±0.031 | 0.102±0.031 | 0.016±0.004 | 0.105±0.026 | 0.090±0.025 | 0.015±0.003 |
| **2013** | **0.141±0.037** | **0.122±0.037** | **0.019±0.004** | **0.125±0.030** | **0.107±0.030** | **0.018±0.004** |
| DJF | 0.267±0.069 | 0.231±0.069 | 0.036±0.008 | 0.236±0.058 | 0.202±0.058 | 0.034±0.008 |
| MAM | 0.159±0.041 | 0.138±0.041 | 0.021±0.005 | 0.141±0.034 | 0.121±0.034 | 0.020±0.004 |
| JJA | 0.040±0.010 | 0.035±0.010 | 0.005±0.001 | 0.035±0.009 | 0.030±0.009 | 0.005±0.001 |
| SON | 0.098±0.025 | 0.085±0.025 | 0.013±0.003 | 0.086±0.021 | 0.074±0.021 | 0.012±0.003 |
| **2014** | **0.187±0.049** | **0.162±0.049** | **0.025±0.006** | **0.166±0.040** | **0.142±0.040** | **0.024±0.005** |
| DJF | 0.295±0.077 | 0.256±0.077 | 0.040±0.009 | 0.261±0.064 | 0.224±0.064 | 0.037±0.008 |
| MAM | 0.182±0.047 | 0.158±0.047 | 0.024±0.005 | 0.161±0.039 | 0.138±0.039 | 0.023±0.005 |
| JJA | 0.046±0.012 | 0.040±0.012 | 0.006±0.001 | 0.041±0.010 | 0.035±0.010 | 0.006±0.001 |
| SON | 0.236±0.061 | 0.204±0.061 | 0.032±0.007 | 0.209±0.051 | 0.179±0.051 | 0.030±0.007 |
| **2015** | **0.137±0.036** | **0.119±0.036** | **0.018±0.004** | **0.121±0.030** | **0.104±0.030** | **0.017±0.004** |
| DJF | 0.144±0.038 | 0.125±0.038 | 0.019±0.004 | 0.128±0.031 | 0.109±0.031 | 0.018±0.004 |
| MAM | 0.180±0.047 | 0.156±0.047 | 0.024±0.005 | 0.160±0.039 | 0.137±0.039 | 0.023±0.005 |
| JJA | 0.033±0.009 | 0.029±0.009 | 0.004±0.001 | 0.029±0.007 | 0.025±0.007 | 0.004±0.001 |
| SON | 0.206±0.054 | 0.178±0.054 | 0.028±0.006 | 0.182±0.044 | 0.156±0.044 | 0.026±0.006 |
| **2016** | **0.110±0.029** | **0.096±0.029** | **0.015±0.003** | **0.098±0.024** | **0.084±0.024** | **0.014±0.003** |
| DJF | 0.184±0.048 | 0.159±0.048 | 0.025±0.005 | 0.162±0.040 | 0.139±0.040 | 0.023±0.005 |
| MAM | 0.112±0.029 | 0.097±0.029 | 0.015±0.003 | 0.099±0.024 | 0.085±0.024 | 0.014±0.003 |

| | $TC_{bb}$ $PM_{10}$ | $OC_{bb}$ $PM_{10}$ | $EC_{bb}$ $PM_{10}$ | $TC_{bb}$ $PM_{2.5}$ | $OC_{bb}$ $PM_{2.5}$ | $EC_{bb}$ $PM_{2.5}$ |
|---|---|---|---|---|---|---|
| JJA | 0.035±0.009 | 0.030±0.009 | 0.005±0.001 | 0.031±0.007 | 0.026±0.007 | 0.004±0.001 |
| SON | 0.116±0.030 | 0.101±0.030 | 0.016±0.003 | 0.103±0.025 | 0.088±0.025 | 0.015±0.003 |
| **2017** | **0.121±0.031** | **0.105±0.031** | **0.016±0.004** | **0.107±0.026** | **0.092±0.026** | **0.015±0.003** |
| DJF | 0.231±0.060 | 0.200±0.060 | 0.031±0.007 | 0.204±0.050 | 0.175±0.050 | 0.029±0.007 |
| MAM | 0.091±0.024 | 0.079±0.024 | 0.012±0.003 | 0.081±0.020 | 0.069±0.020 | 0.012±0.003 |
| JJA | 0.033±0.009 | 0.029±0.009 | 0.004±0.001 | 0.029±0.007 | 0.025±0.007 | 0.004±0.001 |
| SON | 0.115±0.030 | 0.100±0.030 | 0.015±0.003 | 0.102±0.025 | 0.087±0.025 | 0.015±0.003 |
| **2018** | **0.143±0.037** | **0.124±0.037** | **0.019±0.004** | **0.127±0.031** | **0.108±0.031** | **0.018±0.004** |
| DJF | 0.198±0.052 | 0.171±0.051 | 0.026±0.006 | 0.175±0.043 | 0.150±0.043 | 0.025±0.006 |
| MAM | 0.200±0.052 | 0.173±0.052 | 0.027±0.006 | 0.177±0.043 | 0.151±0.043 | 0.025±0.006 |
| JJA | 0.020±0.005 | 0.018±0.005 | 0.003±0.001 | 0.018±0.004 | 0.015±0.004 | 0.003±0.001 |

**Table S 17: Equations showing the relationship between EC, OC and TC for ambient $PM_{2.5}$ aerosol filter samples collected at Birkenes in 2014, obtained by temperature calibrated Quartz and EUSAAR-2 temperature programs.**

| | | | | |
|---|---|---|---|---|
| EC | $EC_{EUSAAR\text{-}2,\,TOT} = EC_{QUARTZ,\,TOT}$ x 1.6118 | $R^2 = 0.876$ | n = 50 | Eq. S 16 |
| OC | $OC_{EUSAAR\text{-}2,\,TOT} = OC_{QUARTZ,\,TOT}$ x 0.8687 | $R^2 = 0.977$ | n = 50 | Eq. S 17 |
| TC | $TC_{EUSAAR\text{-}2,\,TOT} = TC_{QUARTZ,\,TOT}$ x 0.9151 | $R^2 = 0.976$ | n = 50 | Eq. S 18 |